PERFORMANCE OF AN INTERNAL COMBUSTION ENGINE USING MIXTURES OF GASOLINE AND HYDROGEN AS THE FUEL

by

Jerry Price Harkey

B.S., Kansas State University, 1976

A MASTER'S THESIS

submitted in partial fulfillment of the

requirements for the degree

MASTER OF SCIENCE

Department of Mechanical Engineering
Kansas State University
Manhattan, Kansas

1978

Approved:

R D Ball

Major Professor

TABLE OF CONTENTS

LIST OF PLATES

LIST OF TABLES

LIST OF FIGURES

Chapter I

Introduction

Because of the increasing scarcity and cost of known reserves of petroleum, interest in alternative fuels has risen. These alternative fuels would be produced from abundant or renewable energy sources, thus freeing the energy market from dependence on scarce and expensive petroleum and natural gas.

Hydrogen is one of the possible alternative fuels on which interest has been focused. In fact a "hydrogen economy" has been proposed, in which hydrogen replaces natural gas and petroleum. In the "hydrogen economy", hydrogen is manufactured by electrolysis or thermochemical cracking. In electrolysis hydrogen is produced by passing an electric current through water. This current would be generated by some process other than fossil fueled power such as nuclear, solar cells, windmills, tidal, solar powered steam turbines, or other processes not yet known.

In thermochemical cracking, a series of high temperature endothermic reactions are used to split water molecules into hydrogen and oxygen. The source of the energy could be nuclear, solar or some other source whose future supply can be reasonably assured.

The question that may be asked at this point is: why hydrogen? Why not use the electricity or heat directly. The

answer is that the hydrogen is a more convenient and practical form of the energy to transport and utilize. Most important perhaps, is the fact that hydrogen can be stored until it is needed, then transported hundreds of miles to be used in much the same way natural gas and liquified petroleum gas is used presently.

In considering the use of hydrogen in place of conventional hydrocarbon fuels in prime movers, additional factors besides ease of storage and transport must be considered, since hydrocarbon fuels are easy to store and a massive hydrocarbon distribution and transportation system already exists. Advantages of hydrogen include: ease of ignition inside the combustion chamber, high energy content per unit weight, high mass diffusivity and low emission of pollutants.

Hydrogen ignition is usually not a problem as hydrogen - air mixtures will ignite over a far wider range of composition and spark plug conditions than will gasoline - air mixtures. Hydrogen ignites so easily that it has been combined with extremely lean gasoline - air mixtures to aid ignition. The purpose of this scheme is to easily ignite the hydrogen which in turn ignites the otherwise inert lean mixture (6, 14).

Hydrogen possesses a high energy content per unit weight. This is a particularly important property when considering the use of hydrogen for aircraft fuel. Reducing the weight of the fuel carried on an aircraft obtains a corresponding increase in payload.

The high mass diffusivity of hydrogen helps offset a disadvantage discussed later - the ease of ignition of hydrogen outside the combustion chamber. The high rate of diffusion helps lessen the chances of formation of combustible mixtures.

Hydrogen fueled engines have the environmental advantage that virtually no carbon monoxide or hydrocarbon pollutants are produced. What little is emitted is formed from engine lubricants.

Disadvantages of hydrogen include: its ease of ignition outside the combustion chamber, volume required for storage, difficulty in sealing lines and tanks, emission of oxides of nitrogen from engines, and the tendency to backfire through the engine intake manifold.

The ease of ignition of hydrogen is caused by its low ignition energy and wide flammability limits (the ability to ignite over a wide range of fuel - air mixtures). For a stoichiometric mixture the minimum spark energy of H_2 (.019 millijoules) is about an order of magnitude lower than that of hydrocarbons. As a result, flammable H_2 - air mixture may be ignited by numerous and relatively weak ignition sources. The lower and upper flammability limits of H_2 when mixed with air are usually between 4 to 75 per cent by volume at standard temperature and pressure. Those of gasoline are about 1.4 to 7.6 per cent by volume (1). However the rapid dissipation of hydrogen as discussed under "advantages" that minimizes the concentration and duration of flammable fuel - air mixtures helps offset this disadvantage.

Hydrogen requires far more volume to store a given amount of energy than does gasoline. There are basically three ways to store hydrogen; compressed gas, cryogenic (very cold) liquid, and metal hydrides. A metal hydride contains hydrogen that can be dissociated via an endothermic reaction, and recharged via an exothermic reaction (2). In Table 1 the three ways of storage of hydrogen are compared with the energy equivalence of 20 gallons of gasoline.

Table 1 Comparison of Fuel Storage Systems for a Vehicle Range of 260 mi (418 km)(Ref. 2)

	Gasoline	Cryogenic LH_2	Compressed GH_2	Metallic Hydride
Fuel:				
weight, lb (kg)	118(53.5)	29.5(13.4)	29.5(13.4)	400(181) ($Mg H_2$)
volume, ft^3 (m^3)	2.6(0.07) (20 gal)	6.7(0.19) (50 gal)	35(1.0) (290 gal)	8(0.23) (60 gal)
Tankage:				
weight, lb (kg)	30(13.6)	400(181)	3000(1361)	100(45.4)
volume, ft^3 (m^3)	3(0.08)	10(0.28)	54(1.53)	9(0.25)
Total:				
weight, lb (kg)	148(67)	430(195)	3030(1374)	500(227)

As can be seen from Table 1, even the "best" method of hydrogen storage requires more than twice the space of gasoline. It can also be seen that whichever of the above methods are used,

that the weight advantage of hydrogen fuel is wiped out by the weight of the tankage (2).

Because of the small size of the hydrogen molecule, hydrogen systems are unusually liable to leak. Special care must be taken in sealing hydrogen systems because the hydrogen can leak through nominally tight seals and escape from systems that appear leak - free when tested with other fluids (1).

The large difference between cryogenic hydrogen temperature (-253^{o}C) and ambient (25^{o}C) causes variant contraction of dissimilar materials. Stresses resulting from this contraction can cause catastrophic failure of equipment. This can be prevented by selecting materials that remain ductile at cryogenic temperatures and whose coefficients of expansion and thermal conductivity are relatively low (1).

Metal hydride systems, where high temperature conditions exist when heat is supplied to dissociate the hydrogen from the hydride storage material, have a tendency to heat treat and hydrogen embrittle. Again this may be prevented by the proper selection of alloys (such as stainless steel) that do not heat treat or embrittle under the expected conditions (3).

Although it is possible, with proper ignition timing, to operate hydrogen engines at high compression ratios without preignition, hydrogen engines seem to have a tendency to backfire. As in a gasoline fueled engine a hydrogen engine produces oxides of nitrogen from the nitrogen and oxygen in the air during the high temperature of combustion. Each case can be

prevented with exhaust gas recirculation or water injection. Exhaust gas recirculation prevents formation of oxides of nitrogen lowering the peak combustion temperature by diluting the combustion mixture with an inert gas. Water injection also limits the peak combustion temperature, but does so by cooling the combustion mixture (4). Since the exhaust of an all hydrogen fueled engine is essentially all water, it can be condensed and used for water injection yielding a self contained water injection system (5). The use of condensed exhaust for water injection, rather than the direct use of the gas, is desirable because a given engine equipped with water injection will have a somewhat higher power output than the same engine with exhaust gas recirculation.

Research so far has been oriented either toward 100 per cent fueled hydrogen engines or adding hydrogen to a gasoline - air mixture to improve the case of ignition of extraordinarily lean mixtures of gasoline and air (6,7).

The desirability of true hydrogen and gasoline mixtures where the hydrogen is used as a fuel and not just to improve the ignition characteristics are two fold. The use of gasoline and hydrogen could increase the range or decrease the bulk of fuel storage components as compared to an all hydrogen fueled vehicle. An optimum mixture of hydrogen and gasoline could hopefully be found maximizing the benefits of each while minimizing the disadvantages of each. This optimum mixture could capitalize on hydrogen's ease of ignition and clean

combustion and gasoline's high energy content per volume. At the same time the heat of vaporization of gasoline could cool the mixture and minimize the tendency of hydrogen mixtures to backfire.

Since no one else has done studies where hydrogen has contributed a significant amount of energy in the fuel, this study was undertaken and the objective was to evaluate the performance of an internal combustion engine using mixtures of gasoline and hydrogen as the fuel.

Chapter II

Literature Review

Most of the published work dealing with hydrogen fueled engines has involved the use of 100% hydrogen fueled engines and engines operating on an extremely lean gasoline - air mixture using hydrogen as a supplement.

According to de Boer, et al. (8), research on hydrogen engines began in the 1920's. By the early 1930's work had progressed to the point where a fleet of hydrogen fueled vehicles were tested. The work was apparently interupted in the late 1930's by the beginning of World War II in Europe. In some of the above work it was found that by using direct injection of hydrogen into the cylinder, controlling the engine by varying the amount of hydrogen injected per engine cycle, and burning lean mixtures, indicated thermal efficiencies as high as 52% were obtained. It was speculated that the high efficiency was obtained in part because of the elimination of pumping losses, and in part because the effective ratio of specific heats is larger in lean mixtures than in nearly stoichiometric mixtures. In theory efficiency increases in Otto and Diesel cycle engines as the ratio of specific heats increase because the efficiency is proportional to the term $\left[1 - \frac{1}{r_v^{k-1}}\right]$ where r_v is the compression ratio and k is the ratio of specific heats.

Interest in hydrogen-fueled engines was revived recently

because they look attractive from the viewpoint of exhaust emissions and the prospects of a hydrogen economy or the availability of hydrogen to replace hydrocarbon fuels.

More recently a great deal of work has been carried out by the Billings Energy Corporation on carbureted hydrogen-fueled engines.

One of the more important areas Billings Energy Corporation has been involved in is that of methods to prevent backfiring in hydrogen fueled engines (9,10). Billings researchers found that any technique for cooling "hot spots" prior to the opening of the intake valve will reduce the backfire problem. These "hot spots" consist of high temperature zones on the interior of the combustion chamber such as a spark plug, an exhaust valve, or a sharp projection such as a casting imperfection or deposits that accumulate during gasoline operation. Exhaust gas recirculation, because it introduces an inert gas in the combustion chamber that lowers the peak temperature of combustion, reduces backfiring. However, injecting what is essentially steam into the intake reduces volumetric efficiency and consequently engine power output and efficiency. Increased conduction via higher surface to volume ratios of the combustion chamber reduces backfiring, and, if accomplished by increasing the compression ratio, increases efficiency. Mixtures with an equivalence ratio (ratio of hydrogen mass in the mixture to the mass of hydrogen for a stoichiometric mixture) less than .6 usually do not exhibit intermittant backfires. Because of

its positive effect on thermal efficiency, liquid water induction was selected as the main method of controlling backfires. However it should be noted that most Billings conversions have included increased compression ratios to a range of about 11:1 to 12:1, and lean operation during normal engine loading. Finally Lynch (10) of Billings Energy Corporation recommended special precautions to insure that all spark plug leads are separated or shielded. This is to prevent the intense current pulses in one spark plug lead from inducing a high enough voltage in an adjacent lead to cause an unwanted spark.

Billings Energy Corporation has researched methods for the control of NO_X, which as was noted in the introduction is the only serious pollutant from hydrogen fueled engines (4). By slightly retarding the spark advance, No_X can be reduced without seriously affecting engine efficiency or power output. Exhaust gas recirculation or water induction can be used to prevent the formation of NO_X, with water induction being the prefered method. It is interesting to see that the last two methods of NO_X control parallel backfire control techniques. Billings researchers found that it required more water for NO_X control than for backfire control.

Billings Energy Corporation has progressed from theoretical and experimental analysis (11) of a hydrogen powered vehicle to real world testing (12). A hydrogen powered bus was operated in the Provo-Orem area with no major problems. In the future Billings plans to market more buses and to

produce at least 10 hydrogen-fueled commuter cars.

Researchers at the Jet Propulsion Lab (JPL) of the California Institute of Technology have been investigating the use of hydrogen enrichment of lean gasoline - air mixtures, particualrly as applied to piston aircraft engines. Menard, Moynihan, and Rupe (6), in a systems analysis study conclude hydrogen enrichment can be used to reduce fuel consumption and exhaust emissions. In this study, hydrogen was catalytically generated from gasoline on the aircraft. By mixing the hydrogen with the normal gasoline fuel, the lean flammability limit of the fuel is extended to ultralean fuel-air mixtures. This improved the thermal efficiency of the engine for the reason that the thermal efficiency of a piston internal combustion engine improves with lean combustion.

In the next phase of the study Chirivella, Duke, and Menard (13) conducted engine tests using hydrogen enriched lean mixtures. It was concluded from the tests that, at least for the engine tested, hydrogen enrichment was not needed to run ultralean and improve fuel economy. Rough engine operation was avoided through the adjustment of spark advance and other engine variables. JPL does, however, intend to flight test a Beech Duke B60 operating ultralean both with and without hydrogen enrichment to obtain more data for comparison.

Stebar and Parks of General Motors Research Laboratories conducted a study (14) of hydrogen supplemented fuel. This study comes as close as any found to investigating a gasoline-

hydrogen mixture where hydrogen actually supplies a significant amount of the energy. In one of the gasoline-hydrogen mixtures studies in the above investigation, hydrogen supplied 23% of the energy, or 10% of the fuel by weight. A 1973 intermediate Oldsmobile was modified to run on the aformentioned mixture. This research effort was predicated on meeting the most stringent federal exhaust emission standards of 0.41 g/mile HC, 3.4 g/mile CO, and 0.40 g/mile NO_X. Although NO_X and CO emissions were at an acceptable level, hydrocarbon emissions were too high. Stebar and Parks reported an equavalent calculated (by carbon balance) gas mileage of 11.0 mpg, averaged over the 1975 Federal Test Procedure. This value surely is not very high when compared with automobiles on the market today and no base line gasoline consumption figures for the automobile tested were given in the report.

Chapter III

Equipment and Testing Procedure

In this chapter experimental equipment, layout, procedures, and the reason why some of the procedures were followed will be explained.

Photographs of the equipment, instrumentation, and controls used in the study are shown in Plates I, II, III. Because of the physical size and layout of the apparatus, and obstructions in the area of the layout, a single photograph could not be taken which would clearly display all the devices. Therefore, the area is pictured in three parts. Accompanying each photograph is a list of equipment numbered corresponding to the numbers in the photograph.

The engine used for this study was a 1968 model, 96.6 cu. in. (1.58 l) displacement, four cylinder, horizontally opposed, electronically fuel injected, air cooled, spark ignition, internal combustion, Volkswagen engine. Table 2 lists important specifications for the engine as it existed for this study.

Table 2

Selected Engine Specifications
(Data from References 17 and 18)

Ignition timing	adjusted for best torque (100% gasoline only) or lean best torque
Ignition type	Bosch distributor modified for operation with Borg-Warner electronic ignition
Spark plug type	Bosch W145 T1
Spark plug gap	.28 in. (17 mm)
Engine oil	Mobile Delvac 1100 SAE30
Bore	3.36 in (85.5 mm)
Stroke	2.72 in. (64 mm)
Displacement	96.6 cu. in. (1.584 l)
Compression Ratio	8.8:1
Torque (SAE)	86.8 ft. lb. @ 2800 rpm
Output (SAE)	65 bhp @ 4600 rpm

It may be noted here that the ignition timing was not left stock, for reasons to be mentioned later.

Gasoline - air mixture control was provided during engine startup, warmup and between tests by the Bosch electronic

EXPLANATION OF PLATE I

Right side of Experimental Layout

Item	Description
1.	Throttle
2.	Hydrogen Mixture Control
3.	Magnetic Speed Pickup
4.	Bosch Electronic Control Unit
5.	Switch to Select Control Mode
6.	Power Supply for Air Flow Transducer
7.	Air Flow Transducer (for Engine Control)
8.	Hydrogen Mixing Valve
9.	Hydrogen Flow Transducer
10.	Modified Propane Convertor
11.	Electrically Operated Hydrogen Flow Shutoff Valve
12.	Hydrogen Line
13.	Location of Tee Junction in Manifold Vacuum Line
14.	Air Flow Measuring Equipment (for Data) A. Surge Tank B. Flow Nozzle
15.	Temperature Measuring Equipment A. Millivolt Potentiometer B. Thermos Bottle Containing Ice Bath
16.	Hydraulic Pump Dynamometer
17.	Thermocouple in Exhaust Stream
18.	Gasoline Flow Measuring Equipment A. Location of "Start-Stop"Switch B. Location of Lever Arm and Trigger Switch
19.	Ignition Switch
20.	Switch for Electrically Operated Hydrogen Flow Shutoff

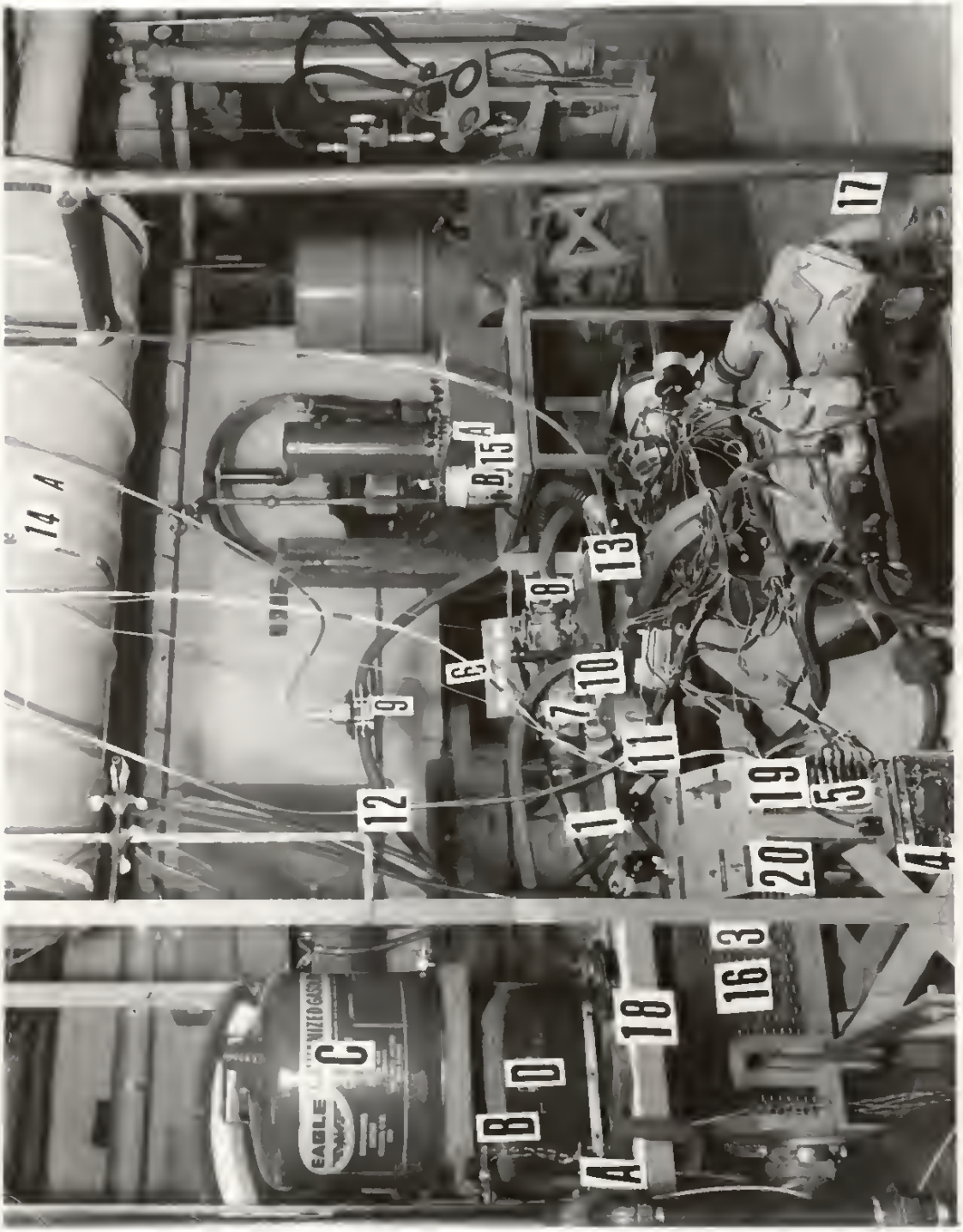

Plate I

EXPLANATION OF PLATE II

Left Side of Experimental Layout

Item	Description
1.	Mercury Manometer
2.	Water Micro Manometer
3.	Cooling Water Supply
4.	Hydraulic Oil Filter
5.	Hydraulic Oil Reservoir
6.	Power Supply for Kim I Microprocessor
7.	Interface Hardware
8.	Kim I Microprocessor
9.	Teletype
10.	Daytronic Modular Instrument System
11.	Cooling Fans
12.	Beckman Counter
13.	Strain Gauge Transducer
14.	Power Supply for Interface and Counter Trigger
15.	Manual Pressure Regulating Valve
16.	Hydrogen Line
17.	Hydrogen Flow Meter
18.	Sling Psychrometer with Distilled Water Bottle
19.	Vise Grips and Sheet Metal Used to Pinch Hydrogen Line

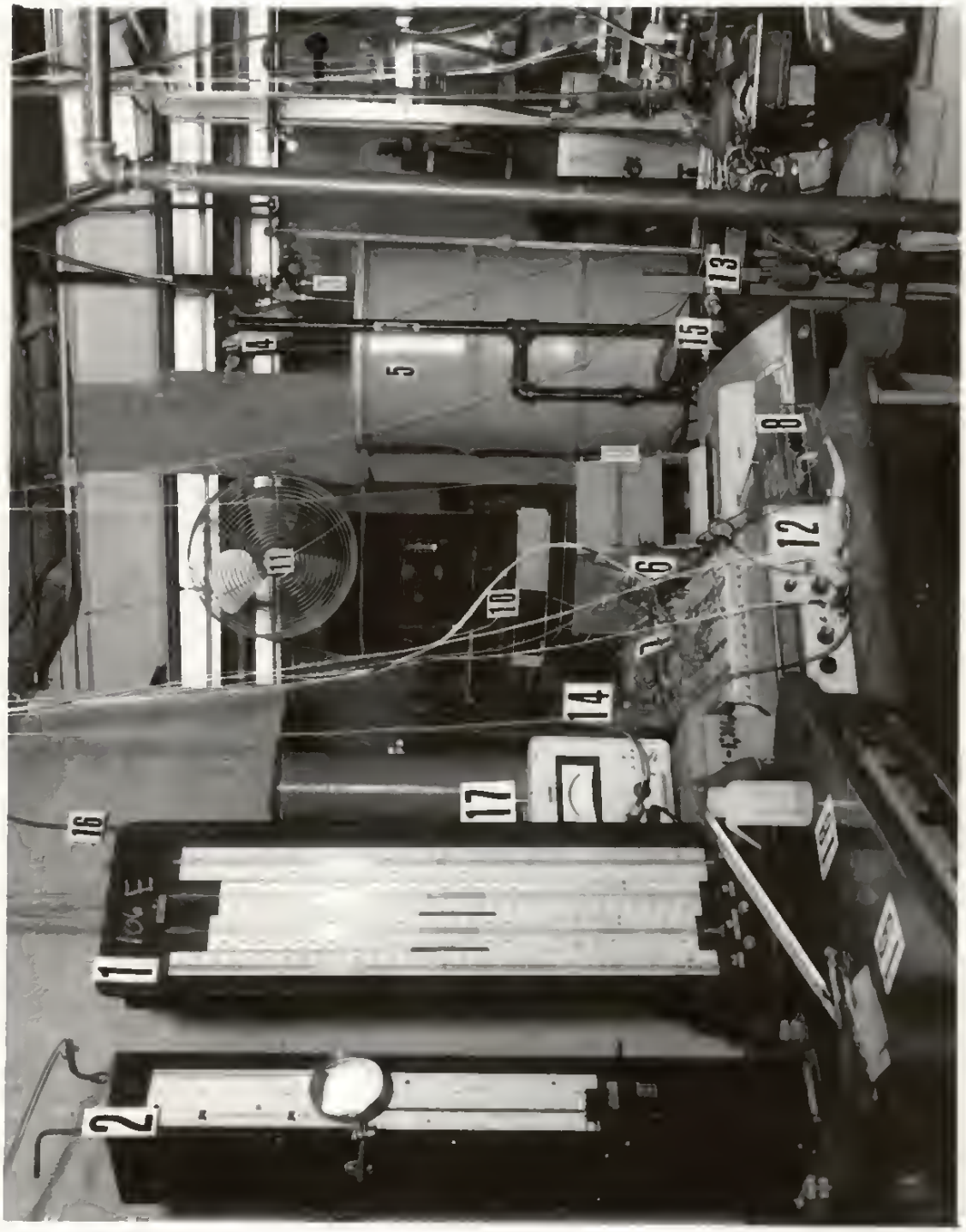

Plate II

EXPLANATION OF PLATE III

Hydrogen Storage Compartment

Item	Description
1.	Hydrogen Tanks
2.	Hydrogen Line Pressure Regulator
3.	Manual Hydrogen Line Shutoff
4.	Hydrogen Tank Hold Downs
5.	Hydrogen Line
6.	Hydrogen Tank Shutoff

Plate III

fuel injection control (Plate I, item 4). For details of this system as well as details on the minor modifications performed on it, the reader is referred to the thesis of Mr. Walt Williams (18). Gasoline - air mixture control was provided during the test runs by the system designed by Mr. Firooz Bakhtiari - Najad and utilizing the Kim 1 microprocessor (Plate II, item 8) and interface hardware (Plate II, item 7). Because this system was used as designed, except for the very minor changes discussed below, and because this control system was itself the subject of a masters degree thesis, very little explanation will be given here and the reader is referred to the masters degree thesis of Mr. Firooz Bakhtiari - Najad (20) for details of the system. There were two minor changes to this system: The values for the gasoline - air mixture that were used in this study, that is 40%, 50%, 60% and 80% of stoichiometric, were placed in the memory of the Kim 1 and the appropriate memory location was loaded into the initialization program as necessary. This system was originally designed to control the spark advance, however for the present work, this control was disconnected. The teletype (Plate II, item 9) was used to print out the control programs of the microprocessor. The print outs were used to check the correctness of the program after it had been loaded. The programs were loaded from paper tapes, again using the teletype.

Hydrogen flow control was accomplished by the operator through a series of manual and electric (solenoid) valves. Each hydrogen tank (Plate III, item 2) came equipped with a valve (Plate III, item 6), kept closed during transport and storage, of course, and when no tests were being run. To insure safety, the hydrogen tanks were stored in a "compartment" between thick, concrete bulkheads. The hydrogen tanks were connected via a manifold to the line pressure regulator (Plate III, item 2) that maintained a line pressure of about 40 psig. After the line pressure regulator, the hydrogen flowed through a manual shutoff valve (Plate III, item 3) that was used when the hydrogen flow was shut for a short time (during equipment adjustments, gasoline refueling etc.). After the manual shutoff valve the hydrogen flowed to the solenoid operated shutoff (Plate I, item 11). This is the valve that was actually used to turn on the hydrogen during conversion from 100% gasoline and Bosch control to hydrogen - gasoline mixtures and microprocessor control. This switch made conversion a simple process of setting the hydrogen mixture rich and flipping two toggle switches. Next the hydrogen flowed through a propane convertor (Plate I, item 10) (in which the water passages were blocked as the hydrogen was already gaseous and hence did not need to be vaporized as does propane). The convertor contained an important safety valve that shut off the hydrogen flow in the absence of any manifold vacuum. This valve performed flawlessly during the

dozen or so backfires that occured and prevented any combustion from continuing. The second function of the convertor was to reduce the line pressure from approximately 40 psig to a pressure near atmospheric. The hydrogen then flowed through a flow transducer (Plate I, item 9). This flow transducer was the transducer for the Gould Datametrics model 800-LM flowmeter, which was used to measure the hydrogen flow. Finally, the hydrogen enters the hydrogen mixing valve (Plate I, item 8) where it is mixed with the engine combustion air. This mixing valve is a standard propane carburetor with the throttle plates removed and the idle passages plugged.

Besides hydrogen mass flow rate the following quantities were recorded; wet and dry bulb termperatures, atmospheric pressure, time of test, engine speed, torque, percent of stoichiometric gasoline mixture, intake manifold vacuum, ignition timing, exhaust gas temperature, pressure drop across the air flow nozzle, and gasoline consumption.

Wet and dry bulb temperatures were obtained through the use of a sling psychrometer (Plate I, item 18) using distilled water on the wet bulb wick. Wet and dry bulb temperatures were always obtained in the area just ahead of the inlet of the air flow nozzle, since their readings were critical in the calculation of air mass flow.

Atmospheric pressure was read from a barometer in a room near the testing area.

Starting and ending times were recorded from the author's Seiko automatic chronograph or Texas Instruments electronic watch.

The engine speed was obtained by using a fixed magnetic pick-up and a 60 tooth metallic gear mounted on the drive shaft between the clutch and dynamometer (Plate I, item 3). A 60 tooth gear was used because the output frequency (in Hertz) is numerically equal to RPM, allowing frequency meters to be used without recalibration (21). Since the speed sensing pickup is obscured by protective mesh in Plate I, detail of the pickup is given in figure 1.

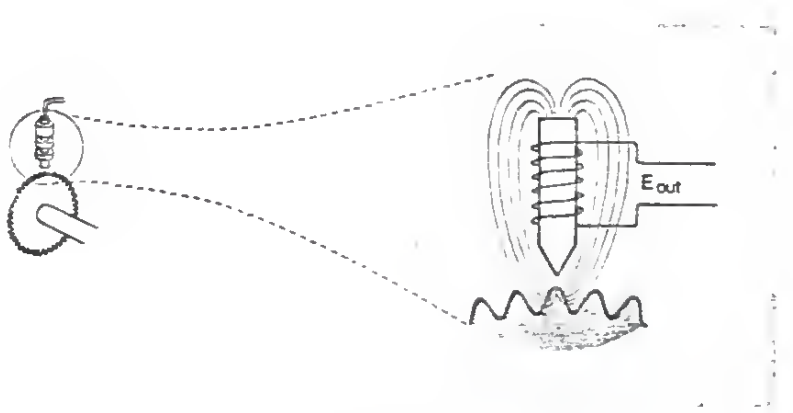

Figure 1 Magnetic Speed Pickup
(from Ref. 21)

The pulses from the pickup were fed into the Daytronic Modular Instrument System (Plate II, item 10) which gave a digital display of the engine speed.

The torque output of the engine was measured using a hydraulic pump dynamometer (Plate I, item 16) exerting force through a moment arm on a strain gauge transducer

(Plate II, item 13). The power absorbing element of this system was an aviation hydraulic pump. This pump drew oil from the hydraulic oil reservoir (Plate II, item 5), pumped it through the pressure regulating valve (Plate II, item 15), hydraulic oil filter (Plate II, item 4) and back to the tank. The oil pressure and thereby pump torque, was manually controlled by the operator, and the torque reading from the lever arm and strain gauge transducer was displayed digitally on the Daytronic modular instrument system. A switch on the Daytronic module selected the display of torque or engine speed. Water was circulated through a coil of copper tubing (Plate II, item 3) inside the hydraulic oil reservoir. Although the tank would become hot to the touch, this cooling system evidentally kept the temperature of the oil sufficiently constant to provide stable power absorption. Before leaving the subject of the dynamometer it should be noted that due to pressure limitations of the hydraulic motor, full power tests could not be run. Instead data were taken at torques of 21.7, 28.9 and 43.4 ft.-lbf., 1/4, 1/3 and 1/2 of the SAE rated torque of the engine, respectively. For the general layout of the Torque Dynamometer see figure 2.

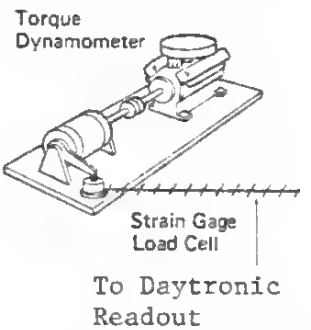

Figure 2. Torque Dynamometer (from reference 21)

The intake manifold vacuum was measured with a vertical mercury manometer (Plate II, item 1). In a previous study (18) the tee (Plate I, item 13) had been placed in the vacuum line from the manifold to the manifold pressure sensor (one of the components of the Bosch fuel injection system) and the tee was connected to the manometer. For the previous study the tee was placed in this location because it was felt the manufacturer placed the manifold tap for the pressure sensor to give a fairly constant and accurate measure of the pressure. The same tee location was employed in the present study for the above reason and to enable this study to be compared to the earlier study.

To facilitate the recording of ignition timing, a degree wheel was constructed and affixed to the cooling fan which was already equipped with a top dead center marker (for no. 1 cylinder). A stationary marker originally supplied with the engine was used as the timing marker. Ignition timing data were taken with a Sears - Penske induction triggered stroboscopic timing light. A handle was attached to the base of the distributor to make it easier to smoothly adjust the spark advance.

Exhaust temperature was found by measuring the electromotive force (emf) produced by a two - junction Chromel - alumel thermocouple with one junction in the exhaust stream (Plate I, item 17) and the other in a thermos bottle containing an ice bath (Plate I, item 15B). The emf was measured with a

null - balance millivolt potentiometer (Plate I, item 15A). After recording the emf, the temperature was determined from a chromel - alumel temperature emf table.

The air mass flow rate was calculated from the pressure drop across a 1.59 in. (4.04 cm.), ASME long radius flow nozzle (Plate I, item 14B), measured with a 10 in. (25.4 cm.) water micro - manometer (Plate II, item 2). The nozzle was placed in one end of a surge tank (Plate I, item 14A), and the engine drew air from the opposite end. The surge tank was used to dampen the intake pulse from the engine to insure stable flow through the airflow nozzle.

Gasoline consumption was measured by timing how long it took to consume a known mass of gasoline. When a gasoline consumption test was to be run, weights were placed on the scales (Plate I, item 18D) on a platform in back of the gasoline tank (Plate I, item 18C) to balance the weight of the gasoline. The counter start - stop switch (Plate I, item 18A) was placed on start. As the gasoline was used, the platform on which the gasoline tank was placed moved upward and the counter trigger switch was released by the lever arm (Plate I, item 18B). Now the counter (Plate II, item 12) was on. A known mass was placed on top of the gasoline tank and the counter start - stop switch was moved to stop. As the tank platform rose again and the known mass consumed, the counter trigger switch was again released and the counter shut off. If another run was to be made, the counter was reset and the above process repeated.

Before engine startup, the gasoline tank was filled, if necessary, full hydrogen tanks were connected, if necessary, the manual line valve and the tank valves were opened (if tests were to be run using hydrogen) and the Daytronic torque and RPM meter was calibrated as per the instructions of Dr. Ralph Turnquist of the Kansas State University Mechanical Engineering Department (15). The torque meter was first adjusted to read zero with the balance adjustment, then a test weight was applied and the meter adjusted to read 60 ft. - lbf. using the span adjustment. This process was repeated until the reading was consistently zero with no load and 60 ft. - lbf. with the test weight. The RPM meter was first adjusted to read zero with the zero adjustment, then the "CAL" button was pushed to feed a signal from an internal crystal oscillator to the meter, and the readout was adjusted to 5,000 RPM. Again the process was repeated until the reading was consistently zero with no input and 5,000 with the input from the internal crystal oscillator. Just before the engine was started, water to the heat exchanger in the dynamometer hydraulic reservoir was turned on as were the auxillary cooling fans (Plate II, item 11).

The engine was started using the Bosch fuel injection control. During warm up the equipment was turned on and checked out, ice was supplied to the reference junction of the thermocouple and a simple calibration procedure was performed on the hydrogen flow meter in accordance with the procedures described in the operating instructions for the meter (16). The hydrogen flow meter is shown in Plate II,

item 17. For detail of the meter, including the location of switches and adjustments see figure 3. Before the meter was turned on the mechanical zero position of the meter was checked and adjusted if need be with the screwdriver adjustment on the panel meter itself. The meter was turned on and, with the engine running on the Bosch System a small flow of hydrogen, in a range from .3 to .5 SCFM, was commenced. It was discovered, that to assure the accuracy of the calabration, this flow should continue for at least 15 to 20 minutes. The speed with which conditions in the transducer became stable seemed to be fairly independent of the rate of hydrogen flow - but it was imperative that some measurable flow did exist. After warmup the calibration procedure continued. The hose line leading from the transducer was pinched lightly shut with a pair of vice grips. To prevent damage to the hose from the jaws of the vice grips it was sandwiched between two small rectangles of sheet metal (Plate II, item 19). The "FUNCTION" switch was set to "CALIBRATE" and the 3 - position toggle switch to "BAL". If the meter read zero, and the last calibration seemed sensible, this was a good sign the warmup had been long enough. If the meter did not read zero, warmup with a small flow of hydrogen was continued for about 10 minutes. If the meter still did not read zero (this rarely happened as this particular adjustment seemed fairly invariant with time) the "BAL" screwdriver potentiometer was adjusted until the reading was zero. The 3 - position switch was positioned at "F.S." and the meter was adjusted to read full scale. The three - position toggle switch was then

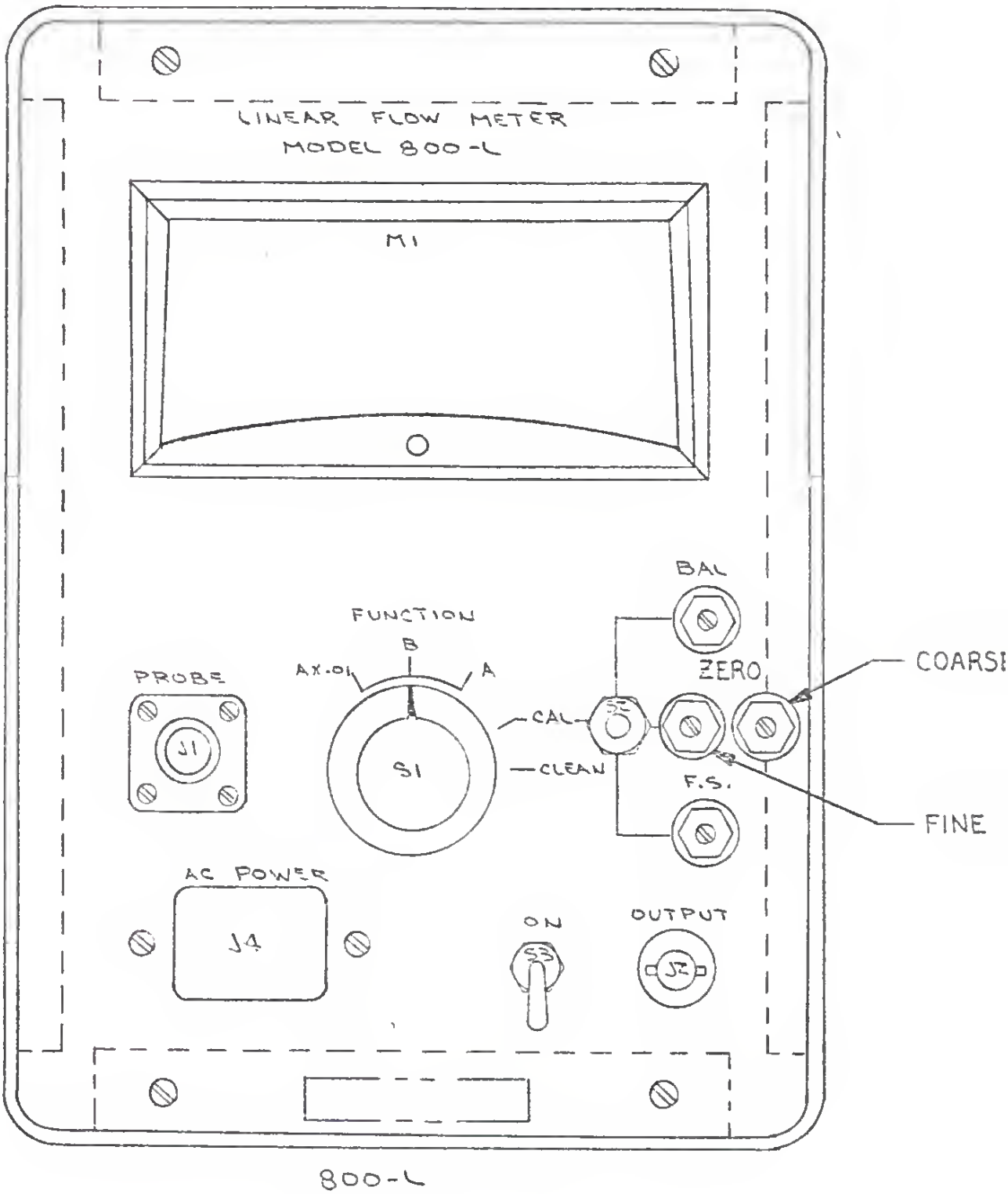

Figure 3. Hydrogen Flowmeter(from reference 16)

returned to its center position and the meter was adjusted to read zero using the "ZERO" and "FINE ZERO" adjustments. The hydrogen was then switched off with the hydrogen toggle switch and the vise grips were released. As a final step before shifting the engine to microprocessor control, the location in memory of the desired air - gasoline ratio, was loaded into the initialization program location 0228. The first location of the initialization program was selected and displayed, all switches on the interface circuit board (Plate II, item 7) were placed in the down (operate) mode and the "GO" button was pushed on the microprocessor. Now the engine was ready for operation on hydrogen - gasoline mixtures or gasoline alone, depending on the gasoline - air mixture selected.

Now switchover to microprocessor control was begun. Concurrently, a procedure called best torque was used to set the ignition timing for tests involving 100% gasoline, and a procedure called lean best torque was used to set the ignition timing and hydrogen flow in the rest of the tests.

Best torque and lean best torque procedures were used in an attempt to optimize ignition timing and fuel - air mixture for each set of hydrogen - gasoline mixtures and test parameters. Although operation could be achieved with the timing left stock for some of the hydrogen - gasoline mixtures it might not be the optimum ignition timing for that mixture, in essence "cheating" that mixture when compared

with the engine running under stock conditions. Furthermore, operation simply could not be obtained for some of the gasoline - hydrogen mixtures utilizing a high precentage of hydrogen, if the timing had not been changed without preignition and/or backfires resulting. The lean best torque procedure was used with hydrogen - gasoline mixtures (with hydrogen as the variable) in an attempt to optimize the fuel - air ratio and to follow a consistent pattern to obtain the desired hydrogen mixture. Operation could be obtained with any number of hydrogen mixtures; however, lean best torque enabled consistent hydrogen mixture selection, and this provided a basis for comparison between the various hydrogen - gasoline fuel mixtures. Furthermore lean best torque and best torque procedures are commonly used in the auto industry and by other I.C. engine researchers, making this study comparable to others. Lean best torque and best torque procedure were related to the author in a conversation with Mr. Walt Williams of Amoco Oil Company (19) and adapted by the author to this particular study. For the 100% gasoline cases, switchover to microprocessor control was obtained by merely moving the gasoline - air ratio control mode switch (Plate I, item 5), mounted on top of the Bosch system control box (Plate II, item 4), to the position marked "MICRO - P". The desired speed and torque was set, if it had not been previous to the switchover. Lean best torque (LBT) was found by first moving the distributor to a obviously retarded position, that is moving it until an obvious RPM drop occured. Then the timing was slowly advanced, with the throttle (Plate I, item 1) being closed to maintain approximately the desired speed. When no more RPM increase was

obtained by advancing the ignition timing, the timing was retarded slightly and process repeated to assure that the minimum spark advance was obtained. For gasoline - hydrogen mixtures the desired speed and torque was obtained for the higher torque in a somewhat different manner than for the lower two torques. In the tests that were conducted under the 43.4 ft-lbf load the engine was set at the desired speed and at an intermediate torque (approximately 25 ft-lbf) while operating on the Bosch system. Just prior to switchover the hydrogen mixture control (Plate I, item 2) was placed in a rich position, as determined by the judgement of the operator. The hydrogen toggle switch was moved to the "HYDROGEN" position, and the gasoline - air control mode switch was moved to "MICRO-P". After this, the torque was slowly increased to 43.4 ft-lbf and the speed kept constant by opening the throttle, all the while the operator was taking care to operate with a rich mixture. The procedure for tests taken at torques of 21.7 ft-lbf and 28.9 ft-lbf was the same except that the desired torque was set before switchover and there was no need for the load increase. Now in both cases the hydrogen mixture was leaned out, while closing the throttle to keep the speed constant. The mixture was leaned out until an RPM drop was noted. The mixture was then richened somewhat to prevent lean operation during RPM increases in the best torque procedure. The best torque condition was obtained in the same manner as described above for 100% gasoline except

when preignition was encountered. When preignition occured the ignition timing was retarded to a point considered safe (that is preignition would not reoccur) by the operator. This safe point was usually about 4^{o} retarded from the point preignition was encountered. After best torque was established, the mixture was leaned out to the minimum needed to sustain the desired engine speed.

After best torque or lean best torque conditions were obtained, the throttle and the hydrogen mixture valve were taped in place, the timing of the gasoline consumption was usually begun first and the following data were all taken during the fuel consumption test if time allowed. If time did not allow it, the data were obtained shortly before or after the gasoline consumption test. These data were: hydrogen flow rate, pressure drop across the air flow nozzle, exhaust gas thermocouple EMF, ignition timing, intake manifold vacuum, mass of fuel measured, and the time of test. Wet and dry bulb temperature were taken during one of the three tests run consecutively, for each set of operating conditions, if time allowed. If time did not allow it, the temperatures were taken just after the three tests. Atmospheric pressure was recorded after a number of operating condition sets were run. An operating condition set consisted of three or more consecutive tests run under the same operating conditions. The number of operating condition sets run were usually two to four before the atmospheric pressure was read. The

length of time involved was never more than an afternoon or evening's length of time. It was assumed atmospheric pressure could be regarded as constant for this length of time.

Chapter IV

Development of Equations

This chapter will present an explanation of the equations used to reduce the data taken in this study. Actual data reduction was done with a Hewlett - Packard 29C programmable calculator. A print out of this program is included in Appendix B. The equations will be presented in the order they appear in the two programs, hence, the programs will essentially be "stepped through". The programs are divided in two, only because of the limitation of program steps imposed by the calculator. Program 2 should be viewed as a logical extension of Program 1.

First the gasoline consumption in lbm per hr was calculated.

$$\text{Gasoline Consumption (lbm/hr)} = \frac{\text{Known Mass Placed on Scale (lbm)}}{\text{Time in Which This Mass was Consumed (sec)}} \times 3600 \left(\frac{\text{sec}}{\text{hr}}\right) \quad (1)$$

The hydrogen consumption calculation was a bit more complicated.

$$\text{Hydrogen Consumption (lbm/hr)} = \frac{\text{SCFM (air equivalent)}}{.141 \left(\frac{\text{SCFM air}}{\text{SCFM hyd.}}\right)} \times 5.612 \times 10^{-3} \left(\frac{\text{lbm}}{\text{ft}^3}\right) \times 60 \left(\frac{\text{min}}{\text{hr}}\right) \quad (2)$$

SCFM is "standard cubic feet per minute". One standard cubic foot of air is that volume whose weight is equal to the weight of one cubic foot of air when the pressure is 29.92" Hg and the temperature is 15^{o}C (16). Since the meter was calibrated

SCFM of air, a conversion factor (.141) had to be applied to obtain SCFM hydrogen. The density of hydrogen (5.612×10^{-3} lbm/ft^3) was found in reference 22.

Power output was calculated with the equation:

$$\text{Power Output (hp)} = \frac{\text{Torque (ft-lbf)} \times \text{RPM}\left(\frac{\text{rev}}{\text{min}}\right) \times 2\pi\left(\frac{\text{radians}}{\text{rev}}\right)}{33000\left(\frac{\text{ft-lbf}}{\text{min}} \Big/ \text{hp}\right)} \quad (3)$$

Brake specific fuel consumption were calculated with the equation:

$$\text{BSFC}\left(\frac{\text{lbm}}{\text{hp-hr}}\right) = \frac{\text{Gasoline Consumption}\left(\frac{\text{lbm}}{\text{hr}}\right) + \text{Hydrogen Consumption}\left(\frac{\text{lbm}}{\text{hr}}\right)}{\text{Power Output (hp)}} \quad (4)$$

Thermal efficiency was calculated using the lower heating value of hydrogen from reference 23. The lower heating value of the gasoline was obtained by measuring its specific gravity (API). Reference 24 was used to reduce the observed specific gravity to that at 60^{o}F. In reference 25 a formula was found to calculate the lower heating value if the specific gravity (d) was known.

$$Q_{LVH} = (22{,}320 - 3{,}780d^2) - 90.8(26-15d) \quad (5)$$

After determining the above, the thermal efficiency could be found using the following equation:

$$N_{th} = \frac{\text{Power Output (hp)} \times 2545.1\left(\frac{\text{BTU}}{\text{hp - hr}}\right)}{\text{Gasoline Consumed}\left(\frac{\text{lbm}}{\text{hr}}\right) \times 19000\left(\frac{\text{BTU}}{\text{lbm}}\right) + \text{Hydrogen Consumed}\left(\frac{\text{lbm}}{\text{hr}}\right) \times 51623\left(\frac{\text{BTU}}{\text{lbm}}\right)} \quad (6)$$

Even though it is customary to use the higher heating value (HHV) of a fuel in thermal efficiency calculations (27), lower heating values (LHV) were used in this study for

three reasons.

First, this was done to facilitate comparison of this study to reference 18. Second, it was believed the LHV represented a more realistic measure of the heat available in the fuels, since it was doubted that condensation occured during the expansion stroke in the engine. Finally, although Obert (27) advocates the use of HHV he also states that LHV is "invariably" used in thermal efficiency calculations involving gaseous fuels. The hydrogen mixed with the gasoline in the tests run for this study was gaseous. If this study is to be compared with others, caution is urged in observing thermal efficiencies and note should be taken whether LHV or HHV is used.

In order to calculate air mass flow, air density and standard density pressure drop across the flow nozzle had to be calculated first. The density equation is taken from reference 26.

$$\text{Density}\left(\frac{\text{lbm}}{\text{ft}^3}\right) = .491\left(\frac{\text{lbf/in}^2}{\text{in-Hg}}\right) \times \text{Atmospheric Pressure (in-Hg)} - .38\left\{\begin{matrix}\text{Pressure of Saturated Vapor @ } T_{\text{wet bulb}} \left(\frac{\text{lbf}}{\text{in}^2}\right) - \left[.491\left(\frac{\text{lbf/in}^2}{\text{in-Hg}}\right) \times \text{Atm Press (in-Hg)} \times \left(T_{\text{wet bulb}}(^{\circ}\text{F}) - T_{\text{wet bulb}}(^{\circ}\text{F})\right)\right] \div 2700\end{matrix}\right\}$$

$$\frac{}{53.34\left(\frac{\text{ft-lbm}}{\text{lbm-}^{\circ}\text{R}}\right) \div 144(\text{in}^2/\text{ft}^2) \times \left[T_{\text{dry bulb}}{}^{\circ}\text{F} + 459.6^{\circ}\text{R}\right]} \qquad (7)$$

The pressure of saturated water vapor at $T_{\text{wet bulb}}$ was obtained from the steam tables. Note that $53.34\left(\frac{\text{ft-lbf}}{\text{lbm-}^{\circ}\text{R}}\right)$ is the gas constant for air.

$$\text{Standard Density Pressure Drop} = \frac{(\text{Measured Drop Across Flow Nozzle})\ (.075)}{(\text{Density})} \quad (8)$$

Now the CFM of air flow could be calculated. In the preparation of reference 18, Mr. Walt Williams performed a calibration procedure on the 1.59 in. (4.04 cm) nozzle and the result was equation 11 in reference 18. It was later found that this equation was somewhat in error (28). The corrected equation, used in this study was:

$$\text{air flow } \left(\text{ft}^3/\text{min}\right) = 59.868 \left[\text{Standard Density Pressure Drop Across the Flow Nozzle}\right]^{.5} \quad (9)$$

The air mass flow was calculated with the relationship:

$$\text{Air Mass Flow Rate } \left(\frac{\text{lbm}}{\text{hr}}\right) = \text{Air Flow}\left(\frac{\text{ft}^3}{\text{min}}\right) \times \text{Density}\left(\frac{\text{lbm}}{\text{ft}^3}\right) \times 60\left(\frac{\text{min}}{\text{hr}}\right) \quad (10)$$

The theoretical maximum air intake was computed from:

$$\text{Theoretical Maximum Air Intake} = \frac{96.6}{2}\left(\frac{\text{in}^3}{\text{rev}}\right) \times \frac{\text{RPM}\left(\frac{\text{rev}}{\text{min}}\right)}{1728\left(\frac{\text{in}^3}{\text{ft}^3}\right)} \times \text{Density}\left(\frac{\text{lbm}}{\text{ft}^3}\right) \times 60\left(\frac{\text{min}}{\text{hr}}\right) \quad (11)$$

Then the value from equation 10 could be divided by the value from equation 11 to obtain volumetric efficiency.

$$N_v = \frac{\text{Air Mass Flow Rate}}{\text{Theoretical Maximum Air Mass Flow}} \quad (12)$$

Values from equations 1, 2 and 10 were used to calculate the air fuel ratio.

$$\text{Air-Fuel Ratio} = \frac{\text{Air Mass Flow Rate}\left(\frac{\text{lbm}}{\text{hr}}\right)}{\text{Gasoline Consumption}\left(\frac{\text{lbm}}{\text{hr}}\right) + \text{Hydrogen Consumption}\left(\frac{\text{lbm}}{\text{hr}}\right)} \quad (13)$$

Likewise the air - gasoline ratio was calculated from equations 1 and 10.

$$\text{Air - Gasoline Ratio} = \frac{\text{Air Mass Flow Rate} \left(\frac{\text{lbm}}{\text{hr}}\right)}{\text{Gasoline Consumption} \left(\frac{\text{lbm}}{\text{hr}}\right)} \tag{14}$$

Chapter V

Presentation of Results

Data reduced by the equations presented in the last chapter yielded the quantities to be discussed in this chapter. These quantities were plotted on the graphs that follow in this chapter.

The first quantity to be discussed is the air-gasoline ratio. The air-gasoline ratio was governed by the KIM - 1 and related control system. A detailed analysis of the control system will not be given here, for reasons mentioned earlier, but a few trends in the air-gasoline ratio will be pointed out. For the torque settings of 21.7 ft-lbf, 28.9 ft-lbf and 43.4 ft-lbf the air-gasoline ratio is shown in Figures 4, 5 and 6 respectively. For a base, 14:1 was used for 100% gasoline mixtures. Hence the desired ratio for 80% gasoline was 17.5:1, for 60% it was 23.3:1, for 50% it was 28:1 and for 40% gasoline the desired ratio was 35:1. The ratios were all fairly close to the desired, but there were some deviations, and the curves seemed to have a "hyperbolic" shape. The reason for this "hyperbolic" shape is not known. Although it would have been desirable for the curves to be more of a straight line and closer to the desired, it should be mentioned that the various air-fuel ratios showed good separation and were free from wild fluctuations.

Air-fuel ratio was dependent on the KIM 1 control system and

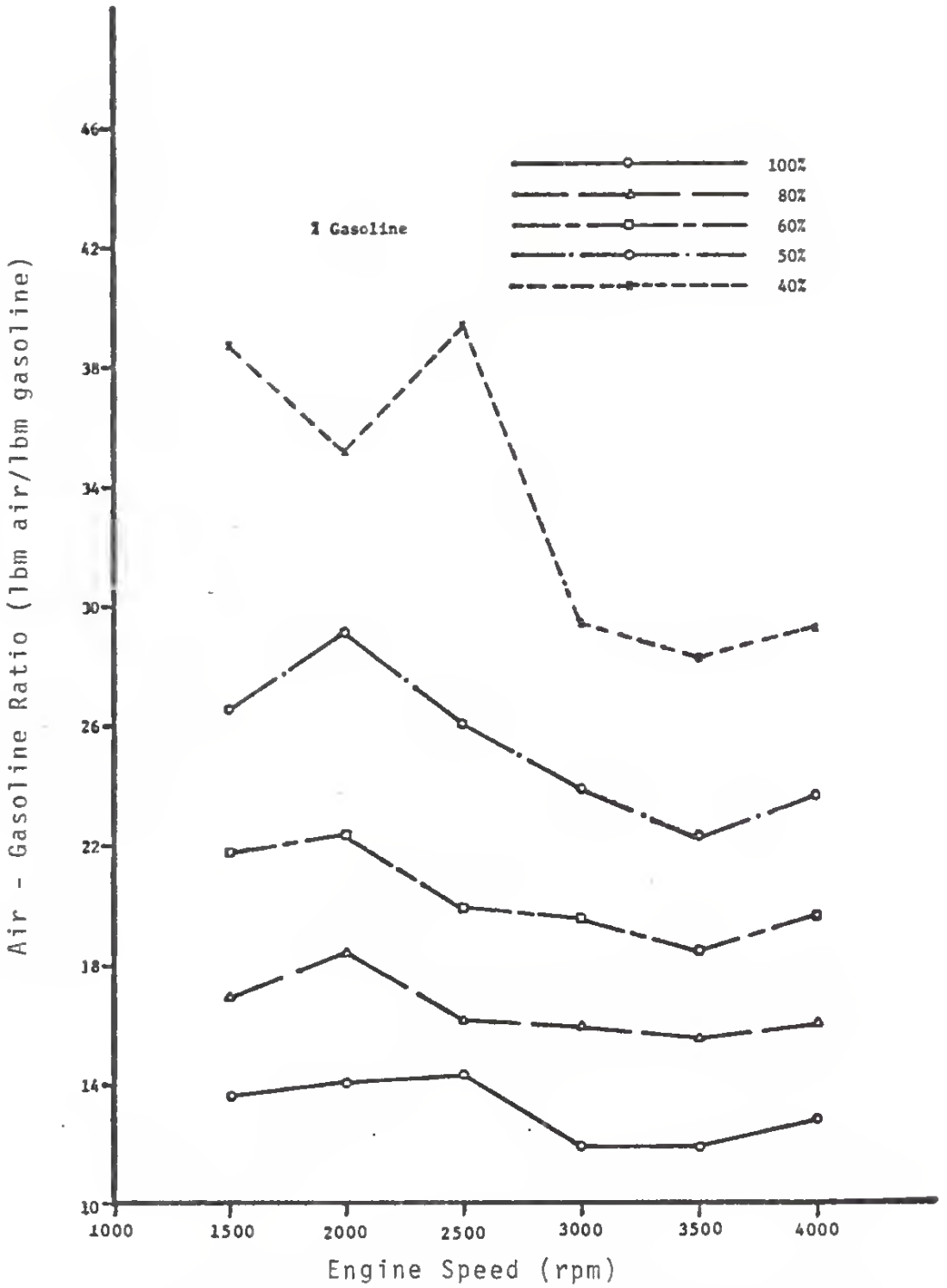

Figure 4 Air - Gasoline Ratio at 21.7 ft-lbf Torque as a Function of Engine Speed and Per Cent Gasoline

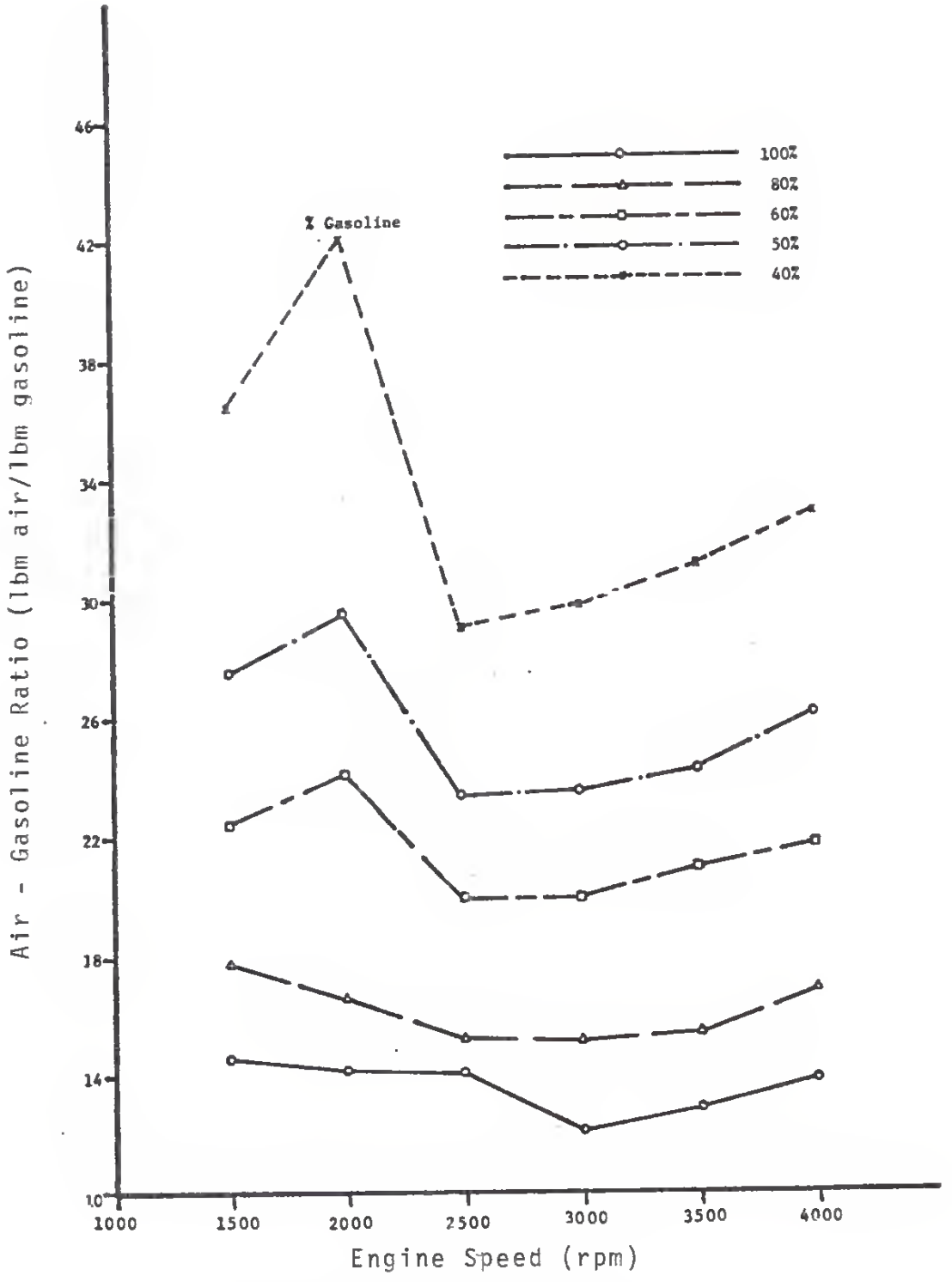

Figure 5 Air - Gasoline Ratio at 28.9 ft-lbf Torque as a Function of Engine Speed and Per Cent Gasoline

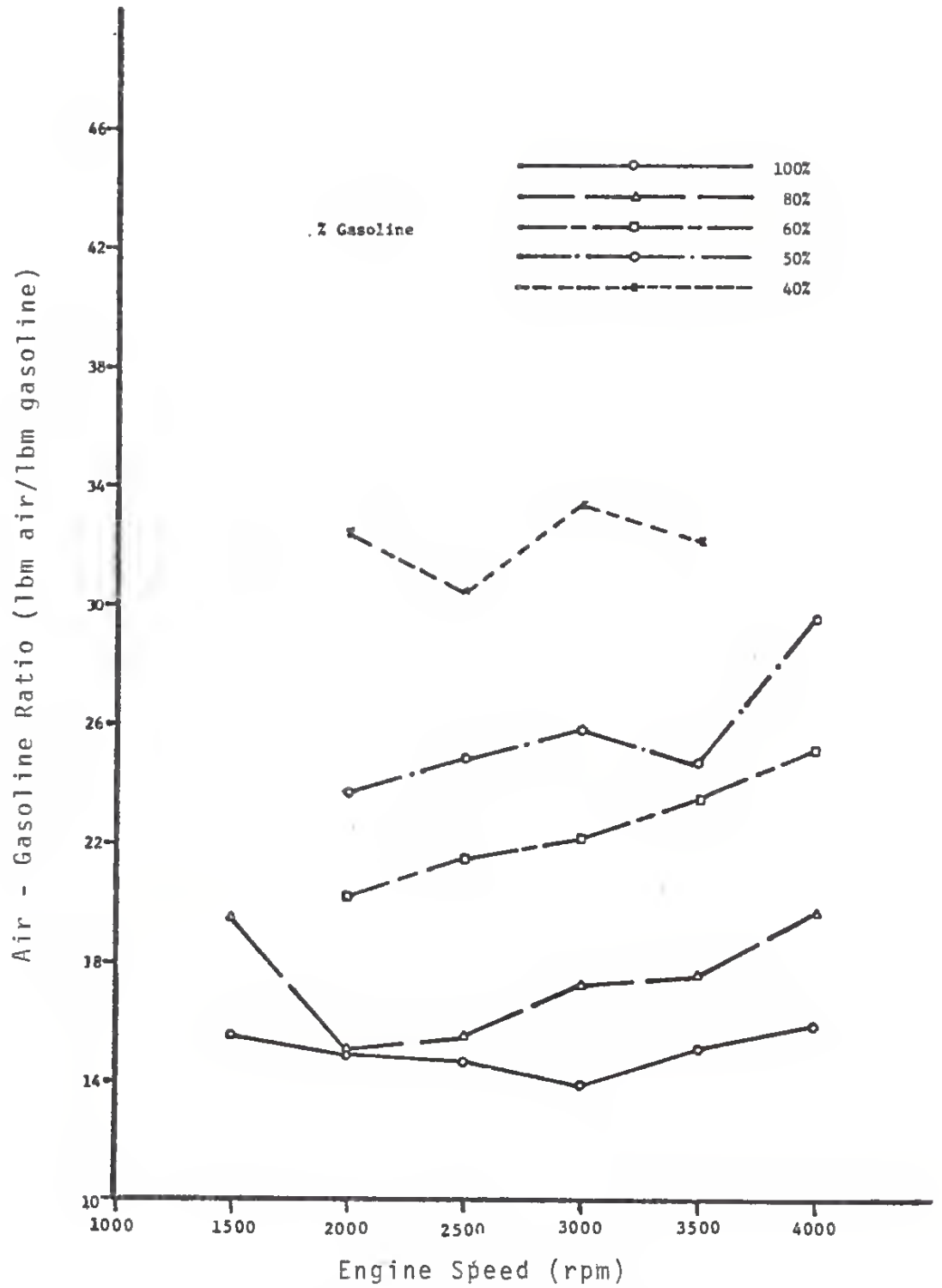

Figure 6 Air - Gasoline Ratio at 43.4 ft-lbf Torque as a Function of Engine Speed and Per Cent Gasoline

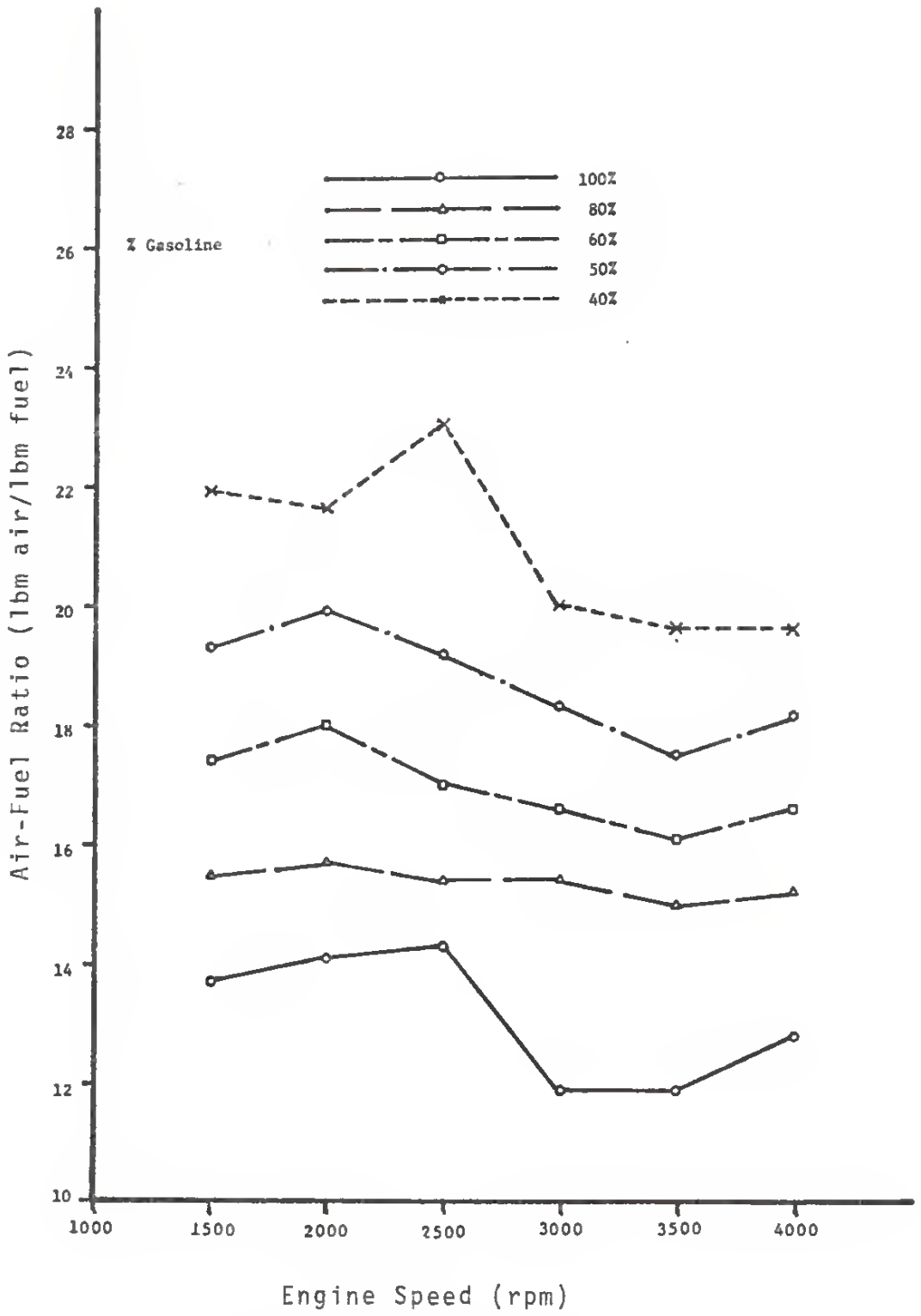

Figure 7 Air-Fuel Ratio at 21.7 ft-lbf Torque as a Function of Engine Speed and Per Cent Gasoline

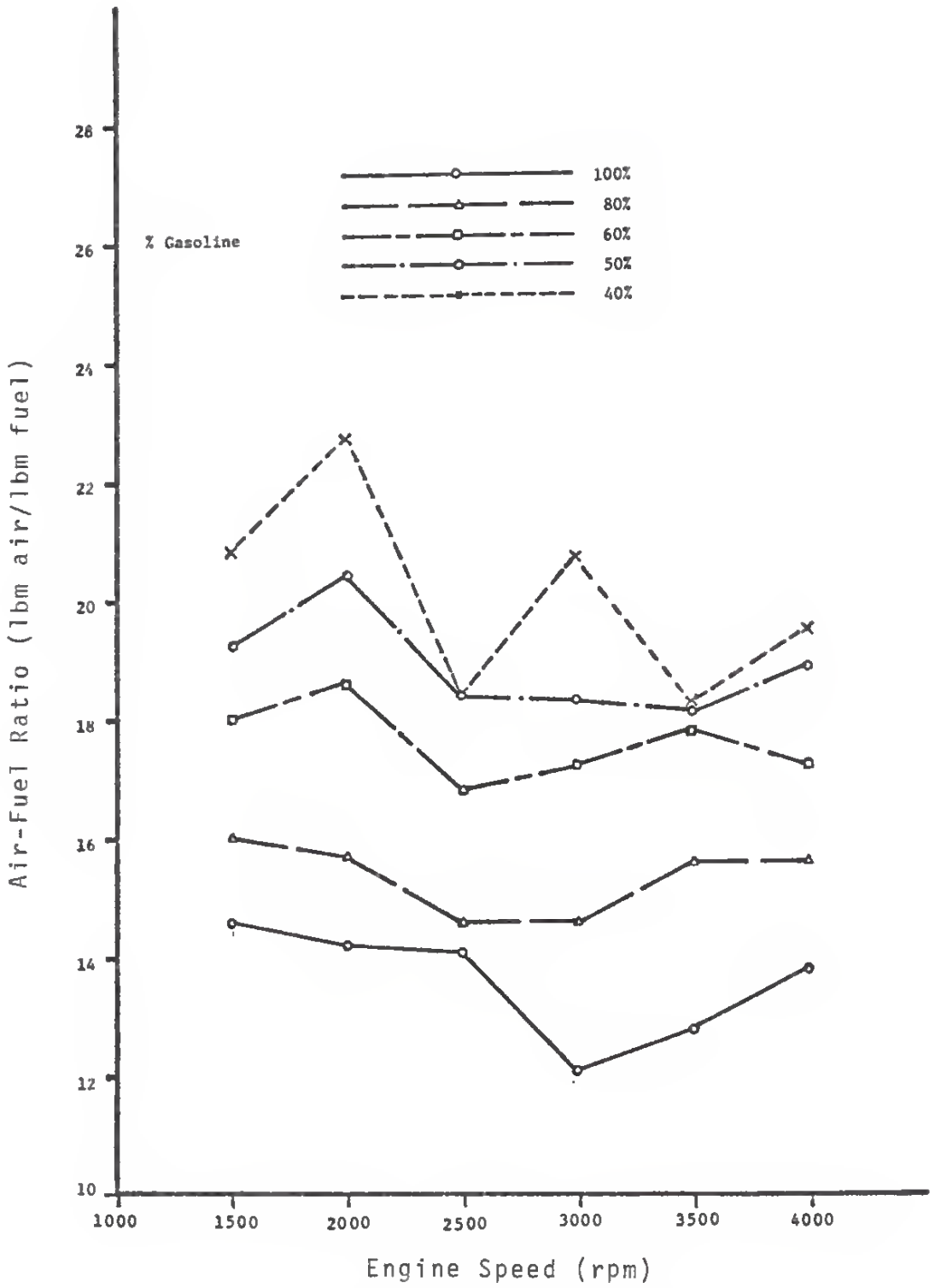

Figure 8 Air-Fuel Ratio at 28.9 ft-lbf Torque as a Function of Engine Speed and Per Cent Gasoline

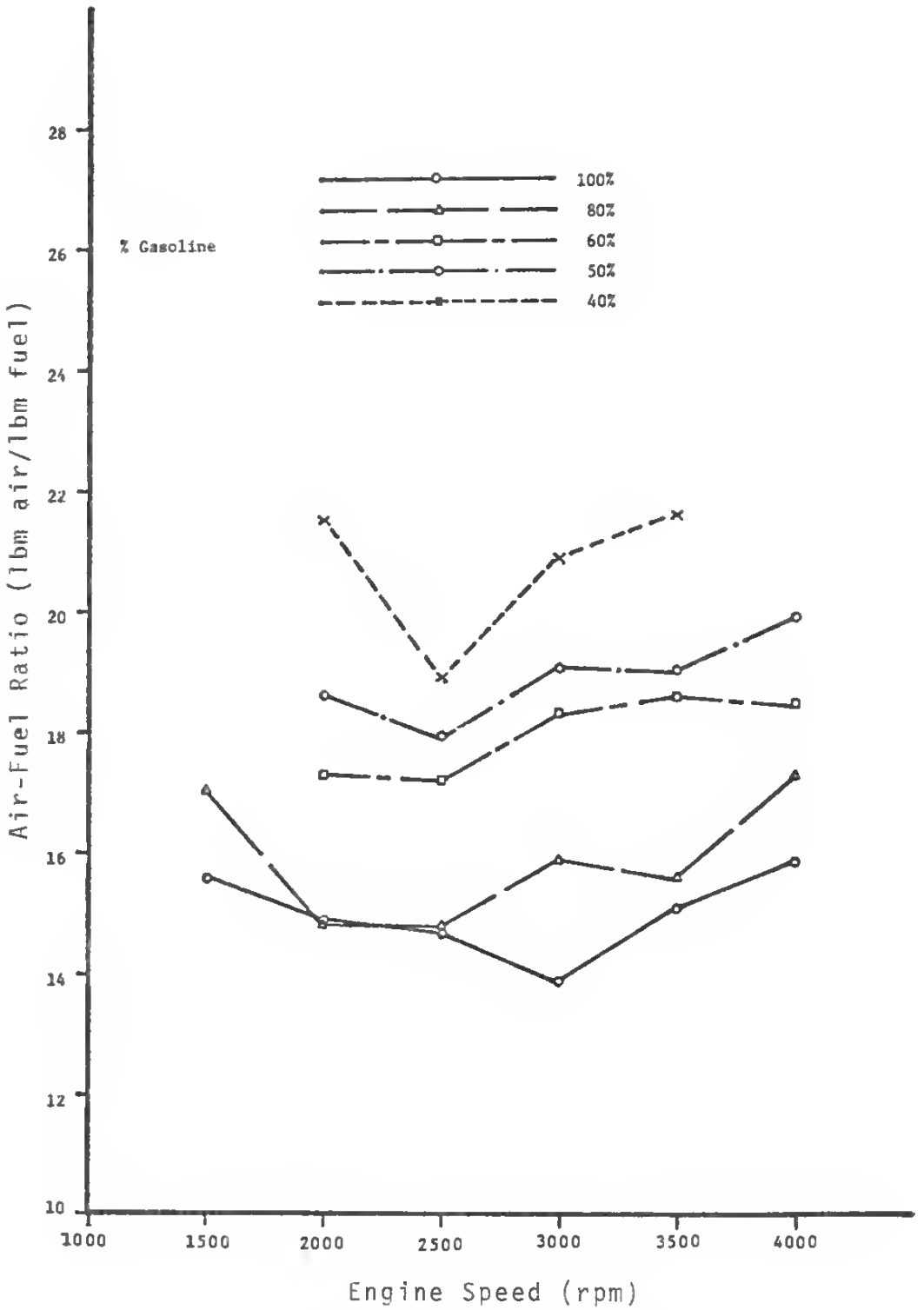

Figure 9 Air-Fuel Ratio at 43.4 ft-lbf Torque as a Function of Engine Speed and Per Cent Gasoline

on the operator's ability to select the correct hydrogen flow. Air-fuel ratios that occured in the 21.7 ft-lbf torque tests are plotted in figure 7 for 21.7 ft-lbf, in figure 8 for 28.9 ft-lbf, and in figure 9 for 43.4 ft-lbf. The smoothness and separation as well as the linearity of the air-fuel ratio lines seemed to support the contention that the LBT procedure was an effective way to obtain consistent air-fuel ratios for a given speed, torque and percentage gasoline. The curves get a bit close at 2,000 and 3,000 rpm with torques of 28.9 ft-lbf and at 2,000 and 2,500 rpm with a torque of 43.4 ft-lbf. However, for a process so dependent upon operator ability, the air-fuel ratio seemed to be satisfactorily controlled.

The curves in figures 10, 11 and 12 represent the trends in intake manifold vacuum. Note that the verticle scale in Figure 12 differs from that in Figures 10 and 11. Two trends that are normal in IC engines can be noted in these curves, regardless of fuel. It can be seen that intake vacuum decreased with speed and load. This occured when the throttle was opened and the manifold pressure increased to provide more air to the cylinders. Two peculiar trends can also be noted, regardless of the fuel. One trend is the comparatively low vacuum at 1500 rpm. This was probably due to the lack of the intake stream momentum effect at low speeds. As the intake stream velocity increases some ram effect occurs from the momentum carried by the air stream. A high intake manifold pressure, obtained by opening the throttle valve, was needed to provide enough air to

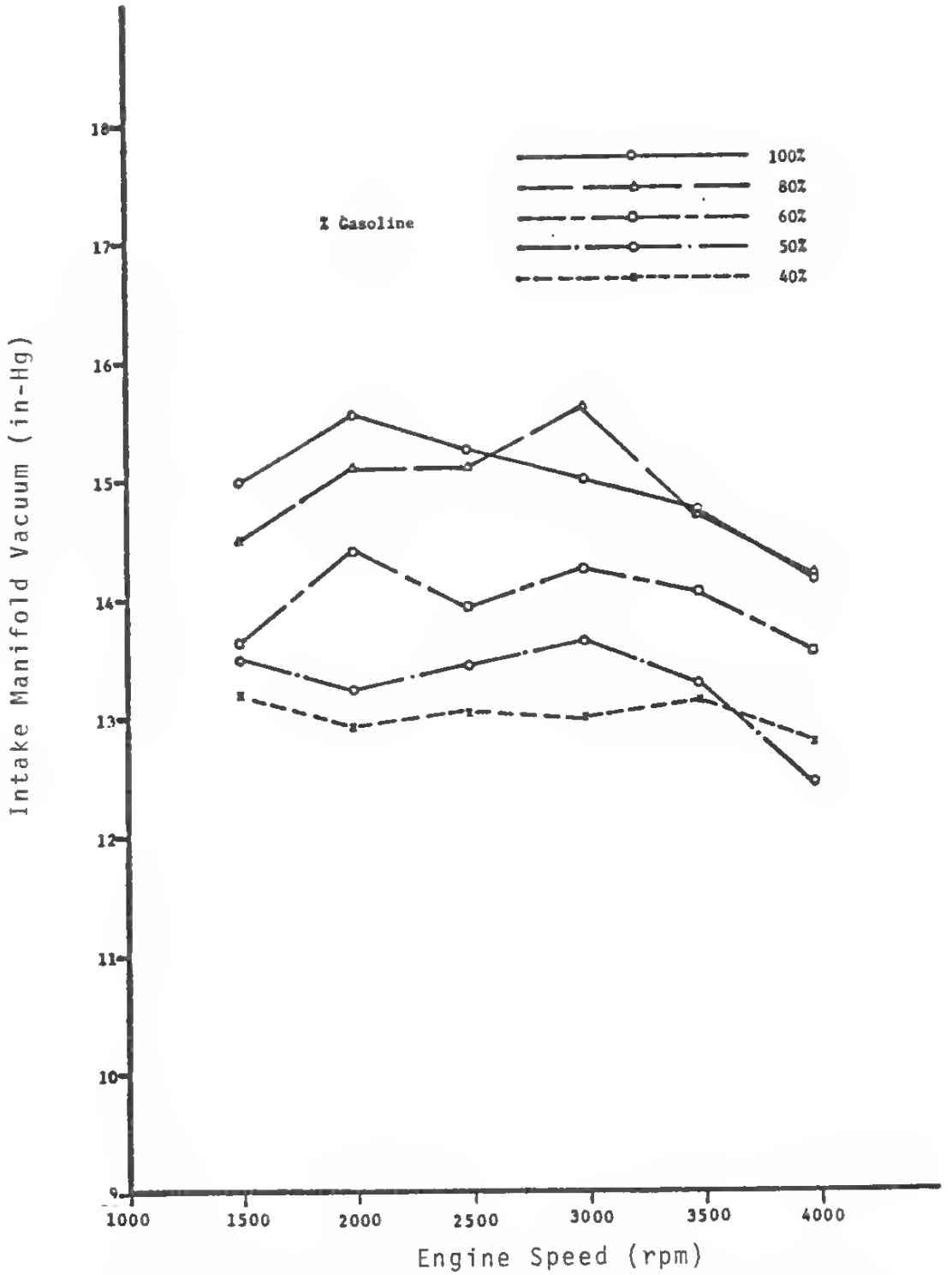

Figure 10 Intake Manifold Vacuum at 21.7 ft-lbf Torque as a Function of Engine Speed and Per Cent Gasoline

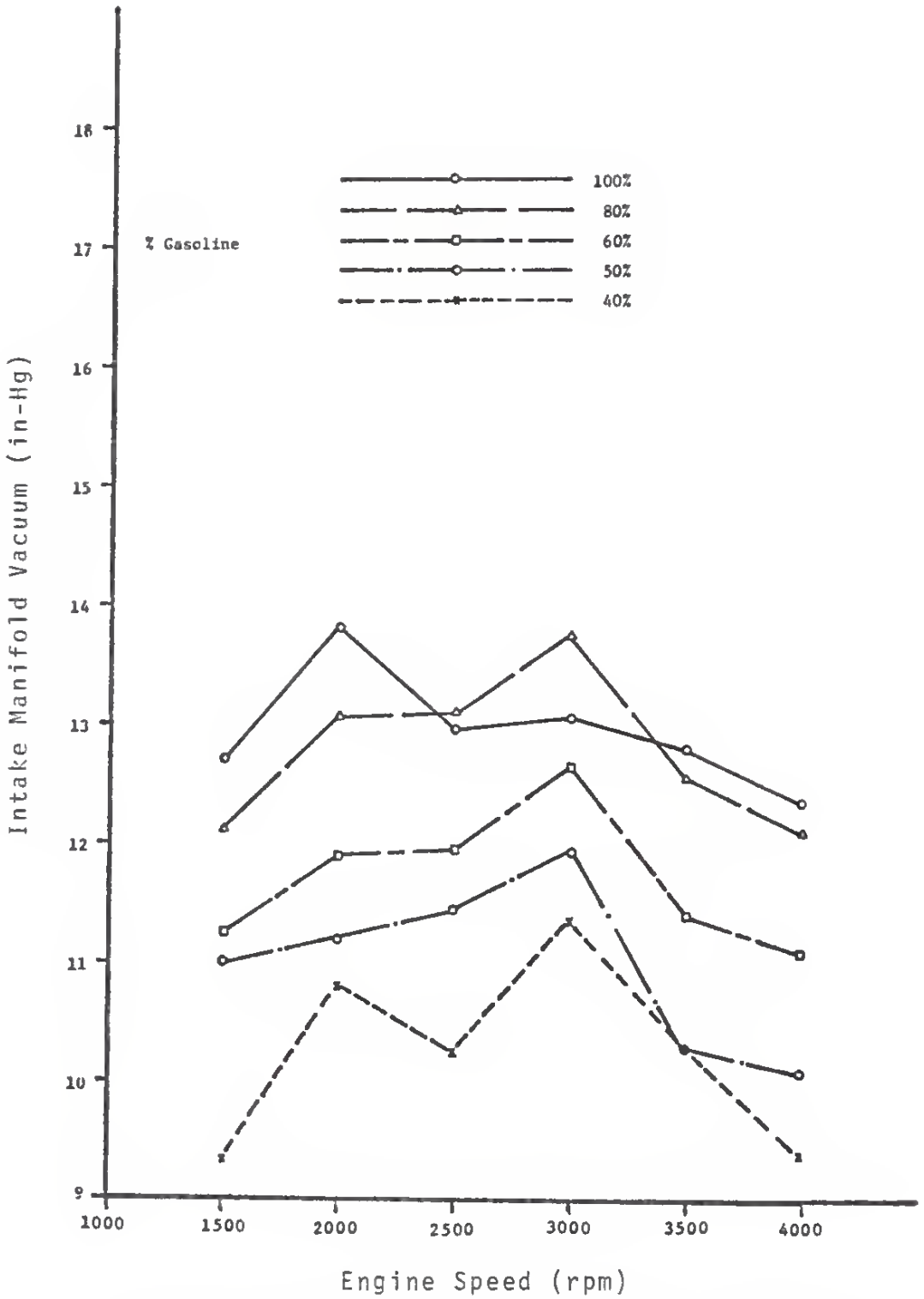

Figure 11 Intake Manifold Vacuum at 28.9 ft-lbf Torque as a Function of Engine Speed and Per Cent Gasoline

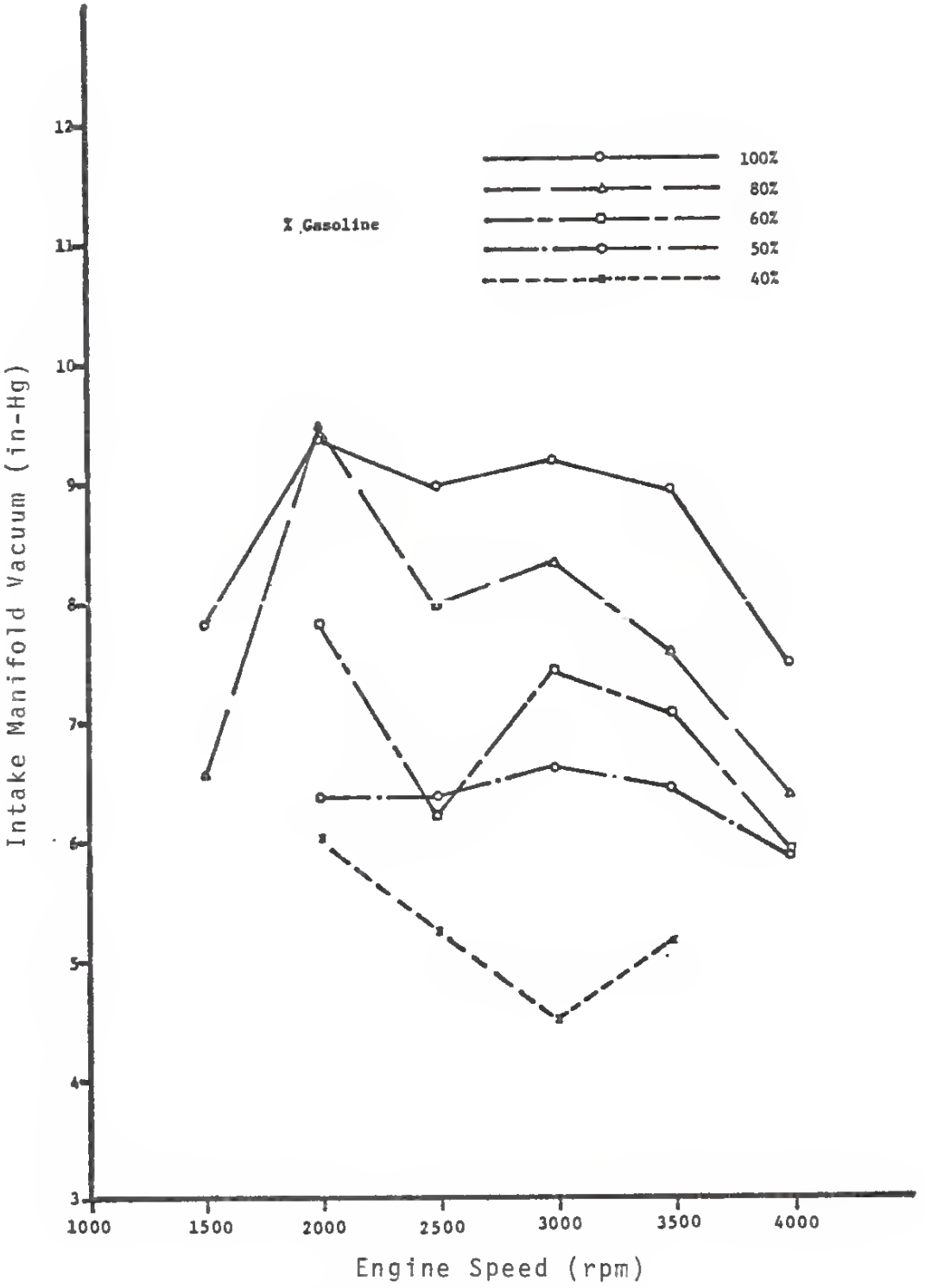

Figure 12 Intake Manifold Vacuum at 43.4 ft-lbf Torque as a Function of Engine Speed and Per Cent Gasoline

the cylinders. A second trend is not so easy to explain, that is the peculiar "dip" in manifold vacuum that occured at 2500 rpm. It can only be speculated that inlet dynamics peculiar to this engine at this speed caused this "dip". There could have been some sonic disturbance wave at this rpm that impeded inlet flow and necessitated raising the manifold pressure. The trend that occured as the hydrogen portion of the fuel was increased was, in general, as expected. As the hydrogen portion of the fuel was increased, this gaseous fuel displaced more and more of the air flow in the manifold passages. To compensate, the throttle was opened to provide more manifold pressure, and hence more air to the cylinders.

Volumetric efficiency is shown in figures 13, 14 and 15. Note that the verticle scale for the last graph differs from the verticle scale of the first two graphs. Volumetric efficiency also exhibited two trends common in spark ignition IC engines. It can be seen from the graphs that volumetric efficiency increased with speed and load. Volumetric efficiency usually increases with speed (due to the momentum ram effect discussed) until a point is reached where fluid friction losses become greater than the gain from the momentum ram effect. Apparently this point was not reached with this engine as the curves show a steady increase with speed. This was probably due to the fact that these were only partial load tests, and the manifold flow was far enough below maximum that this trend did not set in. Volumetric efficiency increased with load due to the fact that

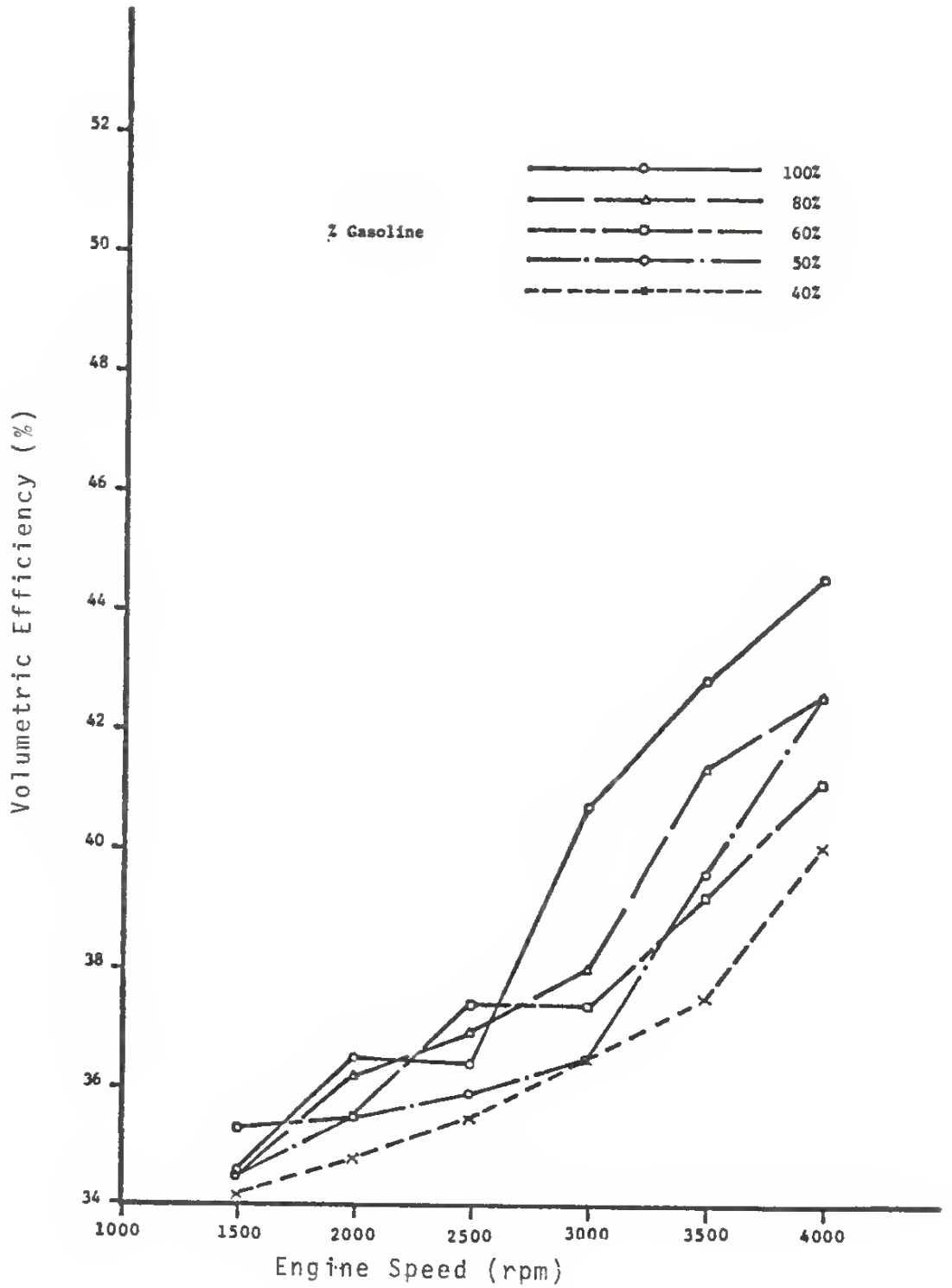

Figure 13 Volumetric Efficiency at 21.7 ft-lbf Torque as a Function of Engine Speed and Per Cent Gasoline

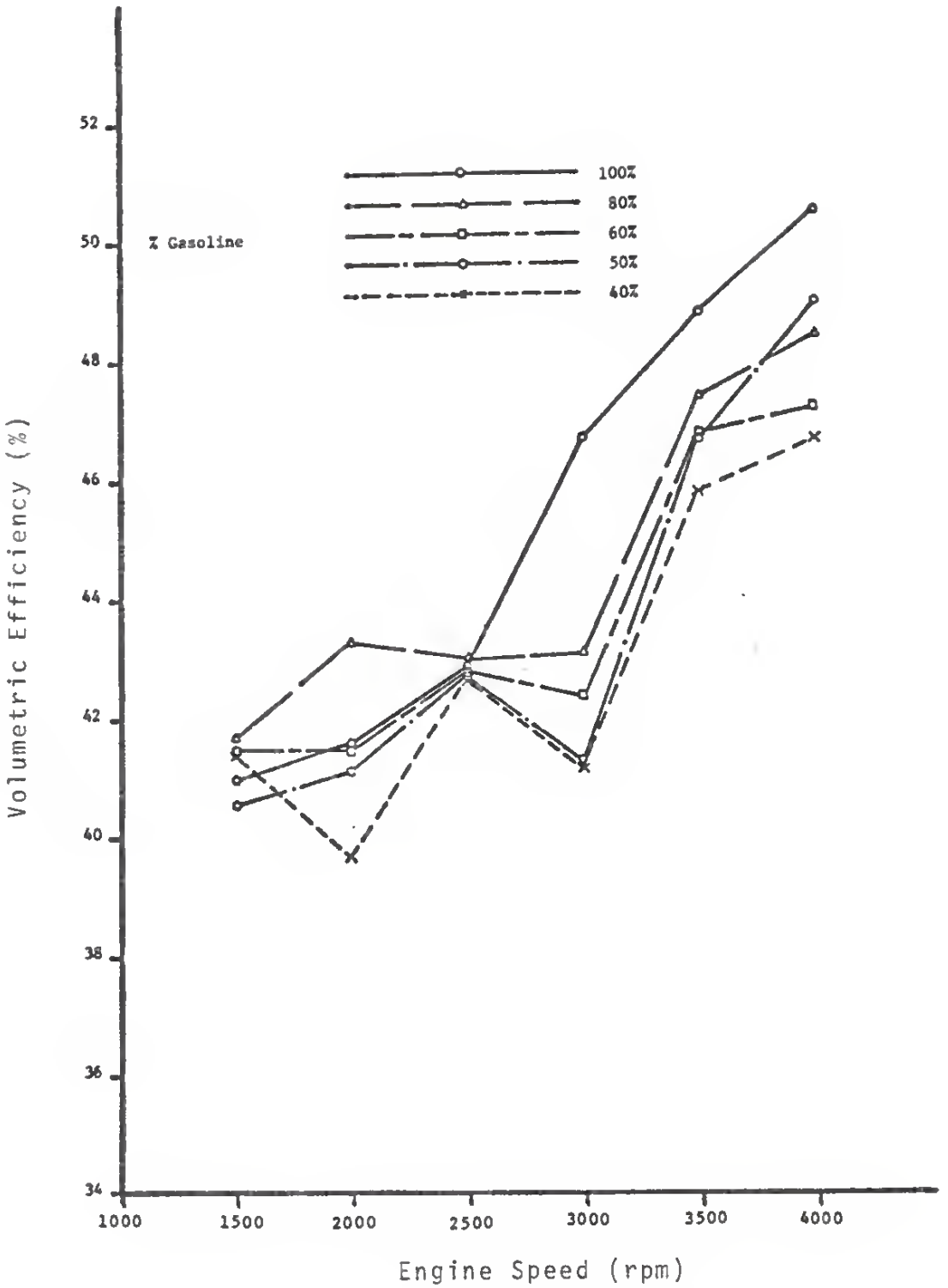

Figure 14 Volumetric Efficiency at 28.9 ft-lbf Torque as a Function of Engine Speed and Per Cent Gasoline

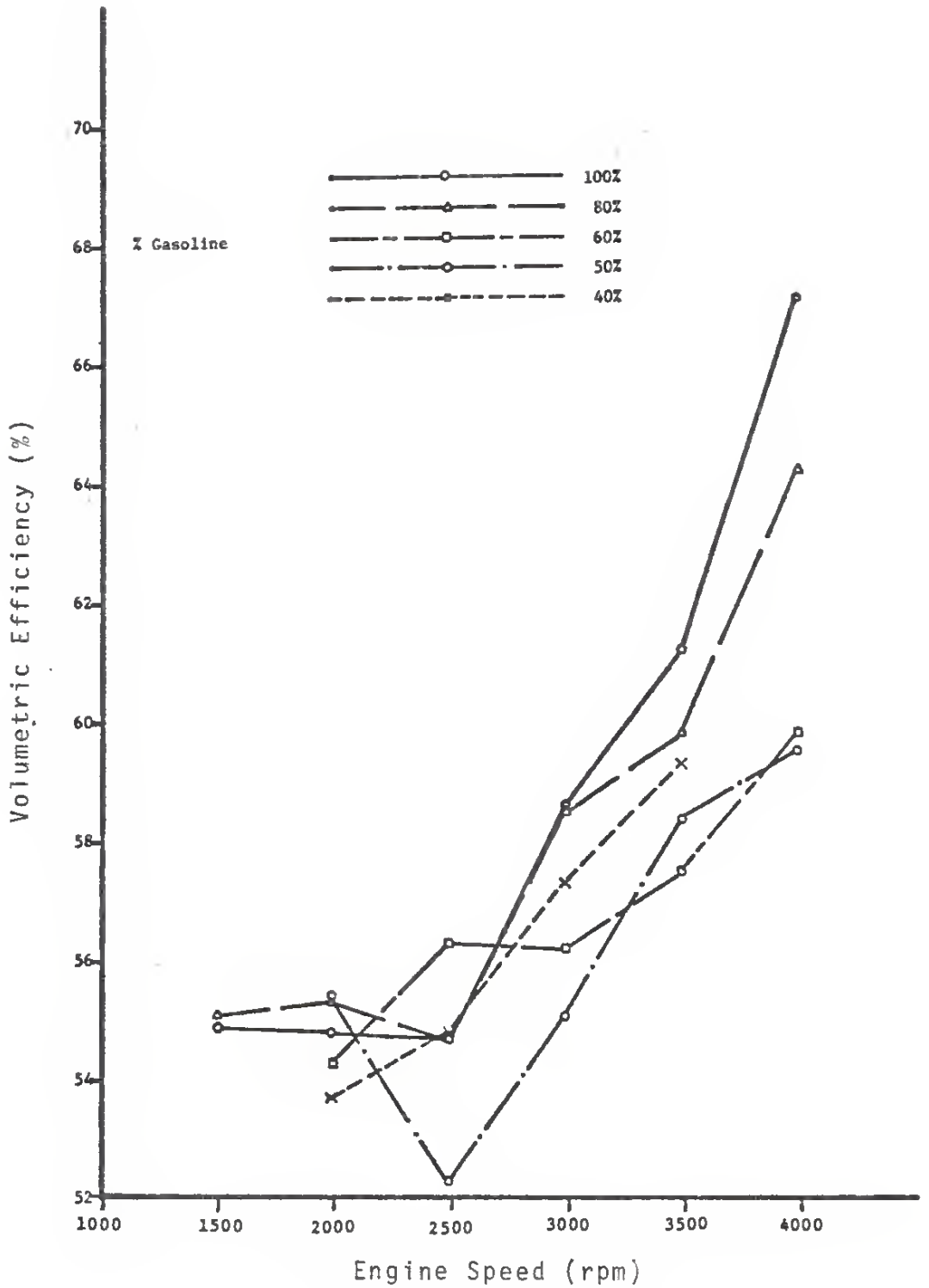

Figure 15 Volumetric Efficiency at 43.4 ft-lbf Torque as a Function of Engine Speed and Per Cent Gasoline

as the throttle was opened to permit a greater load (at constant speed) the pressure drop across the throttle plate decreased, increasing volumetric efficiency. One curious occurence in volumetric efficiency can be found in the 28.9 ft-lbf torque graph at 2500 rpm. Here the volumetric efficiency values seem to be abnormally "clustered" together. It is conjectured that this occurance was caused by the same circumstances that caused the "dip" in manifold vacuum at this point. However it is difficult to explain then, why this behavior was absent from the other two torque settings. In general, as the proportion of hydrogen in the fuel mixture increased, volumetric efficiency decreased. As the hydrogen displaced air in the fixed manifold volume, the throttle was opened to compensate. This increased the speed and density of the air which increased the losses due to fluid friction.

This exhaust gasoline temperature shown in figures 16, 17 and 18 tended to increase with speed and load. This was expected. As the speed was increased less time was available for heat transfer to the walls of the combustion chamber and the exhaust temperature rose accordingly. Compounding the effect was the fact that as speed was increased with a given torque, power output was increased. More fuel and air was being burned per unit time to increase the output. Again, less heat, as a per cent of the total, could be transfered through the cylinder walls and the exhaust temperature rose, and more heat was transfered by the exhaust stream. The same phenomenon took place as the

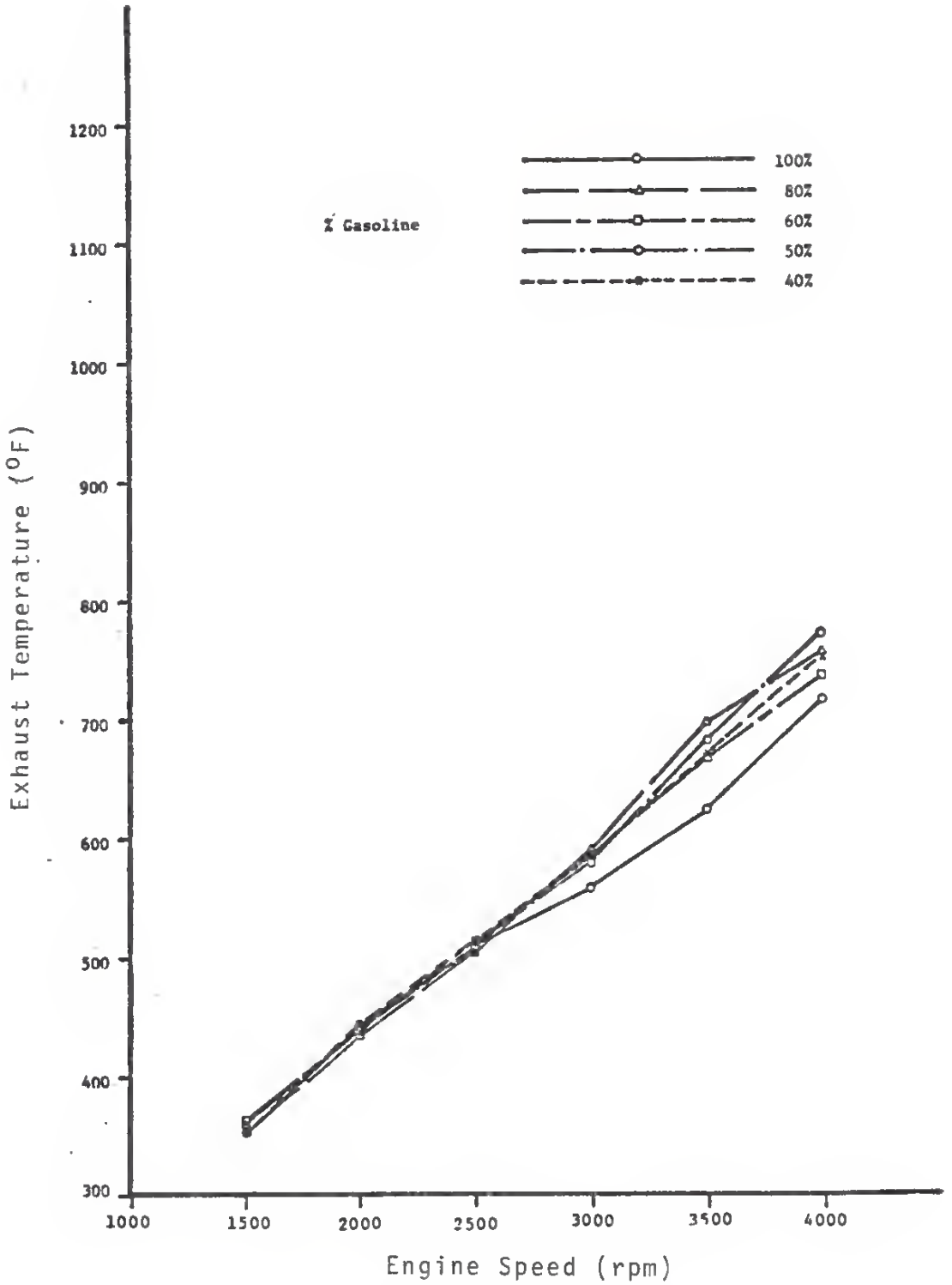

Figure 16 Exhaust Temperature at 21.7 ft-lbf Torque as a Function of Engine Speed and Per Cent Gasoline

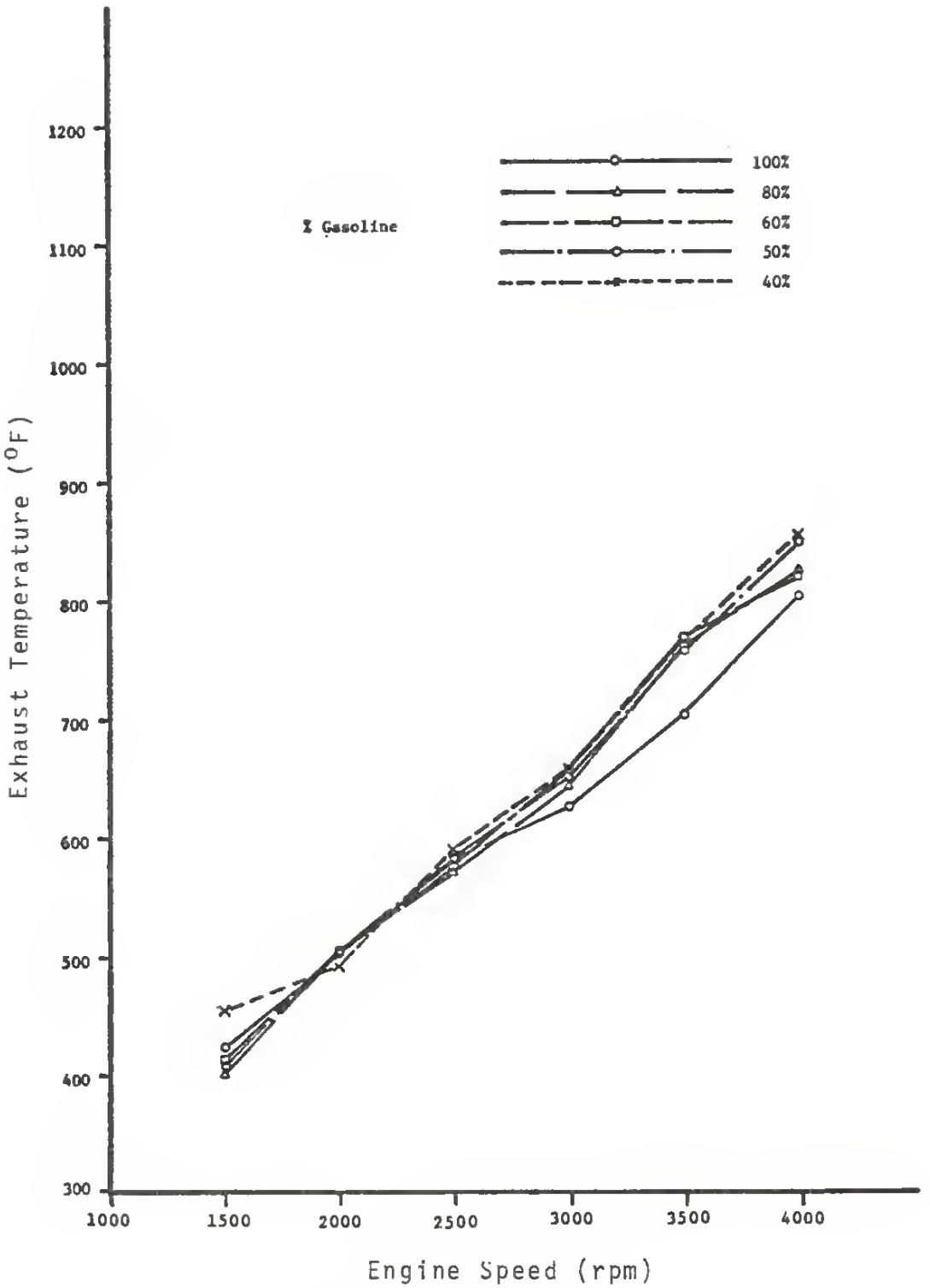

Figure 17 Exhaust Temperature at 28.9 ft-lbf Torque as a Function of Engine Speed and Per Cent Gasoline

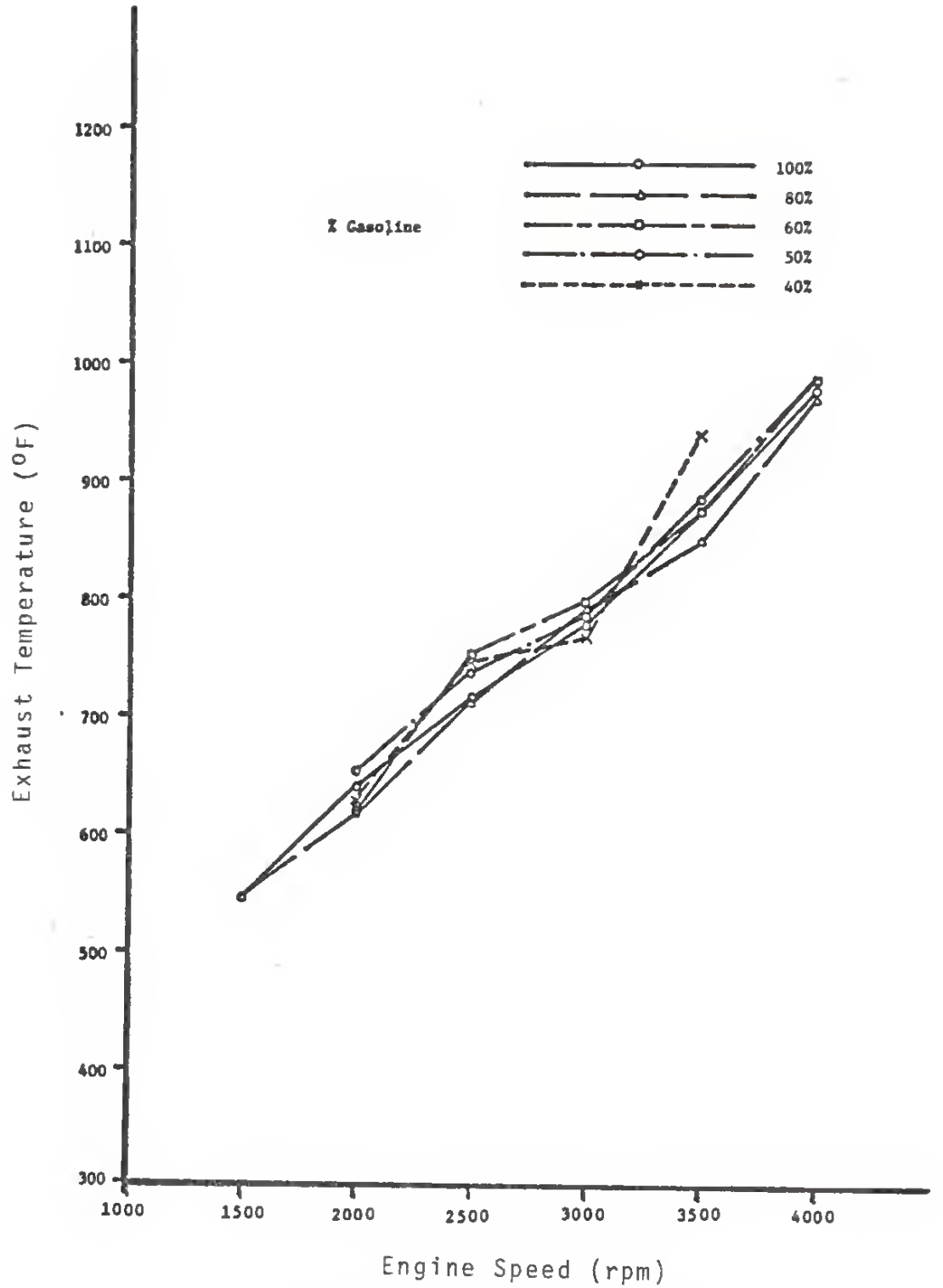

Figure 18 Exhaust Temperature at 43.4 ft-lbf Torque as a Function of Engine Speed and Per Cent Gasoline

load was increased. It was expected that as the proportion of gasoline in the fuel decreased and the cooling effect of the heat of vaporization of the gasoline decreased along with it, the exhaust temperature would rise. While this trend did appear to a small degree, more significant perhaps was the lack of any alarming temperature increases with increasing hydrogen. There certainly were no equipment-threatening temperatures. In fact the greatest temperature experienced at a given speed and torque was rarely more than 50°F greater than the temperature experienced with 100% gasoline and never more than 100°F greater. One note of caution should be interjected however, in that these tests all took place substantially below full power and temperatures could exceed safe values if the load was increased. Oespite the general trend of increasing temperature with increasing hydrogen proportion of fuel, there were many small deviations from this trend. These deviations were probably caused by slight deviations from the desired fuel-air ratio, which in turn caused these deviations in the exhaust gas temperature.

Brake specific fuel consumption, shown in figures 19, 20 and 21 decreased as the proportion of hydrogen in the fuel increased. The more obvious reason for this was the high heat content per pound of hydrogen. Whether this gain in BSFC would be enough to offset the volume disadvantage of hydrogen cannot be determined by this study, but in the author's opinion, in light of the studies discussed in the literature review, it would not. As an example, it can be generally said that is BSFC at 40% gasoline is just a little over half that of 100% gasoline. However,

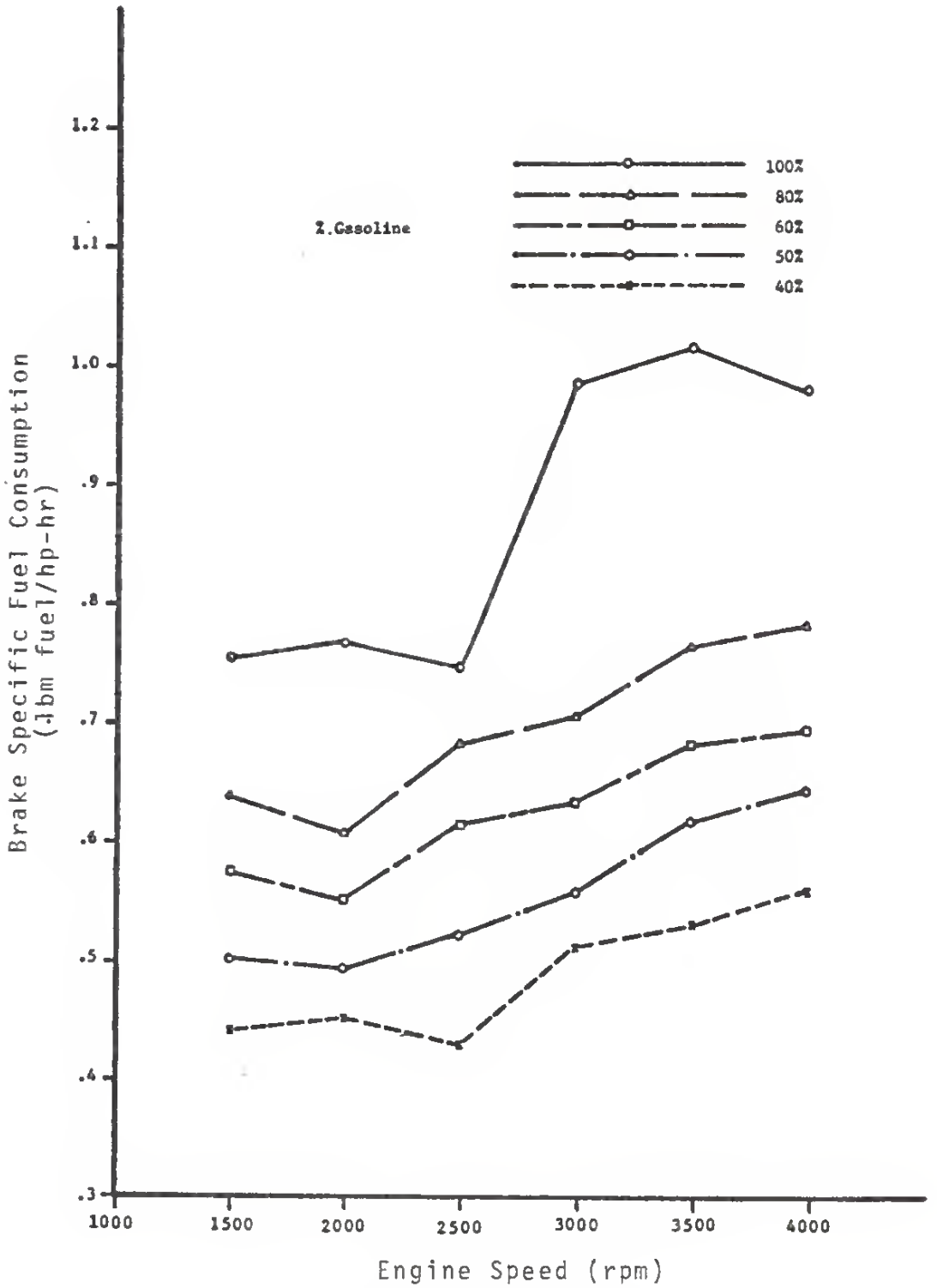

Figure 19 Brake Specific Fuel Consumption at 21.7 ft-lbf Torque as a Function of Engine Speed and Per Cent Gasoline

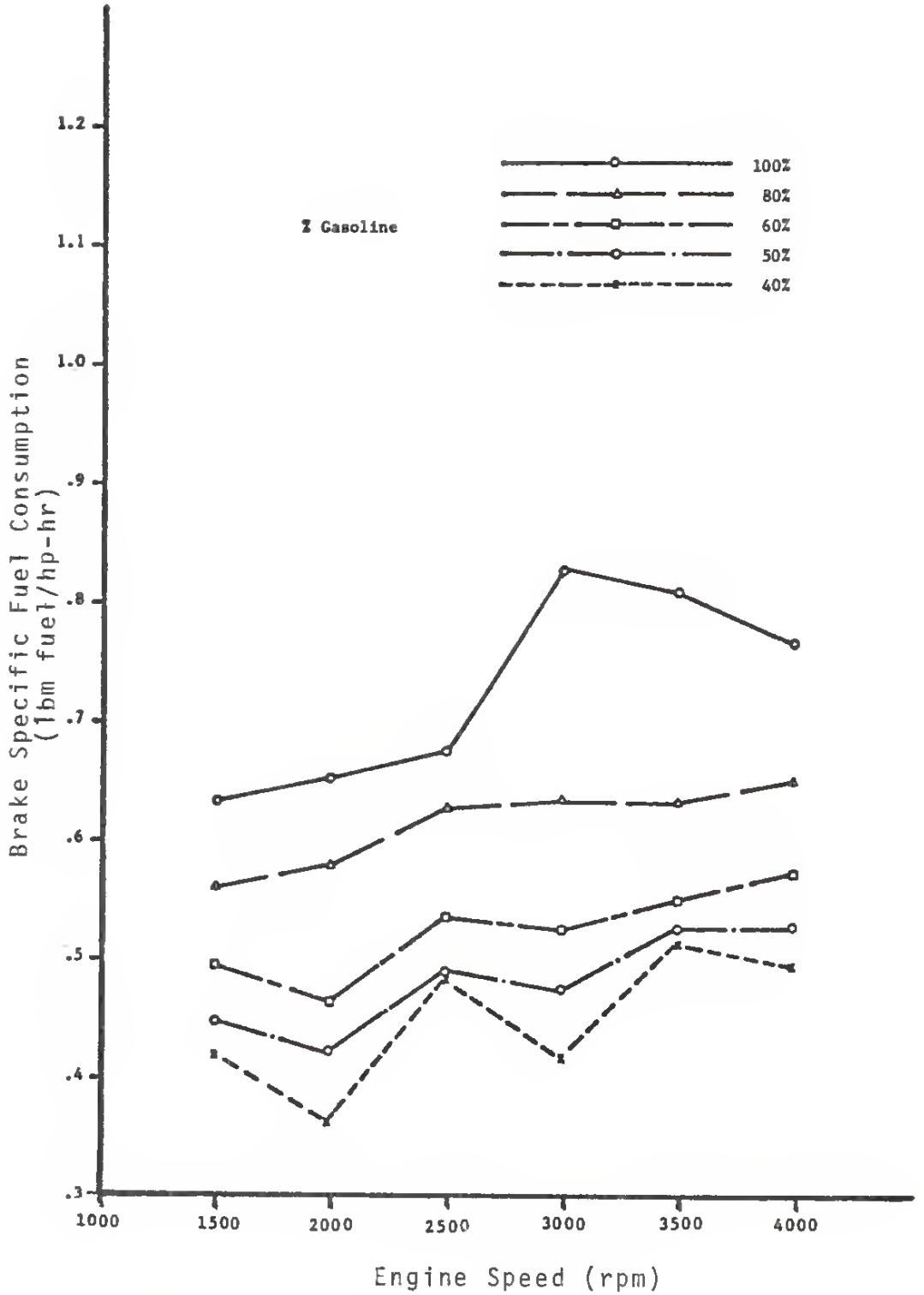

Figure 20 Brake Specific Fuel Consumption at 28.9 ft-lbf Torque as a Function of Engine Speed and Per Cent Gasoline

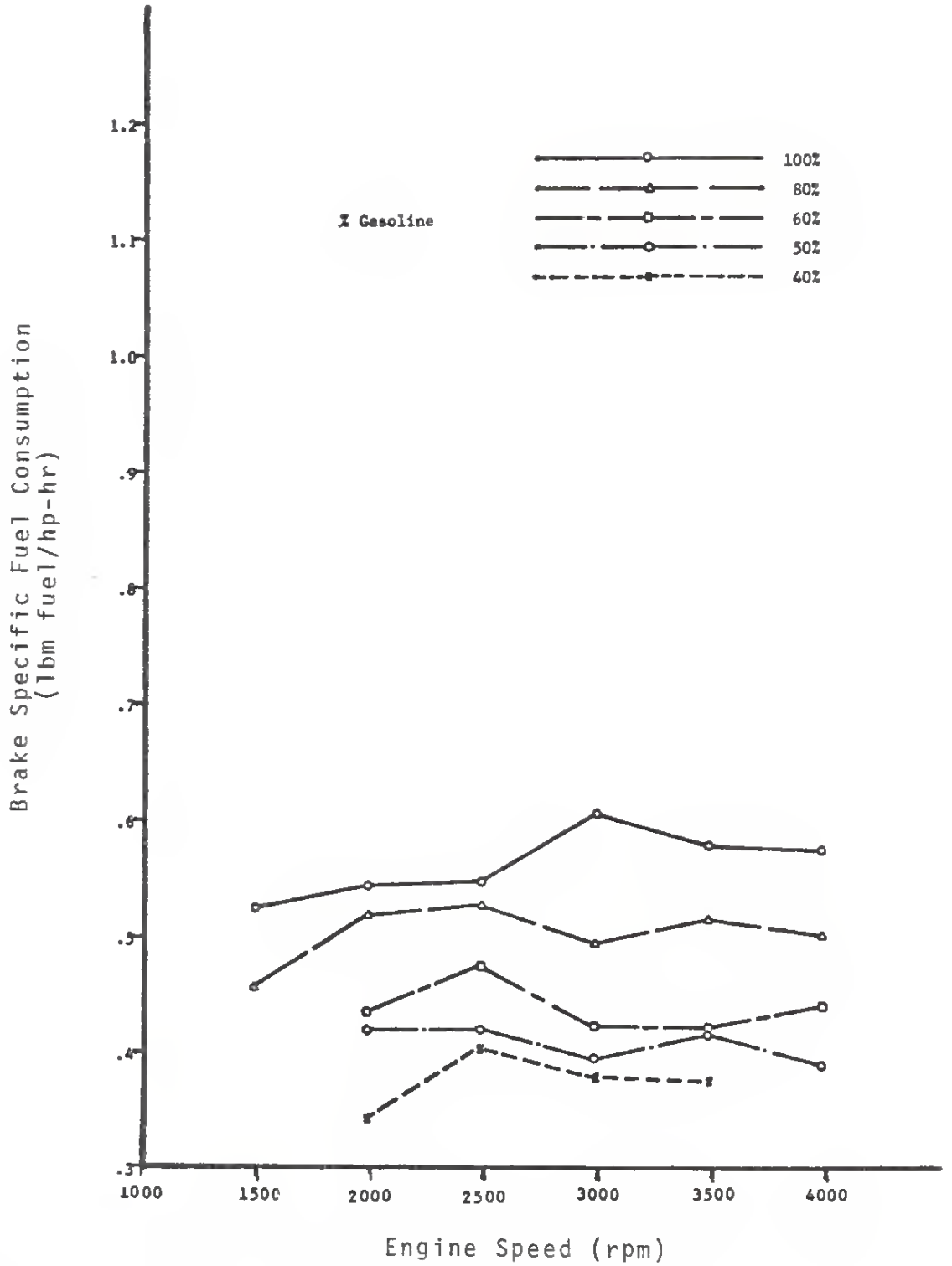

Figure 21 Brake Specific Fuel Consumption at 43.4 ft-lbf Torque as a Function of Engine Speed and Per Cent Gasoline

using data from reference 2 it would also take a little more than double the volume and also a little over twice the weight (if the hydrogen was stored cryogenically) to store the hydrogen and gasoline than it would take to store the gasoline if the engine was run on 100% gasoline.

Before leaving the subject of BSFC one trend that in general applies to IC engines that was in evidence here will be noted. That was the reduction in BSFC which occured when the load was increased for a given speed. This was due to the relative constancy (for a given speed) of the power consumed by internal friction losses.

In the area of thermal efficiency a general decline as engine speed increases can be seen in figures 22, 23 and 24 regardless of the fuel used. This is due to an increase in friction losses with speed. In figure 22 which illustrates the thermal efficiency at 21.7 ft-lbf, the 80% gasoline data would make this seem to be the optimum ratio. The data is a bit more difficult to interpret for the other torques, but the 80% mixture seems to perform consistently well. The 60% and 50% curves tended to fall a little below the 80% figure, but not necessarily in that order, and there tended to be more crossovers with the 50% and 60% mixtures. The 40% gasoline mixture performed well at the lower torque, but at the higher torques often exhibited the lowest thermal efficiency. This may reflect the difficulty that was encountered at this mixture, in providing optimum spark advance without preignition. This will be discussed further in the spark timing section.

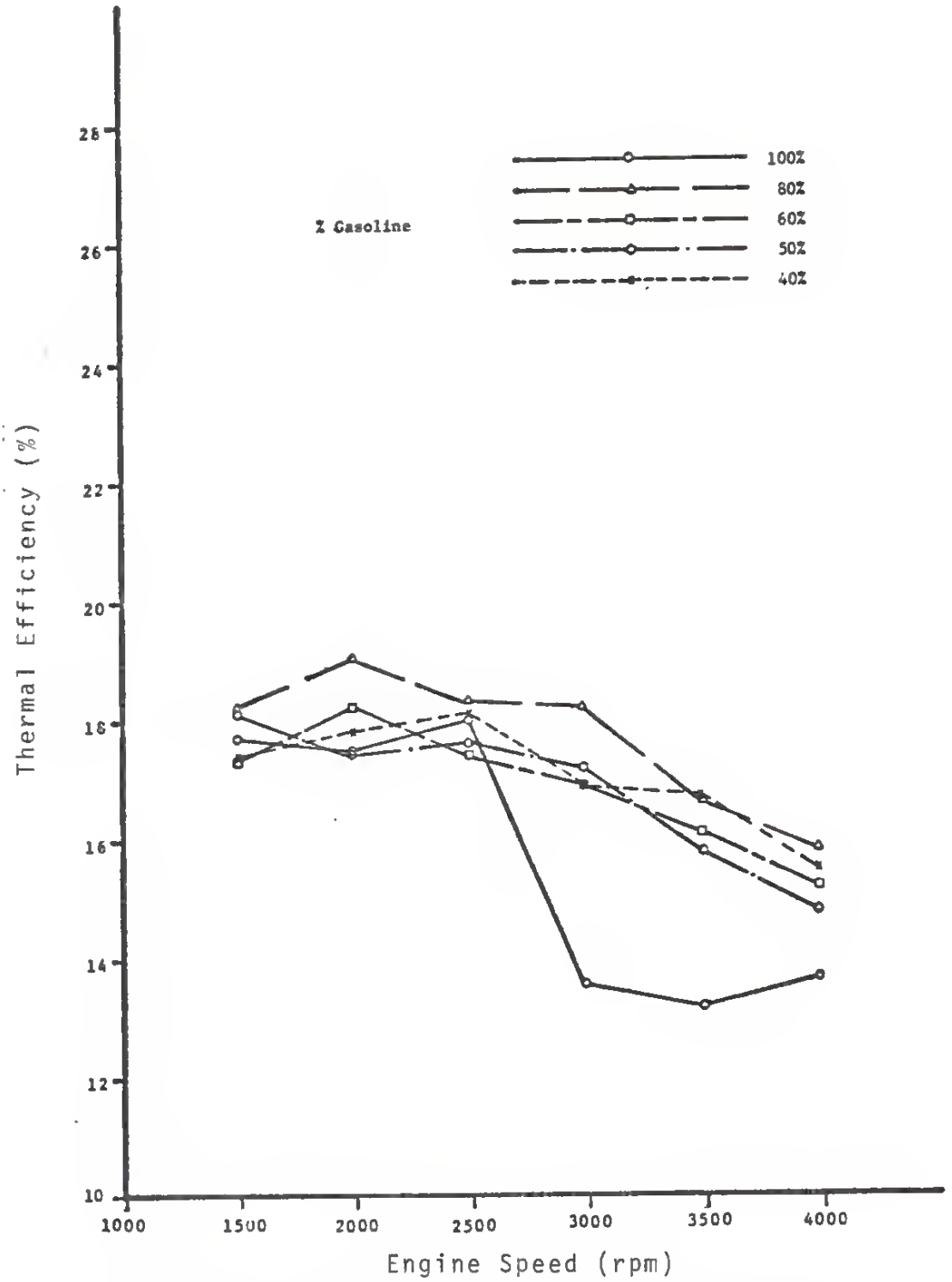

Figure 22 Thermal Efficiency at 21.7 ft-lbf Torque as a Function of Engine Speed and Per Cent Gasoline.

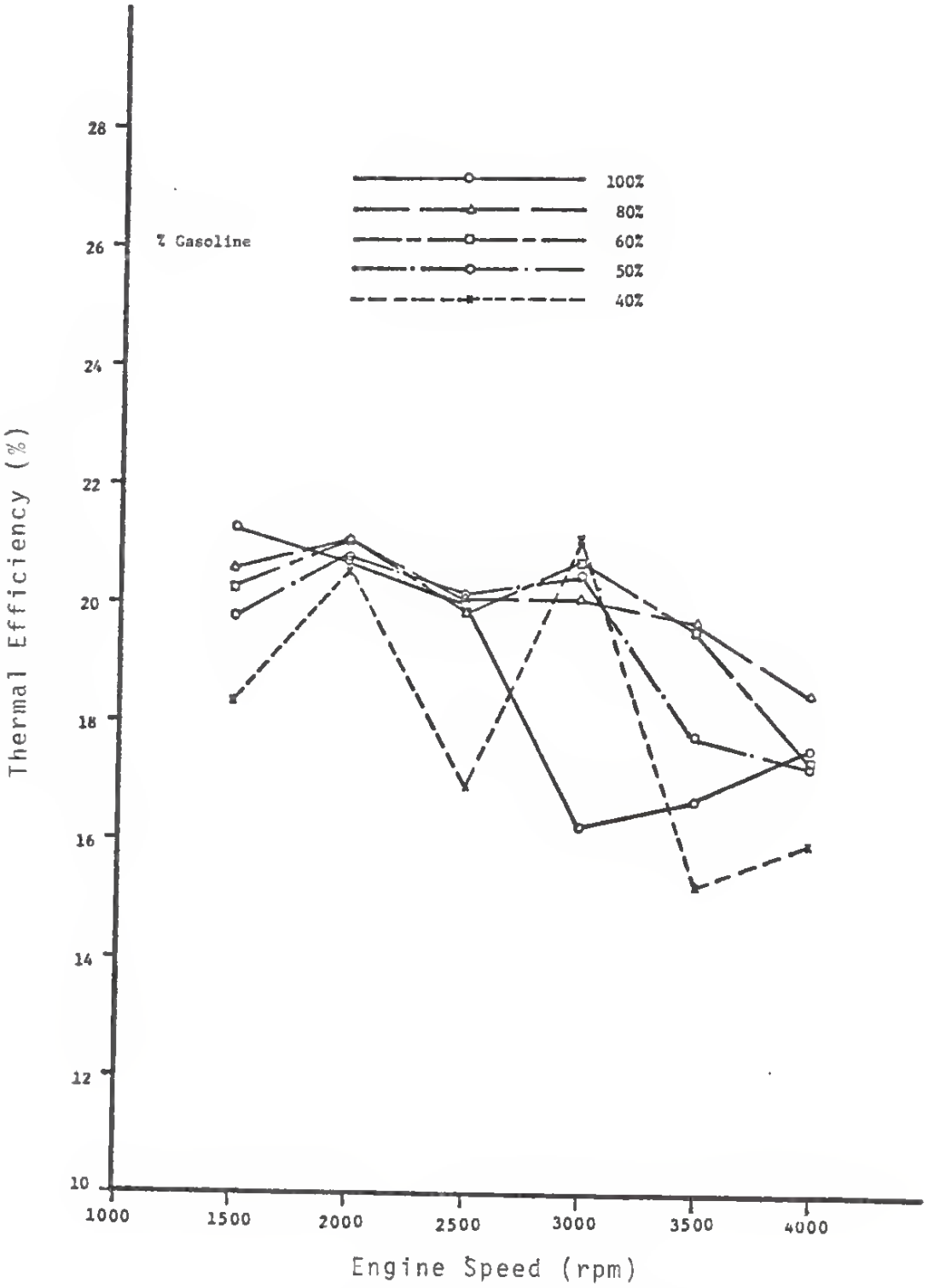

Figure 23 Thermal Efficiency at 28.9 ft-lbf Torque as a Function of Engine Speed and Per Cent Gasoline.

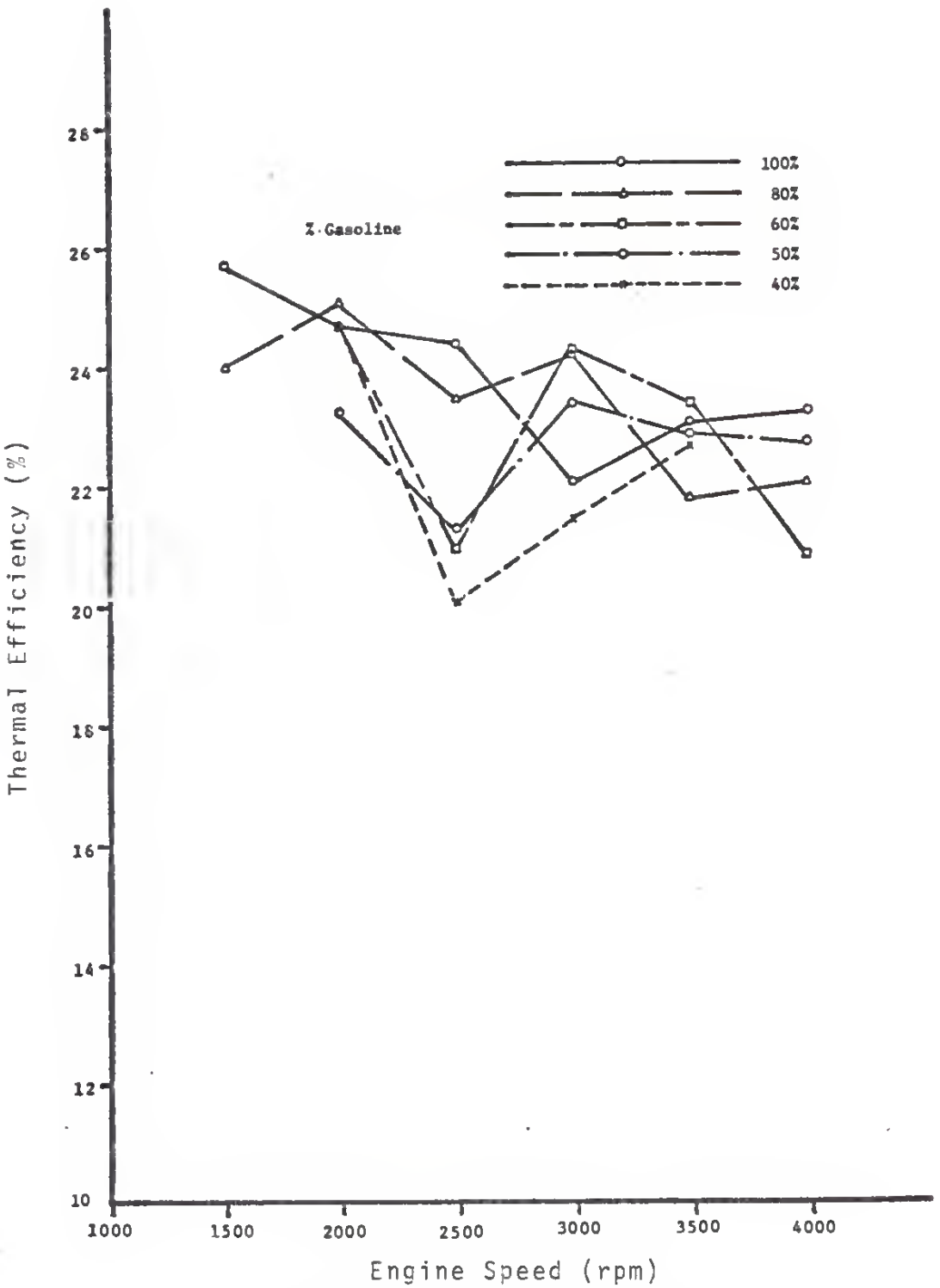

Figure 24 Thermal Efficiency at 43.4 ft-lbf Torque as a Function of Engine Speed and Per Cent Gasoline.

Performance of the 100% gasoline mixture was surprisingly irratic. This may be explained, in part at least, by comparing the thermal efficiency curves for the 100% gasoline mixture, with the air-gasoline ratio curves. The thermal efficiency curves for 100% gasoline tend to assume the "hyperbolic" shape seen in the air-gasoline curves for the 100% gasoline mixture. The low thermal efficiency of the 100% gasoline mixture above 2500 rpm then may be explained, at least in part, by the overly rich mixture provided by the KIM - 1 control system.

Figures 25, 26, and 27 show the spark advance curves for 21.7 ft-lbf, 28.9 ft-lbf and 43.4 ft-lbf torque in that order. The decrease in optimum spark advance as the hydrogen proportion was increased was marked. This in general was due to the high flame speed of hydrogen. However, the knock limited spark advance points for 40% hydrogen at 28.9 ft-lbf and 40% hydrogen at 43.4 ft-lbf demonstrate the preignition problems enocuntered with hydrogen. As hydrogen proportion and load were increased it became more difficult to operate the engine without preignition or backfires. It became clear that if a high hydrogen proportion is used to operate an engine under heavy load, some measure, in addition to decreased spark advance, is needed to control backfires and preignition. In fact, stable operation simply could not be obtained at some points because of preignition and/or backfiring. This is illustrated by the absence of data points at 40%, 50% and 60% gasoline and 1500 rpm and 40% gasoline at 4000 rpm at 43.4 ft-lbf. The difficulties encountered

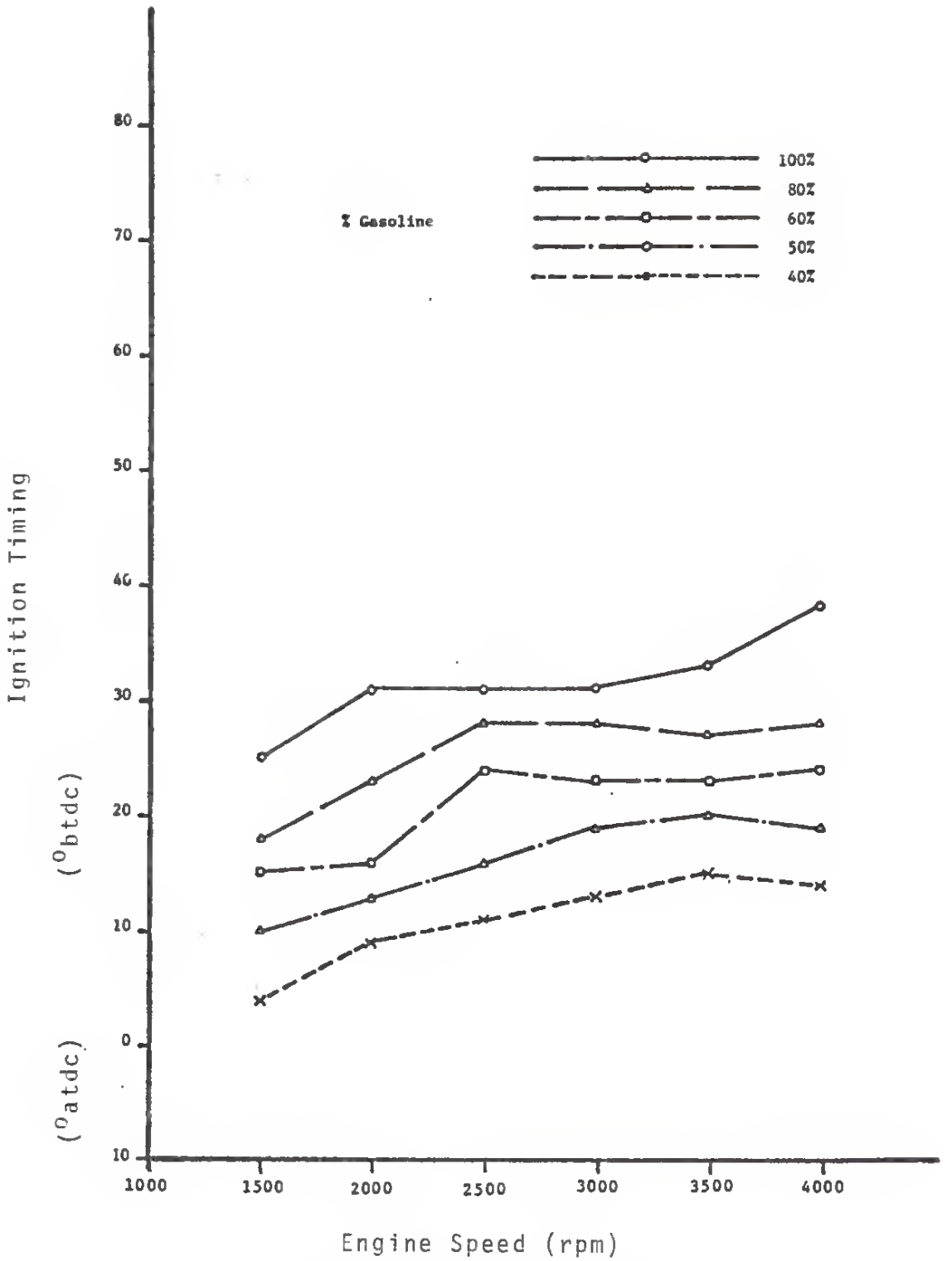

Figure 25 Ignition Timing at 21.7 ft-lbf Torque as a Function of Engine Speed and Per Cent Gasoline

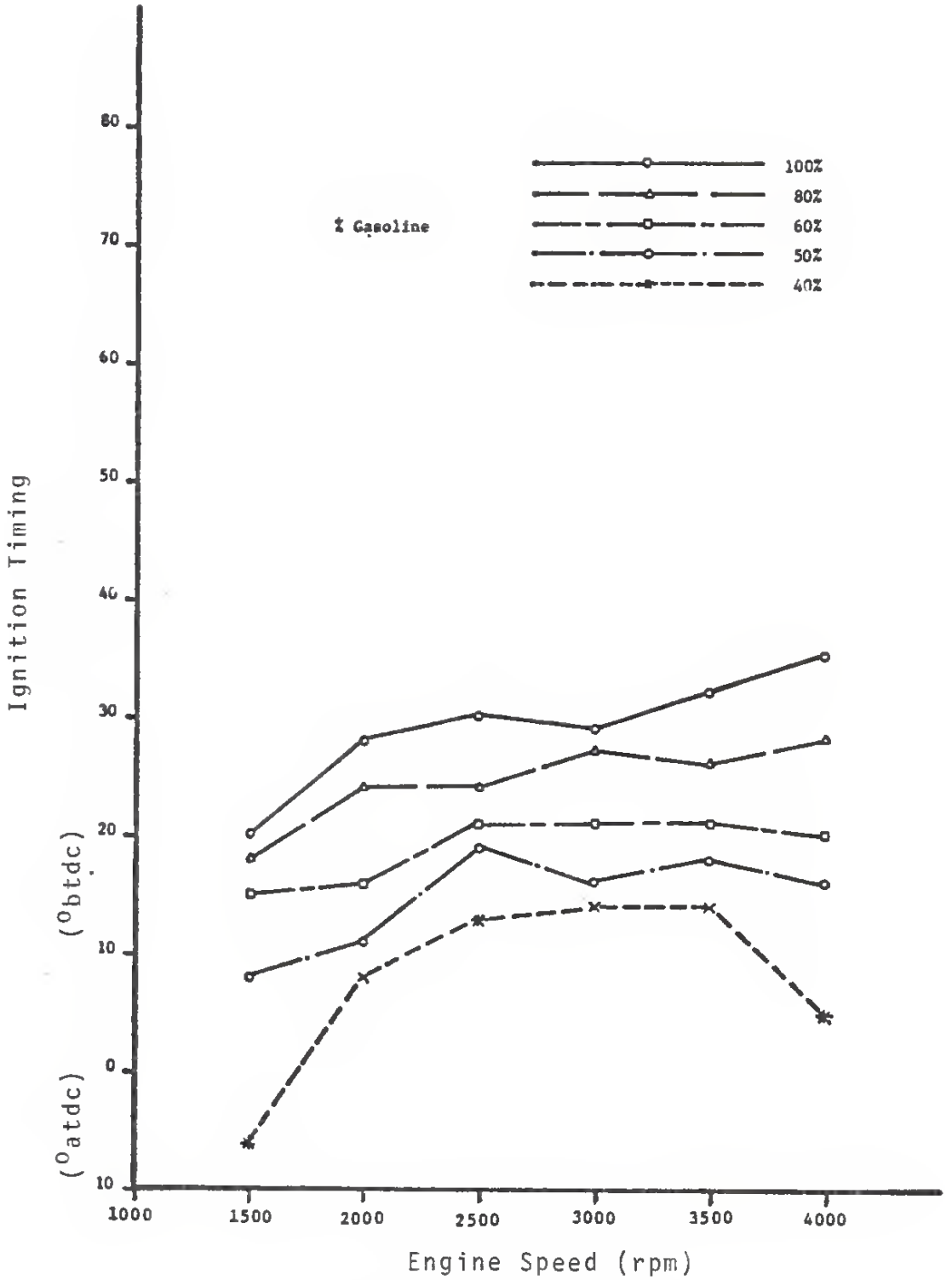

Figure 26 Ignition Timing at 28.9 ft-lbf Torque as a Function of Engine Speed and Per Cent Gasoline

*signifies knock limited spark advance

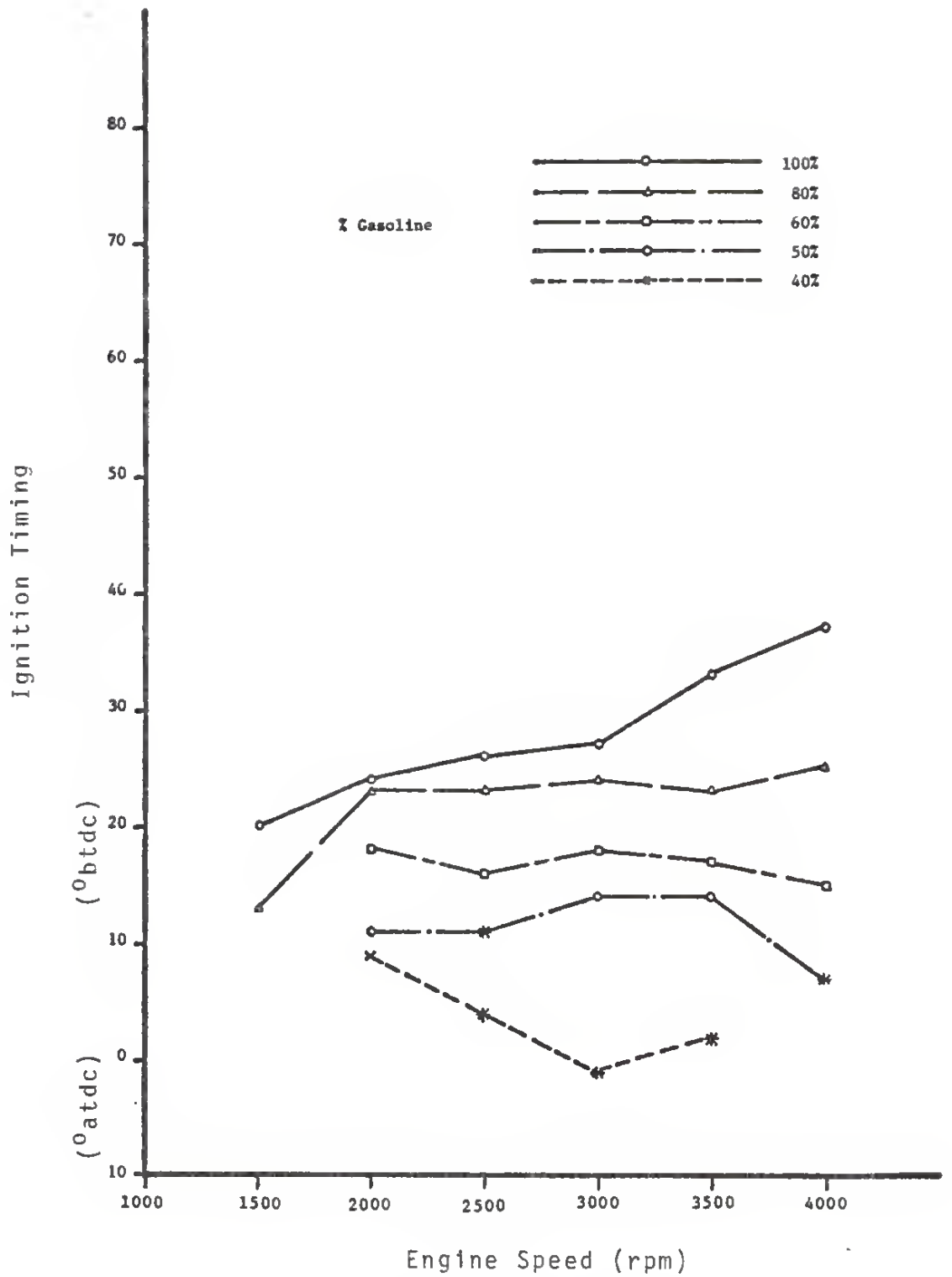

Figure 27 Ignition Timing at 43.4 ft-lbf Torque as a Function of Engine Speed and Per Cent Gasoline

*signifies knock limited spark advance

at 4000 rpm and 43.4 ft-lbf and 40% gasoline were believed to have resulted from insufficient hydrogen flow due to an undersized line from the regulator to the convertor, rather than problems inherent with using hydrogen. It was observed that to maintain hydrogen flow at 4000 rpm and high torque the regulator pressure had to be continually increased in order to maintain sufficient hydrogen flow as the hydrogen proportion increased. Because of this it was concluded that even with increased pressure sufficient flow could not be maintained at the 40% gasoline condition and a lean mixture resulted, which in turn, led to incessant back-fires. In observing the graphs a legitimate question arises: Why does knock limited spark advance (indicating preignition) occured at some rpm values of a given mixture and not others, especially when knock limited spark advance occurs above and below some rpm values where it does not? The answer to this question is that although it can be said that detonation is more prevalent at low rpm, detonation (or preignition) is also dependent upon many other variables. Humidity, for instance, is an important variable. High humidity will tend to suppress detonation. Also detonation can be caused by "hot spots" on the surface of the combustion chamber. These hot spots can be caused by such things as casting imperfections or combustion deposits. These combustion deposits have a certain randomness associated with their formation. These two factors above may explain why preignition was encountered one day and not the next under the same mixture and output conditions. The above mentioned deposits constitute one disadvantage of hydrogen-gasoline mixtures. As

long as gasoline is burned, the deposits will occur, and as long as hydrogen is used as a large proportion of the fuel (50% or 60%) detonation problems are bound to exist. If 100% gasoline is used the effects of the deposits are minimized, while if 100% hydrogen is used, their formation is by and large prevented. One curious situation can be seen in the plots, that is the optimum timing decreased after 3500 rpm for 60, 50, and 40% gasoline. In usual gasoline operation it should increase or stay constant. Perhaps at 4000 rpm there was some turbulance effect that increased the flame speed of the above hydrogen-gasoline mixtures, because of the low thermal energy required to ignite hydrogen, while not having an effect on the 80% and 100% gasoline mixtures. One final observation was made, one that would seem to contradict a statement made by Lynch (10) that "we (should) stop thinking of backfires as a positive indication of preignition". It was noted in this study that significant preignition was often followed by a backfire. This is not meant to say that the idea put forward by Lynch, that is raising the compression actually prevents backfiring, was incorrect, as this was not attempted in this study. It is instead meant as a note to future researchers, that for this engine, as it now exists, preignition can be interpreted as a warning of imminent back-fire.

Chapter VI

Summary and Conclusions

Engine performance tests on a 1968, electronically fuel injected 96.6 cu-in, horizontally opposed, air-cooled Volkswagen engine were conducted. Tests were conducted at engine torques of 21.7, 28.9 and 43.4 ft-lbf with fuel that consisted of a mixture of gasoline and hydrogen. The gasoline-hydrogen mixtures that were used were: 100% gasoline, 80% gasoline-20% hydrogen, 60% gasoline-40% hydrogen, 50% gasoline-50% hydrogen, 40% gasoline-60% hydrogen. These tests were conducted at engine speeds of from 1500 rpm to 4000 rpm in 500 rpm increments. The air-gasoline ratio was controlled by a KIM 1 microprocessor and associated hardware. The spark advance was set manually by the best torque procedure for tests using 100% gasoline. For tests using gasoline-hydrogen mixtures the hydrogen mixture and the spark advance were set manually with the lean best torque procedure. Hydrogen was introduced into the intake stream through a modified propane fuel system and carburetor.

The results or this testing showed that:

1. Although its performance could have been improved the KIM 1 and associated hardware provided satisfactory control of the air-gasoline ratio.
2. The lean best torque, and best torque procedures provided satisfactory control of spark timing and air-

fuel ratio.

3. Intake manifold vacuum, in general, decreased as the proportion of hydrogen in the fuel increased. In addition a few trends, not usually found in spark ignition IC engines, were found and were attributed to inlet dynamics.
4. Volumetric efficiency, in general, decreased as the proportion of hydrogen in the fuel increased. A few unusual trends were noticed in volumetric efficiency and were attributed to the same circumstances as the unusual trends in intake manifold vacuum.
5. No dangerously high temperatures were encountered while operating under the conditions of this test, although temperatures rose slightly as the hydrogen proportion of the fuel increased.
6. The brake specific fuel consumption decreased as the proportion of hydrogen in the fuel increased. If the BSFC curves are viewed in light of thermal efficiency, it would appear that this trend, for the most part, was due to the increased energy content per pound of hydrogen.
7. Although the 40% gasoline mixture may hold some promise for light loads, the 80% gasoline mixture seemed to generally produce the best thermal efficiency. This could be interpreted to support the "hydrogen enrichment" concept as discussed in the literature review,

however, caution is urged because lean operation was not intended here and usually was in the previous studies discussed in the literature review.

8. As the proportion of hydrogen was increased it was necessary to retard the spark timing in order to maintain optimum spark advance or, in some cases, to maintain engine operation.
9. For high torques and high hydrogen fuel proportions it was difficult to operate the engine without preignition or backfires.

Chapter VII

Recommendations

The next step, it would seem, would be to add some device or system to help prevent backfiring when operating with a high torque output and high hydrogen proportion of fuel. From the literature review, water injection seems particularly promising. If a study was then undertaken to repeat the tests found in this study on the engine with water injection, it might prove to be a valuable adjunct to this study. Another promising modification, in light of its beneficial effects on thermal efficiency, would be the raising of the compression ratio as suggested by Lynch (10).

In the area of controls, the performance of the gasoline control system could be improved, in particular at engine speeds of 3000 rpm and above.

In the area of equipment, it would be desirable that a dynamometer were made available that had the capacity for full power tests. There is nothing wrong with partial power tests, but alone, they can only provide a partial picture of engine performance.

If the existing equipment is to be used two suggestions to improve it can be offered. The first, and most simple suggestion, is to replace the line from the hydrogen tank regulator to the convertor with a line of larger diameter. This recommendation

is made in regard with the problems noted in the presentation of results section, dealing with insufficient hydrogen flow at high rpm, torque, and hydrogen proportion. Secondly, it is recommended that the manual engine controls (throttle, hydrogen mixture control, etc.) be moved out of the plane that the engine is in. This would help prevent injury if the engine did happen to fail catastrophically, and would also provide a degree of peace of mind to the operator. This could be easily accomplished by lengthening control cables and wiring and moving the controls to the front or rear of the engine, rather than the present location to the side of the engine.

List of References

1. Bowen, Thomas L., and Taylor, David W., "Hazards Associated with Hydrogen Fuel," 1976 Intersociety Energy Conversion Engineering Conference Proceedings, pp. 997-1002.

2. Edeskuty, F. J., and Stewart, W. F., "Alternate Fuels for Transportation," Mechanical Engineering, June 1974, pp. 22-28.

3. Hoffman, K. C., et al., Metal Hydride Storage for Mobile and Stationary Applications, SAE Pub. No. 760569, Warrendale, 1976.

4. Billings, Roger E., and Lynch, Frank E., Performance and Nitric Oxide Control Parameters of the Hydrogen Engine, Billings Energy Corporation Pub. No. 73002, Provo, (Prepared under contract with the Charles F. Kettering Foundation), 1973.

5. Billings, Robert E.,"Performance of a Hydrogen Powered Transit Vehicle," Hydrogen Progress, 2nd quarter 1977, pp. 16-21.

6. Menard, W. A., Moynihan, P. I., and Rupe, J. H., New Potentials for Conventional Aircraft When Powered by Hydrogen - Enriched Gasoline, SAE Pub. No.760469, Warrendale, 1976.

7. "Hydrogen - Supplemented Fuel," Mechanical Engineering, June 1974, p. 46.

8. de Boer, P. C. T., et al., "An Analytical and Experimental Study of the Performance and Emissions of a Hydrogen Fueled Reciprocating Engine." 1974 Intersociety Energy Conversion Conference Proceedings, pp. 479-486.

9. Wooley, Ronald L., and Hendriksen, D. L., Water Induction in Hydrogen Powered I C Engines, Billings Energy Corporation Pub. No. 76004, Provo, 1976.

10. Lynch, Frank E., Backfire Control Techniques for Hydrogen Fueled Internal Combustion Engines, Billings Energy Corporation Pub. No. 74001, Provo, 1974.

11. Wolley, Ronald L., and, Germane, G. V. Dynamic Tests of Hydrogen - Powered I C Engines, 8illings Energy Corporation Pub. No. 76002, Provo, 1976.

12. Dangerfield, Jim, "Mass Transit in a Hydrogen Economy," Hydrogen Progress, 2nd quarter 1977, pp. 7-13.

13. Chirivilla, J. E., Duke, L. A., Menard, W. A., High Fuel Economy in an Aircraft Piston Engine When Operating Ultralean, SAE Pub. No. 770488, Warrendale, 1977.

14. Stebar, R. F., and Parks, F. 8., Emission Control with Lean Operation Using Hydrogen - Supplemented Fuel, SAE Pub. No. 740187, Warrendale, 1974.

15. Turnquist, R. O., Private Communication.

16. 8ulletin 568-800-LM Operating Instructions, Theory, and Maintenance Model 800-LM Flowmeter, 7-77 edition, Gould Inc., Control and Systems Division, Wilmington, Mass., 1977.

17. Robinson, Jeff, ed., Volkswagen Service - Repair Handbook, Clymer, Los Angeles, Cal., 1972.

18. Williams, W., "Operational Characteristics of an Internal Combustion Engine Using Mixtures of Gasoline and Propane as the Fuel" (unpublished masters thesis, Kansas State University, 1976).

19. Williams, W., Private Communication.

20. 8aktiari - Nijad, F., "Design and Testing of a Microcomputer Air-Fuel Ratio, Ignition Timing System, for an Electronically Fuel Injected Internal Combustion Engine" (unpublished masters thesis, Kansas State University, 1978).

21. "800" System Instruction Manual, Daytronic Corporation, Dayton, Ohio, 1973.

22. Weast, Robert, editor, CRC Handbook of Chemistry and Physics, 57th edition, CRC Press, Cleveland, 1976.

23. Steam/Its Generation and Use, 38th edition, Babcock and Wilcox, New York, 1972.

24. National Standard Petroleum Oil Tables, Circular of the 8ureau of Standards, No. 154, Government Printing Office, Washington, 1924.

25. Baumeister, Theodore, editor, Standard Handbook for Mechanical Engineers, McGraw-Hill, New York, 1967.

26. "Standards, Definitions, Terms and Test Codes for Centrifugal, Axial and Propeller Fans," Bulletin No, 110, 2nd edition, National Association of Fan Manufacturers, Inc., Detroit, 1952.

27. Dbert, Edward F., editor. Internal Combustion Engines and Air Pollution, Intext Educational Publishers, New York, 1973.

28. Ball, H. D., Private Communication.

29. Schneck, Gary, "Design, Implementation, and Testing of a Real - Time Microcomputor Air - Fuel Ratio and Speed Controller for an Electronically Fuel Injected Internal Combustion Engine," (unpublished masters thesis, Kansas State University, 1976).

3D. Sprague, C. H., and Nash, R. T., Introduction to Engineering Experimentation, Kansas State University, Manhattan, Kansas, 1972.

APPENDIX A

Uncertainty Analysis

The uncertainty in each of the performance parameters will be calculated with the suggested equations of Sprague and Nash (30). For a variable which is a function of various independently measured values:

$$H = \sqrt{f\ (y_1,\ y_2,\ y_3, \cdots y_n)}. \tag{15}$$

The uncertainty in H is:

$$\lambda_H = S_1^{\ 2}\ \lambda_1^{\ 2} + S_2^{\ 2}\ \lambda_{\ 2}^{\ 2} + \cdots S_n^{\ 2}\ \lambda_n^{\ 2} \tag{16}$$

where S_n is defined as:

$$S_n = \frac{\partial f}{\partial y_n}\ \frac{y_n}{f(y_1,\ y_2 \cdots\ y_n)} \tag{17}$$

and where λ_n is the uncertainty in the n'th measured value.

If a portion of the measured values are not independent, as would be the case if they were measured with the same instrument, then the equation for the uncertainty is:

$$\lambda_H = \sqrt{(S_1\ \lambda_1 + S_2\ _2 + \cdots S_i\ \lambda_i)^2 + S_{i+1}^2\ \lambda_{i+1}^2 + S_{i+2}^2\ \lambda_{i+2}^2 \cdots S_n^2\ \lambda_n^2} \tag{18}$$

where the values 1 through i are dependent measurements and values i+1 through n are independent measurements.

For the calculations presented here, λ_n will be in per cent of reading wherever possible. The uncertainties will

be calculated using the smallest measured values in order to find the largest uncertainties encountered. Also, manufacturer's literature was not available for some of the instruments used. In these cases, resolution and linearity uncertainties will both be assumed equal to one-half of the smallest scale division of the particular instrument.

Thermal Efficiency

The thermal efficiency calculation was the end calculation in a long series of measurements and calculations. The uncertainties in the measurements will be found first, then the uncertainties in the intermediate calculations will be found, and from these uncertainties, the uncertainty in thermal efficiency will be found.

The Daytronic modular instrument system manual listed the accuracies of the various modules as .05 per cent of full scale for the torque from the strain guage conditioner amplifier, .05 per cent of scale for the speed output derived from the frequency-to-voltage convertor and a .02 per cent ± one digit accuracy associated with the display of these quantities.

The .05 per cent of full scale for the torque can be converted to per cent of smallest reading as follows by knowing full scale is 150 ft-lb.

$$\lambda_{Torque} = \sqrt{(\lambda^2)_{Linearity} + (\lambda^2)_{Accuracy\ of\ display} + (\lambda^2)_{Resolution}}$$

$$\lambda_{Torque} = \sqrt{(.0005)^2 + (.0002)^2 + \left(\frac{.1}{150}\right)^2} = .086\%$$

$$= (.00086)\ (150) = .129 \text{ ft-lb} = \frac{.129}{21.7} = .594\%$$

Since full scale of the engine speed was 5,000 rpm, the uncertainty in the speed can be changed to per cent of reading as follows:

$$\lambda_{RPM} = \sqrt{(\lambda^2)_{Linearity} + (\lambda^2)_{Accuracy\ of\ Display} + (\lambda^2)_{Resolution}}$$

$$\lambda_{RPM} = \sqrt{(.0005)^2 + (.0002)^2 + \left(\frac{5}{5000}\right)^2} = .114\% = (.0014)\ (5000) =$$

$$5.70 RPM = \frac{5.7}{1500} = .380\%$$

From equation three, it can be seen that the sensitivity of rpm and torque in the horsepower calculation was 1. So:

$$\lambda_{Power\ Output} = \sqrt{(.0038)^2 + (.00594)}$$

$$\lambda_{Power\ Output} = .705\%$$

The manual for the Oatametrics 800-LM hydrogen flow meter lists the accuracy of the system as 2% of reading or .025 SCFM whichever is worse. The smallest flow reading encountered was .065 SCFM. This is near the lower end of the smallest scale and was assumed to be the worst case. Full scale of the smallest scale is .5 SCFM. The smallest division is .005 SCFM. In this case .025 SCFM is worse than 2% of reading.

$$\lambda_{Hydrogen\ Consumption} = \sqrt{\left(\frac{.025}{.5}\right)^2 + \left(\frac{.0025}{.5}\right)^2}$$

$$= 5.02\%$$

$$= 5.02\% \times .5 = .0251 \text{ SCFM}$$

$$= \frac{.0251 \text{ SCFM}}{.065 \text{ SCFM}}$$

$$= 38.7\%$$

The Beckman Counter instruction book lists the accuracy of the counter as .3% ± 1 count.

$$\lambda_{Counter} = \sqrt{(.003)^2 + \left(\frac{.01}{74.65}\right)^2}$$

$$\lambda_{Counter} = .3\%$$

Another error component in the timing of the fuel flow was that due to the scales, counter trigger switch, and related hardware. This error component was the subject of a statistiscal analysis carried out by Mr. Gary Schneck in the uncertainty analysis appendix of his masters thesis (29). The study concluded that the value of this error was 2.9%. The total uncertainty in timing the gasoline flow was:

$$\lambda_{Timing\ of\ Fuel\ Flow} = \sqrt{(.003)^2 + (.0290)^2}$$

$$\lambda_{Timing\ of\ Fuel\ Flow} = 2.92\%$$

A known mass was used to determine the fuel mass flow rate. The smallest mass used was .2 lb. The uncertainty in this mass lies in the certainty with which the .2 lb mass could

be measured. This measurement was done using a Sartorius Model 2253-AL Balance. The uncertainty in this measurement is calculated as:

$$\lambda_{Mass} = \sqrt{\left(\frac{.05}{90.7}\right)^2 + \left(\frac{.1}{90.7}\right)^2}$$

$$\lambda_{Mass} = .123\%$$

The sensitivities of mass and timing with respect to gasoline consumption were +1 and -1 respectively so:

$$\lambda_{\text{Gasoline Consumption}} = \sqrt{(.00123)^2 = (.0292)^2}$$

$$= 2.92\%$$

It can be seen from equation six that the sensitivity of power output with respect to thermal efficiency is 1. Finding the sensitivities of hydrogen consumption and gasoline consumption and gasoline consumption is a bit more complicated:

$$S_{\substack{\text{Gasoline}\\ \text{Consumption}}} = \frac{\frac{\partial \eta_{th}}{\partial \left(\begin{smallmatrix}\text{Gasoline}\\ \text{Consumption}\end{smallmatrix}\right)} \left(\begin{smallmatrix}\text{Gasoline}\\ \text{Consumption}\end{smallmatrix}\right)}{\frac{\text{Power Output} \times 2545.1}{\left(\begin{smallmatrix}\text{Gasoline}\\ \text{Consumption}\end{smallmatrix}\right)(19000) + \left(\begin{smallmatrix}\text{Hydrogen}\\ \text{Consumption}\end{smallmatrix}\right)(51623)}}$$

$$= \frac{\left(\begin{smallmatrix}\text{Gasoline}\\ \text{Consumption}\end{smallmatrix}\right)(19000)}{\left(\begin{smallmatrix}\text{Gasoline}\\ \text{Consumption}\end{smallmatrix}\right)(19000) + \left(\begin{smallmatrix}\text{Hydrogen}\\ \text{Consumption}\end{smallmatrix}\right)(51623)}$$

Similarly:

$$S_{\substack{\text{Hydrogen}\\ \text{Consumption}}} = \frac{\left(\begin{smallmatrix}\text{Hydrogen}\\ \text{Consumption}\end{smallmatrix}\right)(51623)}{\left(\begin{smallmatrix}\text{Gasoline}\\ \text{Consumption}\end{smallmatrix}\right)(19000) + \left(\begin{smallmatrix}\text{Hydrogen}\\ \text{Consumption}\end{smallmatrix}\right)(51623)}$$

Now substituting values from the test used to calculate the uncertainty in the hydrogen flowmeter, that is the first test at 2,000 rpm, 43.4 ft-lbs and 80% gasoline, it was found that:

$$S_{\substack{\text{Gasoline}\\\text{Consumption}}} = .952$$

$$S_{\substack{\text{Hydrogen}\\\text{Consumption}}} = .048$$

finally:

$$\lambda_{n_{th}} = \sqrt{(S^2\lambda^2)_{\substack{\text{Gasoline}\\\text{Consumption}}} + (S^2\lambda^2)_{\substack{\text{Hydrogen}\\\text{Consumption}}} + (S^2\lambda^2)_{\substack{\text{Power}\\\text{Output}}}}$$

$$\lambda_{n_{th}} = \sqrt{(.952)^2\ (.0292)^2 + (.048)^2\ \ (.387)^2 + (.00705)^2}$$

$$\lambda_{n_{th}} = 3.417\%$$

Brake Specific Fuel Consumption

From equation 4, the sensitivities of gasoline consumption, hydrogen consumption, and power output with respect to brake specific fuel consumption can be found.

$$S_{\substack{\text{Gasoline}\\\text{Consumption}}} = \frac{\dfrac{\text{Gasoline Consumption}}{\text{Power Output}}}{\dfrac{\left(\begin{matrix}\text{Gasoline}\\\text{Consumption}\end{matrix}\right) + \left(\begin{matrix}\text{Hydrogen}\\\text{Consumption}\end{matrix}\right)}{\text{Power Output}}}$$

$$S_{\substack{\text{Hydrogen}\\\text{Consumption}}} = \frac{\dfrac{\text{Hydrogen Consumption}}{\text{Power Output}}}{\dfrac{\left(\begin{matrix}\text{Gasoline}\\\text{Consumption}\end{matrix}\right) + \left(\begin{matrix}\text{Hydrogen}\\\text{Consumption}\end{matrix}\right)}{\text{Power Output}}}$$

$$S_{\text{Power Output}} = \frac{\left(\begin{matrix}\text{Gasoline}\\ \text{Consumption}\end{matrix}\right) + \left(\begin{matrix}\text{Hydrogen}\\ \text{Consumption}\end{matrix}\right)}{\text{Power Consumption}} = 1$$

$$\frac{\left(\begin{matrix}\text{Gasoline}\\ \text{Consumption}\end{matrix}\right) + \left(\begin{matrix}\text{Hydrogen}\\ \text{Consumption}\end{matrix}\right)}{\text{Power Output}}$$

Again using data from the first test at 2,000 rpm, 43.4 ft-lbf and 80% gasoline it was found that:

$$S_{\begin{matrix}\text{Gasoline}\\ \text{Consumption}\end{matrix}} = .982$$

$$S_{\begin{matrix}\text{Hydrogen}\\ \text{Consumption}\end{matrix}} = .018$$

so:

$$\lambda_{BSFC} = \sqrt{(S^2\lambda^2)_{\begin{matrix}\text{Power}\\ \text{Output}\end{matrix}} + (S^2\lambda^2)_{\begin{matrix}\text{Hydrogen}\\ \text{Consumption}\end{matrix}} + (S^2\lambda^2)_{\begin{matrix}\text{Gasoline}\\ \text{Consumption}\end{matrix}}}$$

$$= \sqrt{(.00705)^2 + (.018)^2\,(.387)^2 + (.982)^2\,(.0292)^2}$$

$$= 3.03\%$$

Volumetric Efficiency

From equation 12 it can be seen that to calculate the uncertainty in volumetric efficiency, the uncertainty in air mass flow rate and theoretical maximum air mass flow rate must be found first. These two quantities depend on the uncertainty in density, volumetric air flow rate (CFM) and

engine speed. These in turn depend upon the uncertainty in $T_{\text{wet bulb}}$, $T_{\text{dry bulb}}$, atmospheric pressure, standard density pressure drop across the flow nozzle, and measured pressure drop across the flow nozzle.

To make the density equation more mathematically manageable it can be exoanded to the form:

$$\text{Density} = 1.33 \frac{\text{Atmospheric Pressure}}{T_{\text{dry bulb}}} - 1.03 \frac{\text{Vapor Pressure of Water @ } T_{\text{wet bulb}}}{T_{\text{dry bulb}}} + .00019 \text{ Atmospheric Pressure} - .00019 \left(\frac{T_{\text{wet bulb}}}{T_{\text{dry bulb}}}\right) \text{Atmospheric Pressure} \quad (15)$$

The uncertainties in $T_{\text{dry bulb}}$ and $T_{\text{wet bulb}}$ are found by assuming the linearity uncertainty equals the resolution uncertainty of .5°F. The smallest value of $T_{\text{dry bulb}}$ was 43°F.

$$\lambda T_{\text{dry bulb}} = \sqrt{(\lambda^2)_{\text{Linearity}} + (\lambda^2)_{\text{Resolution}}}$$

$$= \sqrt{\left(\frac{.5}{60}\right)^2 + \left(\frac{.5}{60}\right)^2}$$

$$= 1.179\%$$

$$\lambda T_{\text{wet bulb}} = \sqrt{(\lambda^2)_{\text{Linearity}} + (\lambda^2)_{\text{Resolution}}}$$

$$= \sqrt{\left(\frac{.5}{43}\right)^2 + \left(\frac{.5}{43}\right)^2}$$

$$= 1.644\%$$

The uncertainty in the barometric pressure is also to be calculated with the linearity and resolution uncertainties equal to 1/2 of the smallest scale division on the barometer. This smallest division was .01 in-Hg and the smallest pressure reading was 28.49 in-Hg.

The uncertainty in atmospheric pressure is:

$$\lambda_{\text{Atmospheric Pressure}} = \sqrt{(\lambda^2)_{\text{Linearity}} + (\lambda^2)_{\text{Resolution}}}$$

$$= \left(\frac{.005}{28.49}\right)^2 + \left(\frac{.005}{28.49}\right)^2$$

$$= .0248\%$$

Now after finding the sensitivities of atmospheric pressure, $T_{\text{dry bulb}}$ and $T_{\text{wet bulb}}$ the uncertainty in density can be computed.

$$S_{\text{Atmospheric Pressure}} = \frac{\frac{\partial\ \text{Oensity}}{\partial\ \text{Atmospheric Pressure}}\ (\text{Atmospheric Pressure})}{\text{Oensity}}$$

$$= \frac{\partial}{\partial\ \text{Atmo. Press.}}\left[1.33\ \frac{\text{Atmo. Press.}}{T_{\text{dry bulb}}} - 1.03\ \frac{\text{Vapor Press. of Water @ } T_{\text{wet bulb}}}{T_{\text{dry bulb}}} + .00019\ \text{Atmo. Press.} - .00019\left(\frac{T_{\text{wet bulb}}}{T_{\text{dry bulb}}}\right)\text{Atmo. Press.}\right]\ \text{Atmo. Press.}$$

$$\frac{}{1.33\ \frac{\text{Atmo. Press.}}{T_{\text{dry bulb}}} - 1.03\ \frac{\text{Vapor Press. of Water @ } T_{\text{wet bulb}}}{T_{\text{dry bulb}}} + .00019\ \text{Atmo. Press.} - .00019\left(\frac{T_{\text{wet bulb}}}{T_{\text{dry bulb}}}\right)\text{Atmo. Press.}}$$

$$= \frac{\frac{1.33}{T_{dry\ bulb}} + .00019 - .00019\frac{T_{wet\ bulb}}{T_{dry\ bulb}}}{\frac{1.33}{T_{dry\ bulb}} - 1.03\frac{\text{Vapor Press. of Water @ } T_{wet\ bulb}}{(T_{dry\ bulb})(\text{Atmo. Press.})} + .00019\left(\frac{T_{wet\ bulb}}{T_{dry\ bulb}}\right)}$$

now for $S_{T_{wet\ bulb}}$:

$$S_{T_{wet\ bulb}} = \frac{\frac{\partial\ \text{Density}}{\partial\ T_{wet\ bulb}} \times T_{wet\ bulb}}{\text{Density}}$$

$$= \frac{- .00019\frac{T_{wet\ bulb}}{T_{dry\ bulb}}(\text{Atmo. Press.})}{1.33\frac{\text{Atmo. Press.}}{T_{dry\ bulb}} - 1.03\frac{\text{Vapor Press. of Water @ } T_{wet\ bulb}}{T_{dry\ bulb}} + .00019\,\text{Atmo. Press.} - .00019\left(\frac{T_{wet\ bulb}}{T_{dry\ bulb}}\right)\text{Atmo. Press.}}$$

next $S_{T_{dry\ bulb}}$:

$$S_{T_{dry\ bulb}} = \frac{\frac{\partial\ \text{Density}}{\partial\ T_{dry\ bulb}}\ T_{dry\ bulb}}{\text{Density}}$$

$$= -1.33 \frac{\text{Atmo. Press.}}{T_{\text{dry bulb}}} + 1.03 \frac{\text{Vapor Press. of Water @ } T_{\text{wet bulb}}}{T_{\text{dry bulb}}} + .00019 \left(\frac{T_{\text{wet bulb}}}{T_{\text{dry bulb}}}\right) \text{Atmo. Press.}$$

$$\overline{1.33 \frac{\text{Atmo. Press.}}{T_{\text{dry bulb}}} - 1.03 \frac{\text{Vapor Press. of Water @ } T_{\text{wet bulb}}}{T_{\text{dry bulb}}} + .00019 \text{ Atmo. Press.} - .00019 \left(\frac{T_{\text{wet bulb}}}{T_{\text{dry bulb}}}\right) \text{Atmo. Press.}}$$

The values of $T_{\text{dry bulb}}$, $T_{\text{wet bulb}}$ and the vapor pressure of water @ $T_{\text{wet bulb}}$ are taken from a test run, judged representative of the tests in general. The particular test chosen was the first test run at the conditions of 3500 rpm, 21.7 ft-lbf torque and 40% hydrogen. The values are:

$T_{\text{dry bulb}} = 93^{\circ}F$

$T_{\text{wet bulb}} = 63^{\circ}F$

Vapor Pressure of Water @ $T_{\text{wet bulb}} = .28496$

A value of 28.9 in-Hg was the mean of the atmospheric pressures and is used in calculation of the sensitivities. When these readings are substituted into the sensitivity equations, the result is:

$S_{\text{Atmo. Press.}} = 1.01$

$S_{T_{\text{wet bulb}}} = -.00903$

$S_{T_{\text{dry bulb}}} = -.987$

Now the uncertainty in density can be found.

$$\lambda_{\text{Density}} = \sqrt{(S^2\lambda^2)_{\text{Atmo. Press.}} + (S^2\lambda^2)_{T_{\text{dry bulb}}} + (S^2\lambda^2)_{T_{\text{wet bulb}}}}$$

$$= \sqrt{(1.01)^2(.000248)^2 + (-.987)^2(.0179)^2 + (-.00903)^2(.01644)^2}$$

$$= 1.77\%$$

From the uncertainty, the uncertainty in the theoretical maximum air mass flow rate can be found.

$$\lambda_{\text{Theoretical Maximum Air Mass Flow}} = \sqrt{(S^2\lambda^2)_{RPM} + (S^2\lambda^2)_{\text{Density}}}$$

since $S_{rpm} = 1$ and $S_{density} = 1$

$$\lambda_{\text{Theoretical Maximum Air Mass Flow}} = \sqrt{(1)^2(.0038)^2 + (1)^2(.0177)^2}$$

$$= 1.81\%$$

To obtain the uncertainty in the air mass flow rate, the uncertainty in the standard density pressure drop and volumetric air flow must first be found. First however

$$\text{Standard Density Pressure Drop} = \frac{(\text{Measured Drop Across Flow Nozzle})\ (.075)}{\text{Density}}$$

the task of finding the uncertainty of the measured drop across flow nozzle must be performed. The only uncertainty associated with the above measurement was the resolution and linearity of the micromanometer. Once again these two uncertainties will be assumed equal to 1/2 of the smallest scale division which is .0005 in-H_2O.

The uncertainty in the measured pressure drop is then:

$$\lambda_{\text{Measured Pressure Drop}} = \sqrt{(\lambda^2)_{\text{Linearity}} + (\lambda^2)_{\text{Resolution}}}$$

$$= \sqrt{\left(\frac{.0005}{.05}\right)^2 + \left(\frac{.0005}{.05}\right)^2}$$

$$= 1.41\%$$

From equation 8, it is seen that:

$$S_{\text{Measured Pressure Drop}} = 1$$

$$S_{\text{Density}} = 1$$

so the uncertainty in the standard density pressure drop is:

$$\lambda_{\text{Standard Density Pressure Drop}} = \sqrt{(S^2\lambda^2)_{\text{Measured Pressure Drop}} (S^2\lambda^2)_{\text{Density}}}$$

$$= \sqrt{(.0141)^2 + (.0177)^2}$$

$$= 2.26\%$$

In order to calculate the uncertainty in CFM the sensitivity of standard density pressure drop across the flow nozzle in equation 9 must be known.

$$S_{\substack{\text{Standard Density} \\ \text{Pressure Drop}}} = \frac{\frac{\partial \text{ CFM}}{\partial \substack{\text{Standard Density} \\ \text{Pressure Drop}}} \left(\substack{\text{Standard Density} \\ \text{Pressure Drop}}\right)}{\text{CFM}}$$

$$= \frac{(59.868)\ .5\ (\text{Standard Density Pressure Drop})}{(59.868)\ (\text{Standard Density Pressure Drop})}$$

$$= .5$$

The uncertainty for volumetric air flow (CFM) may now be found:

$$\lambda_{CFM} = \sqrt{(.5)^2\ (.0226)^2}$$

$$\lambda_{CFM} = 1.13\%$$

The uncertainty in air mass flow rate may be found as:

$$\lambda_{\substack{\text{Air} \\ \text{Mass} \\ \text{Flow}}} = \sqrt{(S^2\lambda^2)_{CFM} + (S^2\lambda^2)_{Density}}$$

$$= \sqrt{(.0113)^2 + (.0177)^2}$$

$$= 2.1\%$$

Continuing on, the sensitivities of air mass flow and theoretical air mass flow in equation 12 are 1 and -1 respectively so:

$$\lambda_{N_V} = \sqrt{(S^2\lambda^2)_{\substack{\text{Air Mass}\\ \text{Flow Rate}}} + (S^2\lambda^2)_{\substack{\text{Theoretical}\\ \text{Air Mass}\\ \text{Flow Rate}}}}$$

$$\lambda_{N_V} = \sqrt{(.021)^2 + (.0181)^2}$$

$$\lambda_{N_V} = 2.77\%$$

Air-Fuel Ratio

The next parameter that the uncertainty will computed for is air-fuel ratio. From equation 13:

$$S_{\substack{\text{Air Mass}\\ \text{Flow Rate}}} = 1$$

$$S_{\substack{\text{Gasoline}\\ \text{Consumption}}} = \frac{(\text{Air Mass Flow Rate})\ (\text{Gasoline Consumption})}{\left[\left(\begin{matrix}\text{Gasoline}\\ \text{Consumption}\end{matrix}\right) + \left(\begin{matrix}\text{Hydrogen}\\ \text{Consumption}\end{matrix}\right)\right]^2}$$

$$\frac{\text{Air Mass Flow Rate}}{\left(\begin{matrix}\text{Gasoline}\\ \text{Consumption}\end{matrix}\right) + \left(\begin{matrix}\text{Hydrogen}\\ \text{Consumption}\end{matrix}\right)}$$

$$= \frac{\text{Gasoline consumption}}{\left(\begin{matrix}\text{Gasoline}\\ \text{Consumption}\end{matrix}\right) + \left(\begin{matrix}\text{Hydrogen}\\ \text{Consumption}\end{matrix}\right)}$$

Similarly:

$$S_{\substack{\text{Hydrogen}\\\text{Consumption}}} = \frac{\text{Hydrogen Consumption}}{\left(\substack{\text{Gasoline}\\\text{Consumption}}\right) + \left(\substack{\text{Hydrogen}\\\text{Consumption}}\right)}$$

From the data of the first test at 2,000 rpm, 43.4 ft-lbf and 80% gasoline:

$$S_{\substack{\text{Gasoline}\\\text{Consumption}}} = .982$$

$$S_{\substack{\text{Hydrogen}\\\text{Consumption}}} = .018$$

so:

$$\lambda_{\substack{\text{Air-Fuel}\\\text{Ratio}}} = \sqrt{(S^2\lambda^2)_{\substack{\text{Air Mass}\\\text{Flow Ratio}}} + (S^2\lambda^2)_{\substack{\text{Gasoline}\\\text{Consumption}}} + (S^2\lambda^2)_{\substack{\text{Hydrogen}\\\text{Consumption}}}}$$

$$\lambda_{\substack{\text{Air-Fuel}\\\text{Ratio}}} = \sqrt{(.021)^2 + (.982)^2\,(.0292)^2 + (.018)^2\,(.387)^2}$$

$$= 3.62\%$$

Air Gasoline Ratio

It can be seen from equation 14 that the sensitivities of air mass flow rate and gasoline consumption with respect to air - gasoline ratio were 1 and -1 respectfully. So:

$$\lambda_{\substack{\text{Air-Gasoline}\\\text{Ratio}}} = \sqrt{(.021)^2 + (.0292)^2}$$

$$= 3.60\%$$

Manifold Vacuum

As explained in an earlier chapter, the manifold vacuum was read from a vertical mercury manometer. The uncertainties associated with this reading consist of linearity and resolution uncertainties only. The smallest scale division of the manometer was .1 in-Hg. The smallest recorded value of intake manifold pressure was 4.5 in-Hg. The uncertainty in the recorded values of manifold pressure was:

$$\lambda_{\text{Intake Pressure}} = \sqrt{(\lambda^2)_{\text{Linearity}} + (\lambda^2)_{\text{Resolution}}}$$

$$= \sqrt{(.05)^2 + (.05)^2} = .071 \text{ in-Hg}$$

$$= \frac{.071 \text{ in-Hg}}{4.5} = 1.57\%$$

Exhaust Temperature

Several uncertainties are associated with the recorded exhaust temperature. These are the uncertainty in temperature sensed by the thermocouple, amounting to 4°F, a linearity uncertainty in the millivolt potentiometer of .03% of reading plus 3 μV and a resolution uncertainty of .00025 μV. The smallest temperature read was 353°F which corresponds to a millivolt output of 7.26. The value of the uncertainty in exhaust temperature in per cent reading is:

$$\lambda_{\text{Exhaust Temperature}} = \sqrt{(\lambda^2)_{\text{Thermocouple}} + (\lambda^2)_{\text{Linearity}} + (\lambda^2)_{\text{Resolution}}}$$

$$= \sqrt{\left(\frac{4}{353}\right)^2 + (.0003)^2 + \left(\frac{.3}{7.23}\right)^2 + \frac{.0023}{7.23}^2}$$

$$= 4.30\%$$

Spark Advance

As stated in an earlier chapter the spark advance was read from a degree wheel mounted on the cooling fan and illuminated with a stroboscopic timing light. The uncertainty associated with this reading consisted of linearity and resolution uncertainties. The error is independent of the number of degrees advance, and because it is so, the error is stated in the number of degrees rather than per cent. The smallest division on the degree wheel was 2 degrees.

$$\lambda_{\text{Spark Advance}} = \sqrt{(\lambda^2)_{\text{Linearity}} + (\lambda^2)_{\text{Resolution}}}$$

$$\lambda_{\text{Spark Advance}} = \sqrt{(1)^2 + (1)^2}$$

$$= 1.41 \text{ degrees}$$

APPENDIX B

HP-29C Data Reduction Program

```
001  *LBL1
002   RCL2
003   RCL4
004     ÷
005   RCL5
006     ^
007     1
008     3
009     6
010     0
011     0
012     ^
013   STO6
014     R
015   RCL6
016     .
017     1
018     4
019     1
020     ÷
021     5
022     .
023     6
024     1
025     2
026    EEX
027    CHS
028     3
029     ^
030     6
031     0
032
033   STO3
034     R
035   RCL2
036   RCL1
037     ÷
038     2
039     ^
040     P
041     ^
042     3
043     3
044     0
045     0
046     0
047     ÷
048   STO7
049     1
050   RCL6
051   RCL5
052     ÷
053     ^
054     R
```

STO 1 RPM
STO 2 Torque
STO 3 Time for measured mass to be consumed
STO 4 Numerator of fractional form of measured mass
STO 5 Denominator of fractional form of measured mass
STO 8 H_2 SCFM (air equivalent)

Result: Gasoline Consumption (lbm/hr)

Result: Hydrogen Consumption (lbm/hr)

Result: Brake Specific Fuel Consumption (lbm/hp-hr)

```
055   RCL6
056     1
057     5
058     0
059     0
060     0
061     X
062   RCL9
063     5
064     1
065     6
066     2
067     3
068     X
069     +
070   1/X
071   RCL7
072     X
073     2
074     5
075     4
076     5
077     .
078     1
079     X
080     1
081     0
082     0
083     X
084   R/S      Result: Thermal Efficiency (%)
085   RCL2
086     1
087     .
088     5
089     6
090     1
091     X
092   RTN
093   R/S      Result: Brake Mean Effective Pressure (lb/in2)
```

```
001  *LBL2
002   RCL0
003     .
004     4
005     9
006     1
007     x
008   RCL2
009   RCL3
010     -
011     x
012     2
013     7
014     0
015     0
016     ÷
017   CHS
018   RCL1
019     +
020     .
021     3
022     8
023     x
024   CHS
025   RCL0
026     .
027     4
028     9
029     1
030     x
031     +
032     .
033     3
034     7
035     ÷
036   RCL2
037     4
038     5
039     9
040     .
041     6
042     +
043     ÷
044   STO8
045   1/X
046     .
047     0
048     7
049     5
050     x
051   RCL4
052     x
053     .
054     5
```

STO 0 Atmospheric pressure (in-Hg)
STO 1 Pressure of saturated water vapor @ wet bulb temperature (lb/in^2)
STO 2 Dry bulb temperature (degrees F)
STO 3 Wet bulb temperature (degrees F)
STO 4 Measured pressure drop across air flow nozzle ($in\text{-}H_2O$)
STO 5 RPM
STO 6 Consumed mass of gasoline (lbm/hr)
STO 7 Consumed mass of H_2 (lbm/hr)

```
055    Y^x
056     5
057     9
058     .
059     8
060     6
061     8
062     x
063   RCL8
064     x
065     6
066     0
067     x
068    R/S
069   STO9
070   RCL5
071   RCL8
072     x
073     1
074     .
075     6
076     7
077     7
078     x
079    1/X
080   RCL9
061     x
082    R/S      Volumetric Efficiency Ratio
083   RCL9
084   RCL6
085   RCL7
086     +
087     ÷
088    R/S      Air-Fuel Ratio
089   RCL9
090   RCL6
091     ÷
092    RTN
093    R/S      Air-Gasoline Ratio
```

APPENDIX C

Computed Results

		run	Gasoline Consumption lbm/hr	Hydrogen Consumption lbm/hr	BSFC $\frac{\text{lbm}}{\text{hp-hr}}$	η_{th} %	Exhaust Temp °F
RPM Torque % fuel	1500 RPM 21.7 ft-lbf 100% gasoline 6.198 hp 33.874 PSI BMEP	1 2 3 Avg	4.739 4.651 4.635	0 0 0	.765 .750 .748 .754	17.5 17.8 17.9 17.7	352 355 354 354
	1500 RPM 21.7 ft-lbf 80% gasoline	1 2 3 Avg	3.640 3.545 3.654	.346 .346 .346	.643 .628 .645 .639	18.1 18.5 18.1 18.2	356 352 352 353
	1500 RPM 21.7 ft-lbf 60% gasoline	1 2 3 Avg	2.898 2.817 2.836	.716 .716 .716	.583 .570 .573 .575	17.1 17.4 17.4 17.3	363 364 365 364
	1500 RPM 21.7 ft-lbf 50% gasoline	1 2 3 Avg	2.277 2.276 2.254	.848 .860 .860	.504 .506 .502 .504	18.1 18.0 18.1 18.1	354 361 362 359
	1500 RPM 21.7 ft-lbf 40% gasoline	1 2 3 Avg	1.487 1.592 1.551	1.182 1.194 1.182	.431 .450 .441 .441	17.7 17.1 17.4 17.4	358 359 357 358
RPM Torque % fuel	1500 RPM 28.9 ft-lbf 100% gasoline 8.254 hp 45.113 PSI BMEP	1 2 3 Avg	5.239 5.178 5.242	0 0 0	.635 .627 .635 .632	21.103 21.352 21.090 21.2	423 424 425 424
	1500 RPM 28.9 ft-lbf 80% gasoline	1 2 3 Avg	4.102 4.225 3.995	.454 .454 .346	.552 .567 .526 .560	20.7 20.3 22.399 20.5	398 401 404 400
	1500 RPM 28.9 ft-lbf 60% gasoline	1 2 3 Avg	3.255 3.308 3.245	.812 .812 .812	.493 .499 .492 .495	20.2 20.1 20.3 20.2	413 413 415 414
	1500 RPM 28.9 ft-lbf 50% gasoline	1 2 3 Avg	2.576 2.589 2.590	1.11 1.11 1.122	.447 .448 .450 .448	19.8 19.7 19.6 19.7	410 412 408 410

		run	Intake Vacuum in-Hg	Ignition Timing °BTDC	η_v %	A/F ratio	Air / Gasoline ratio
RPM Torque % fuel	1500 RPM 21.7 ft-lbf 100% gasoline 6.198 hp 33.874 PSI BMEP	1	14.95	25	35.1	13.7	13.7
		2	15.05	25	34.5	13.7	13.7
		3	15.05	25	34.2	13.6	13.6
		Avg	15.0	25	34.6	13.7	13.7
	1500 RPM 21.7 ft-lbf 80% gasoline	1	14.5	18	34.5	15.4	16.8
		2	14.5	18	34.5	15.7	17.3
		3	14.5	18	34.5	15.3	16.8
		Avg	14.5	18	34.5	15.5	17.0
	1500 RPM 21.7 ft-lbf 60% gasoline	1	13.65	15	35.3	17.2	21.4
		2	13.7	15	35.3	17.6	22.1
		3	13.65	15	35.3	17.5	21.9
		Avg	13.65	15	35.3	17.4	21.8
	1500 RPM 21.7 ft-lbf 50% gasoline	1	13.8	10	33.8	18.9	26.0
		2	13.6	10	34.8	19.4	26.7
		3	13.6	10	34.8	19.5	27.0
		Avg	13.5	10	34.5	19.3	26.6
	1500 RPM 21.7 ft-lbf 40% gasoline	1	13.2	4	34.8	22.8	40.9
		2	13.2	4	34.8	21.8	38.2
		3	13.25	4	33.1	21.2	37.4
		Avg	13.2	4	34.2	21.9	38.8
RPM Torque % fuel	1500 RPM 28.9 ft-lbf 100% gasoline 8.254 hp 45.113 PSI BMEP	1	12.7	21	41.0	14.5	14.5
		2	12.65	20	41.0	14.7	14.7
		3	12.7	20	41.0	14.5	14.5
		Avg	12.7	20	41.0	14.6	14.6
	1500 RPM 28.9 ft-lbf 80% gasoline	1	12.15	18	41.7	16.2	18.0
		2	12.1	18	41.7	15.8	17.5
		3	~~12.05~~	~~18~~			
		Avg	12.1	18	41.7	16.0	17.8
	1500 RPM 28.9 ft-lbf 60% gasoline	1	11.25	15	41.5	18.0	22.5
		2	11.2	15	41.5	17.8	22.1
		3	11.25	15	41.5	18.1	22.6
		Avg	11.25	15	41.5	18.0	22.4
	1500 RPM 28.9 ft-lbf 50% gasoline	1	10.95	8	40.6	19.3	27.6
		2	11	8	40.6	19.2	27.5
		3	11.1	8	40.6	19.2	27.5
		Avg	11.0	8	40.6	19.2	27.5

		run	Gasoline Consumption lbm/hr	Hydrogen Consumption lbm/hr	BSFC $\frac{\text{lbm}}{\text{hp-hr}}$	η_{th} %	Exhaust Temp °F
	1500 RPM	1	1.965	1.493	.419	18.4	447
	28.9 ft-lbf	2	2.034	1.493	.427	18.2	456
	40% gasoline	3	1.960	1.493	.418	18.4	460
		Avg			.421	18.3	454
	1500 RPM	1	6.474	0	.522	25.7	546
	43.4 ft-lbf	2	6.548	0	.528	25.4	539
	100% gasoline	3	6.422	0	.518	25.9	546
	12.395 hp	Avg			.523	25.7	544
	67.747 PSI BMEP						
	1500 RPM	1	5.129	.728	.473	23.4	548
	43.4 ft-lbf	2	4.682	.728	.436	24.9	543
	80% gasoline	3	5.023	.716	.463	23.8	538
		Avg			.457	24.0	543
	1500 RPM						
	43.3 ft-lbf						
	60% gasoline						
	1500 RPM						
	43.4 ft-lbf						
	50% gasoline						
	1500 RPM						
	43.4 ft-lbf						
	40% gasoline						
RPM	2000 RPM	1	6.352	0	.769	17.4	442
Torque	21.7 ft-lbf	2	6.305	0	.763	17.6	449
% fuel	100% gasoline	3	6.327	0	.766	17.5	442
	8.263 hp	Avg			.766	17.5	442
	33.874 PSI BMEP						
	2000 RPM	1	4.555	.478	.609	18.9	436
	21.7 ft-lbf	2	4.496	.478	.602	19.1	435
	80% gasoline	3	4.574	.478	.611	18.9	436
		Avg			.607	19.0	436
	2000 RPM	1	3.740	.896	.561	17.9	438
	21.7 ft-lbf	2	3.581	.896	.542	18.4	439
	60% gasoline	3	3.626	.896	.547	18.3	439
		Avg			.550	18.2	439

		run	Intake Vacuum in-Hg	Ignition Timing ^{o} BTDC	η_v %	A/F ratio	Air / Gasoline ratio
	1500 RPM 28.9 ft-lbf 40% gasoline	1 2 3 Avg	9.4 9.35 9.35 9.35	*6^{o}ATDC *6^{o}ATDC *6^{o}ATDC *6^{o}ATDC	41.4 41.4 41.4 41.4	20.9 20.5 21.0 20.8	36.9 35.6 37.0 36.5
	1500 RPM 43.4 ft-lbf 100% gasoline 12.395 hp 67.747 PSI BMEP	1 2 3 Avg	7.7 7.9 7.7 7.8	20 19 20 20	54.8 55.0 54.9 54.9	15.6 15.5 15.8 15.6	15.6 15.5 15.8 15.6
	1500 RPM 43.4 ft-lbf 80% gasoline	1 2 3 Avg	6.5 6.5 6.65 6.55	12 13 13 13	55.1 55.1 55.1 55.1	16.5 17.8 16.8 17.0	18.8 20.6 19.2 19.5
	1500 RPM 43.4 ft-lbf 60% gasoline						
	1500 RPM 43.4 ft-lbf 50% gasoline						
	1500 RPM 43.4 ft-lbf 40% gasoline						
RPM Torque % fuel	2000 RPM 21.7 ft-lbf 100% gasoline 8.263 hp 33.874 PSI BMEP	1 2 3 Avg	15.55 15.6 15.55 15.55	31 30 31 31	36.6 36.3 36.6 36.5	14.1 14.1 14.2 14.1	14.1 14.1 14.2 14.1
	2000 RPM 21.7 ft-lbf 80% gasoline	1 2 3 Avg	15.1 15.1 15.1 15.1	23 23 23 23	36.3 36.3 36.1 36.2	16.6 16.8 16.7 16.7	18.3 18.6 18.5 18.5
	2000 RPM 21.7 ft-lbf 60% gasoline	1 2 3 Avg	14.4 14.4 14.35 14.4	16 16 16 16	35.4 35.6 35.6 35.5	17.6 18.3 18.1 18.0	21.8 22.9 22.6 22.4

*knock limited spark advance

		run	Gasoline Consumption lbm/hr	Hydrogen Consumption lbm/hr	BSFC $\frac{\text{lbm}}{\text{hp-hr}}$	η_{th} %	Exhaust Temp ^{o}F
	2000 RPM	1	2.741	1.313	.491	17.5	440
	21.7 ft-lbf	2	2.815	1.313	.500	17.3	439
	50% gasoline	3	2.806	1.313	.498	17.4	437
		Avg			.496	17.4	439
	2000 RPM	1	2.374	1.433	.461	17.7	445
	21.7 ft-lbf	2	2.296	1.433	.451	17.9	443
	40% gasoline	3	2.172	1.493	.444	17.8	443
		Avg			.452	17.8	444
RPM	2000 RPM	1	7.165	0	.651	20.6	497
Torque	28.9 ft-lbf	2	7.176	0	.652	20.5	502
% fuel	100% gasoline	3	7.154	0	.650	20.6	500
	11.005 hp	Avg			.651	20.6	500
	45.113 PSI BMEP						
	2000 RPM	1	6.028	.382	.582	20.9	503
	28.9 ft-lbf	2	6.069	.382	.586	20.7	504
	80% gasoline	3	5.863	.382	.567	21.4	503
		Avg			.578	21	503
	2000 RPM	1	4.013	1.134	.468	20.8	503
	28.9 ft-lbf	2	3.886	1.134	.456	21.2	504
	60% gasoline	3	3.973	1.134	.464	20.9	504
		Avg			.463	21.0	504
	2000 RPM	1	3.200	1.433	.421	20.8	504
	28.9 ft-lbf	2	3.219	1.433	.423	20.7	505
	50% gasoline	3	3.232	1.433	.424	20.7	505
		Avg			.423	20.7	505
	2000 RPM	1	2.126	1.851	.361	20.6	492
	28.9 ft-lbf	2	2.116	1.851	.360	20.6	492
	40% gasoline	3	2.226	1.851	.370	20.3	490
		Avg			.364	20.5	491
RPM	2000 RPM	1	8.961	0	.542	24.7	637
Torque	43.4 ft-lbf	2	8.978	0	.543	24.7	640
% fuel	100% gasoline	3	8.996	0	.544	24.6	641
	16.527 hp	Avg			.543	24.7	639
	67.747 PSI BMEP						
	2000 RPM	1	8.437	.155	.520	25	615
	43.4 ft-lbf	2	8.607	.155	.530	24.5	615
	80% gasoline	3	8.167	.155	.504	25.8	615
		Avg			.518	25.1	615

		run	Intake Vacuum in-Hg	Ignition Timing ^{o}BTDC	η_v %	A/F ratio	Air / Gasoline ratio
	2000 RPM	1	13.2	12	35.6	20.2	29.8
	21.7 ft-lbf	2	13.3	13	35.5	19.7	28.9
	50% gasoline	3	13.3	13	35.5	19.8	29.0
		Avg	13.25	13	35.5	19.9	29.2
	2000 RPM	1	12.95	9	34.7	21.0	33.6
	21.7 ft-lbf	2	12.95	9	34.7	21.4	34.8
	40% gasoline	3	12.9	9	35.1	22.4	37.1
		Avg	12.95	9	34.8	21.6	35.2
RPM	2000 RPM	1	13.85	28	41.6	14.2	14.2
Torque	28.9 ft-lbf	2	13.75	28	41.6	14.2	14.2
% fuel	100% gasoline	3	13.75	28	41.6	14.2	14.2
	11.005 hp	Avg	13.8	28	41.6	14.2	14.2
	45.113 PSI BMEP						
	2000 RPM	1	13.05	24	43.4	15.6	16.6
	28.9 ft-lbf	2	13.05	24	43.4	15.5	16.4
	80% gasoline	3	13.05	24	43.1	15.9	16.9
		Avg	13.05	24	43.3	15.7	16.6
	2000 RPM	1	11.9	16	41.5	18.5	23.8
	28.9 ft-lbf	2	11.9	16	41.5	19.0	24.5
	60% gasoline	3	11.85	16	41.5	18.7	24.0
		Avg	11.9	16	41.5	18.7	24.1
	2000 RPM	1	11.2	11	41.1	20.4	29.6
	28.9 ft-lbf	2	11.25	11	41.1	20.4	29.4
	50% gasoline	3	11.2	11	41.1	20.3	29.3
		Avg	11.2	11	41.1	20.4	29.4
	2000 RPM	1	10.85	8	39.7	22.8	42.7
	28.9 ft-lbf	2	10.75	8	39.7	22.9	42.9
	40% gasoline	3	10.85	8	39.7	22.3	40.8
		Avg	10.8	8	39.7	22.7	42.1
RPM	2000 RPM	1	9.4	24	54.8	15.0	15.0
Torque	43.4 ft-lbf	2	9.35	24	54.8	14.9	14.9
% fuel	100% gasoline	3	9.35	24	54.7	14.9	14.9
	16.527 hp	Avg	9.35	24	54.8	14.9	14.9
	67.747 PSI BMEP						
	2000 RPM	1	9.45	23	55.3	14.8	15.0
	43.4 ft-lbf	2	9.45	23	55.3	14.5	14.7
	80% gasoline	3	9.45	23	55.3	15.2	15.5
		Avg	9.45	23	55.3	14.8	15.1

		run	Gasoline Consumption lbm/hr	Hydrogen Consumption lbm/hr	BSFC $\frac{\text{lbm}}{\text{hp-hr}}$	η_{th} %	Exhaust Temp °F
	2000 RPM	1	6.158	1.027	.435	24.7	619
	43.4 ft-lbf	2	6.097	1.027	.431	24.9	618
	60% gasoline	3	6.263	1.027	.441	24.5	618
		Avg			.436	24.7	618
	2000 RPM	1	5.571	1.493	.427	23.0	656
	43.4 ft-lbf	2	5.326	1.493	.413	23.6	657
	50% gasoline	3	5.466	1.493	.421	23.3	648
		Avg			.420	23.3	654
	2000 RPM	1	3.724	1.910	.341	24.8	630
	43.4 ft-lbf	2	3.889	1.910	.351	24.4	628
	40% gasoline	3	3.727	1.910	.341	24.8	627
		Avg			.344	24.7	628
RPM	2500 RPM	1	7.750	0	.750	17.9	509
Torque	21.7 ft-lbf	2	7.713	0	.747	17.9	512
% fuel	100% gasoline	3	7.657	0	.741	18.1	511
	10.329 hp	Avg			.746	18.0	511
	33.874 PSI BMEP						
	2500 RPM	1	6.494	.322	.660	18.8	508
	21.7 ft-lbf	2	6.710	.322	.681	18.2	508
	80% gasoline	3	6.905	.322	.700	17.8	508
		Avg			.680	18.3	508
	2500 RPM	1	5.463	.931	.619	17.3	512
	21.7 ft-lbf	2	5.355	.943	.610	17.5	512
	60% gasoline	3	5.463	.931	.619	17.3	511
		Avg		.935	.616	17.4	512
	2500 RPM	1	3.981	1.433	.524	17.6	508
	21.7 ft-lbf	2	3.958	1.433	.522	17.6	506
	50% gasoline	3	3.942	1.433	.520	17.7	506
		Avg			.522	17.6	507
	2500 RPM	1	2.645	1.851	.435	18.0	521
	21.7 ft-lbf	2	2.557	1.851	.427	18.2	515
	40% gasoline	3	2.575	1.851	.429	18.2	514
		Avg			.430	18.1	517
RPM	2500 RPM	1	9.279	0	.675	19.9	581
Torque	28.9 ft-lbf	2	9.210	0	.669	20.0	583
% fuel	100% gasoline	3	9.286	0	.675	19.8	582
	13.756 hp	Avg			.673	19.9	582
	45.113 PSI BMEP						

		run	Intake Vacuum in-Hg	Ignition Timing ^{o}BTOC	η_v %	A/F ratio	Air / Gasoline ratio
	2000 RPM	1	7.75	18	54.3	17.4	20.3
	43.4 ft-lbf	2	7.85	18	54.3	17.5	20.5
	60% gasoline	3	7.85	18	54.3	17.1	19.9
		Avg	7.80	18	54.3	17.3	20.2
	2000 RPM	1	6.35	11	55.4	18.3	23.2
	43.4 ft-lbf	2	6.35	11	55.4	18.9	24.2
	50% gasoline	3	6.3	11	55.4	18.6	23.6
		Avg	6.35	11	55.4	18.6	23.7
	2000 RPM	1	6.0	9	53.7	21.8	32.9
	43.4 ft-lbf	2	6.0	9	53.7	21.1	31.5
	40% gasoline	3	6.0	9	53.7	21.7	32.9
		Avg	6.0	9	53.7	21.5	32.4
RPM	2500 RPM	1	15.25	31	36.5	14.3	14.3
Torque	21.7 ft-lbf	2	15.25	31	36.4	14.3	14.3
% fuel	100% gasoline	3	15.25	31	36.2	14.3	14.3
	10.329 hp	Avg	15.25	31	36.4	14.3	14.3
	33.874 PSI BMEP						
	2500 RPM	1	15.10	28	36.9	15.9	16.7
	21.7 ft-lbf	2	15.10	28	36.9	15.4	16.1
	80% gasoline	3	15.10	28	36.9	15.0	15.7
		Avg	15.10	28	36.9	15.4	16.2
	2500 RPM	1	13.95	24	37.4	16.9	19.8
	21.7 ft-lbf	2	13.95	24	37.4	17.2	20.2
	60% gasoline	3	13.95	24	37.4	16.9	19.8
		Avg	13.95	24	37.4	17.0	19.9
	2500 RPM	1	13.45	16	35.9	19.1	26.0
	21.7 ft-lbf	2	13.45	16	35.9	19.2	26.1
	50% gasoline	3	13.45	16	35.9	19.2	26.2
		Avg	13.45	16	35.9	19.2	26.1
	2500 RPM	1	13.05	11	35.5	22.7	38.6
	21.7 ft-lbf	2	13.05	11	35.5	23.2	39.9
	40% gasoline	3	13.05	11	35.5	23.1	39.6
		Avg	13.05	11	35.5	23.0	39.4
RPM	2500 RPM	1	12.95	30	42.9	14.0	14.0
Torque	28.9 ft-lbf	2	12.95	30	42.7	14.1	14.1
% fuel	100% gasoline	3	12.95	30	43.1	14.1	14.1
	13.756 hp	Avg	12.95	30	42.9	14.1	14.1
	45.113 PSI BMEP						

		run	Gasoline Consumption lbm/hr	Hydrogen Consumption lbm/hr	BSFC $\frac{\text{lbm}}{\text{hp-hr}}$	η_{th} %	Exhaust Temp ^{o}F
	2500 RPM	1	8.329	.346	.631	19.9	571
	28.9 ft-lbf	2	8.162	.346	.618	20.2	571
	80% gasoline	3	8.389	.346	.635	19.8	570
		Avg			.628	20.0	571
	2500 RPM	1	6.198	1.134	.533	19.9	576
	28.9 ft-lbf	2	6.246	1.134	.537	19.8	575
	60% gasoline	3	6.261	1.134	.538	19.7	575
		Avg			.536	19.8	575
	2500 RPM	1	5.297	1.433	.489	20.1	583
	28.9 ft-lbf	2	5.325	1.433	.491	20.0	583
	50% gasoline	3	5.258	1.433	.486	20.1	583
		Avg			.489	20.1	583
	2500 RPM	1	4.293	2.448	.490	16.8	590
	28.9 ft-lbf	2	4.150	2.448	.480	17.1	589
	40% gasoline	3	4.254	2.448	.487	16.9	587
		Avg			.486	16.9	589
RPM	2500 RPM	1	11.302	0	.547	24.5	715
Torque	43.4 ft-lbf	2	11.404	0	.552	24.3	714
% fuel	100% gasoline	3	11.289	0	.546	24.5	713
	20.658 hp	Avg			.548	24.4	714
	67.747 PSI BMEP						
	2500 RPM	1	10.501	.513	.533	23.3	711
	43.4 ft-lbf	2	10.405	.513	.529	23.5	710
	80% gasoline	3	10.3	.513	.523	23.6	711
		Avg			.528	23.5	711
	2500 RPM	1	7.788	1.97	.472	21.1	751
	43.4 ft-lbf	2	7.765	1.97	.471	21.1	760
	60% gasoline	3	7.859	1.97	.476	20.9	738
		Avg				21.0	750
	2500 RPM	1	6.221	2.448	.420	21.5	740
	43.4 ft-lbf	2	6.106	2.507	.417	21.4	736
	50% gasoline	3	6.200	2.567	.424	21.0	736
		Avg			.420	21.3	737
	2500 RPM	1	5.178	3.164	.404	20.1	744
	43.4 ft-lbf	2	5.131	3.164	.402	20.2	744
	40% gasoline	3	5.255	3.164	.408	20.0	744
		Avg			.405	20.1	744

		run	Intake Vacuum in-Hg	Ignition Timing °BTDC	η_v %	A/F ratio	Air / Gasoline ratio
	2500 RPM	1	13.1	24	43.0	14.5	15.1
	28.9 ft-lbf	2	13.1	24	43.0	14.8	15.4
	80% gasoline	3	13.1	24	43.0	14.4	15.0
		Avg	13.1	24	43.0	14.6	15.2
	2500 RPM	1	11.95	21	42.8	16.9	20.0
	28.9 ft-lbf	2	11.95	21	42.8	16.8	19.8
	60% gasoline	3	11.95	21	42.8	16.8	19.8
		Avg	11.95	21	42.8	16.8	19.9
	2500 RPM	1	11.45	19	42.8	18.4	23.4
	28.9 ft-lbf	2	11.45	19	42.8	18.3	23.3
	50% gasoline	3	11.45	19	42.8	18.5	23.6
		Avg	11.45	19	42.8	18.4	23.4
	2500 RPM	1	10.25	12*	42.7	18.2	28.6
	28.9 ft-lbf	2	10.25	13*	42.7	18.6	29.6
	40% gasoline	3	10.25	13*	42.7	18.3	28.8
		Avg	10.25	13*	42.7	18.4	29.0
RPM	2500 RPM	1	8.95	26	54.6	14.7	14.7
Torque	43.4 ft-lbf	2	8.9	27	54.9	14.6	14.6
% fuel	100% gasoline	3	8.95	26	54.6	14.7	14.7
	20.658 hp	Avg	8.95	26	54.7	14.7	14.7
	67.747 PSI BMEP						
	2500 RPM	1	7.95	23	54.7	14.7	15.4
	43.4 ft-lbf	2	7.95	23	54.7	14.8	15.5
	80% gasoline	3	7.95	23	54.7	14.9	15.7
		Avg	7.95	23	54.7	14.8	15.5
	2500 RPM	1	6.1	15	56.3	17.2	21.5
	43.4 ft-lbf	2	6.1	16	56.3	17.2	21.6
	60% gasoline	3	6.3	17	56.3	17.1	21.3
		Avg	6.2	16	56.3	17.2	21.5
	2500 RPM	1	6.3	11*	52.3	17.9	25.0
	43.4 ft-lbf	2	6.4	11*	52.3	18.0	24.5
	50% gasoline	3	6.4	11*	52.3	17.7	25.1
		Avg	6.35	11*	52.3	17.9	24.9
	2500 RPM	1	5.25	4*	54.8	18.9	30.4
	43.4 ft-lbf	2	5.2	5*	54.8	19.0	30.7
	40% gasoline	3	5.25	4*	54.8	18.7	30.0
		Avg	5.25	4*	54.8	18.9	30.4

*knock limited spark advance

		run	Gasoline Consumption lbm/hr	Hydrogen Consumption lbm/hr	BSFC $\frac{lbm}{hp\text{-}hr}$	η_{th} %	Exhaust Temp °F
RPM Torque % fuel	3000 RPM 21.7 ft-lbf 100% gasoline 12.395 hp 33.874 PSI BMEP	1 2 3 Avg	12.125 12.282 12.140	0 0 0	.978 .991 .979 .983	13.7 13.5 13.7 13.6	559 558 558 558
	3000 RPM 21.7 ft-lbf 80% gasoline	1 2 3 Avg	8.334 8.556 8.486	.251 .251 .251	.693 .711 .705 .703	18.417 18.0 18.1 18.2	592 592 593 592
	3000 RPM 21.7 ft-lbf 60% gasoline	1 2 3 Avg	6.599 6.754 6.643	1.170 1.170 1.170	.627 .639 .630 .632	17.0 16.7 16.9 16.9	588 588 588 588
	3000 RPM 21.7 ft-lbf 50% gasoline	1 2 3 Avg	5.445 5.244 5.243	1.612 1.612 1.612	.569 .553 .553 .558	16.9 17.3 17.3 17.2	582 579 579 580
	3000 RPM 21.7 ft-lbf 40% gasoline	1 2 3 Avg	4.323 4.297 4.303	2.030 2.030 2.030	.513 .510 .511 .511	16.9 16.9 16.9 16.9	591 589 589 590
RPM Torque % fuel	3000 RPM 28.9 ft-lbf 100% gasoline 16.508 hp 45.113 PSI BMEP	1 2 3 Avg	13.682 13.644 13.605	0 0 0	.829 .827 .824 .827	16.2 16.2 16.3 16.2	624 624 626 625
	3000 RPM 28.9 ft-lbf 80% gasoline	1 2 3 Avg	9.696 10.454 9.957	.382 .382 .382	.611 .656 .626 .631	20.6 19.2 20.1 20.0	642 641 641 641
	3000 RPM 28.9 ft-lbf 60% gasoline	1 2 3 Avg	7.529 7.493 7.416	1.194 1.194 1.194	.528 .526 .522 .525	20.5 20.6 20.7 20.6	656 657 657 657
	3000 RPM 28.9 ft-lbf 50% gasoline	1 2 3 Avg	6.053 6.250 6.097	1.731 1.731 1.731	.472 .483 .474 .476	20.6 20.2 20.5 20.4	653 652 652 652

		run	Intake Vacuum in-Hg	Ignition Timing °BTDC	η_v %	A/F ratio	$\frac{\text{Air}}{\text{Gasoline}}$ ratio
RPM Torque % fuel	3000 RPM 21.7 ft-lbf 100% gasoline 12.395 hp 33.874 PSI BMEP	1 2 3 Avg	14.95 15.0 15.05 15.0	31 31 31 31	40.8 40.8 40.6 40.7	11.9 11.8 11.9 11.9	11.9 11.8 11.9 11.9
	3000 RPM 21.7 ft-lbf 80% gasoline	1 2 3 Avg	15.6 15.6 15.55 15.6	28 28 29 28	38.0 38.0 38.0 38.0	15.6 15.2 15.3 15.4	16.1 15.7 15.8 15.9
	3000 RPM 21.7 ft-lbf 60% gasoline	1 2 3 Avg	14.25 14.25 14.25 14.25	23 23 23 23	37.4 37.4 37.4 37.4	16.7 16.4 16.6 16.6	19.7 19.2 19.5 19.5
	3000 RPM 21.7 ft-lbf 50% gasoline	1 2 3 Avg	13.7 13.65 13.65 13.65	19 19 19 19	36.5 36.5 36.5 36.5	17.9 18.5 18.5 18.3	23.3 24.1 24.2 23.9
	3000 RPM 21.7 ft-lbf 40% gasoline	1 2 3 Avg	13.05 13.0 13.0 13.0	13 13 13 13	36.5 36.5 36.5 36.5	19.9 20.0 20.0 20.0	29.3 29.5 29.4 29.4
RPM Torque % fuel	3000 RPM 28.9 ft-lbf 100% gasoline 16.508 hp 45.113 PSI BMEP	1 2 3 Avg	13.05 13.05 13.00 13.05	29 29 29 29	46.8 46.6 46.6 46.7	12.1 12.1 12.1 12.1	12.1 12.1 12.1 12.1
	3000 RPM 28.9 ft-lbf 80% gasoline	1 2 3 Avg	13.7 13.8 13.7 13.75	27 27 27 27	43.1 43.1 43.1 43.1	15.1 14.0 14.7 14.6	15.6 14.5 15.2 15.1
	3000 RPM 28.9 ft-lbf 60% gasoline	1 2 3 Avg	12.65 12.65 12.65 12.65	21 21 21 21	42.4 42.4 42.4 42.4	17.1 17.1 17.3 17.2	19.8 19.9 20.1 19.9
	3000 RPM 28.9 ft-lbf 50% gasoline	1 2 3 Avg	11.95 11.95 11.95 11.95	16 16 16 16	41.3 41.3 41.3 41.3	18.6 18.1 18.3 18.3	23.9 23.2 23.4 23.5

		run	Gasoline Consumption lbm/hr	Hydrogen Consumption lbm/hr	BSFC $\frac{\text{lbm}}{\text{hp-hr}}$	η_{th} %	Exhaust Temp ^{o}F
	3000 RPM	1	4.843	2.090	.420	21.0	656
	28.9 ft-lbf	2	4.753	2.090	.415	21.2	656
	40% gasoline	3	4.950	2.090	.426	20.8	656
		Avg			.420	21.0	656
RPM	3000 RPM	1	15.138	0	.611	21.9	775
Torque	43.4 ft-lbf	2	14.975	0	.604	22.2	776
% fuel	100% gasoline	3	14.959	0	.603	22.2	775
	24.790 hp	Avg			.606	22.1	775
	67.747 PSI BMEP						
	3000 RPM	1	11.274	.860	.489	24.4	789
	43.4 ft-lbf	2	11.489	.860	.498	24.0	789
	80% gasoline	3	11.417	.872	.496	24.1	789
		Avg			.494	24.2	789
	3000 RPM	1	8.626	1.851	.423	24.3	794
	43.4 ft-lbf	2	8.727	1.851	.427	24.1	794
	60% gasoline	3	8.526	1.851	.419	24.5	794
		Avg			.423	24.3	794
	3000 RPM	1	7.154	2.537	.391	23.6	784
	43.4 ft-lbf	2	7.342	2.567	.400	23.2	783
	50% gasoline	3	7.254	2.567	.396	23.3	788
		Avg			.396	23.4	785
	3000 RPM	1	5.741	3.463	.371	21.9	861
	43.4 ft-lbf	2	6.055	3.522	.386	21.3	866
	40% gasoline	3	5.891	3.582	.382	21.3	868
		Avg			.380	21.5	865
RPM	3500 RPM	1	14.474	0	1.001	13.4	624
Torque	21.7 ft-lbf	2	14.672	0	1.015	13.2	623
% fuel	100% gasoline	3	14.754	0	1.020	13.1	626
	14.461 hp	Avg			1.012	13.2	624
	33.874 PSI BMEP						
	3500 RPM	1	10.729	.334	.765	16.6	693
	21.7 ft-lbf	2	10.838	.346	.773	16.4	697
	80% gasoline	3	10.503	.346	.750	16.9	698
		Avg			.763	16.6	696
	3500 RPM	1	8.571	1.254	.679	16.2	667
	21.7 ft-lbf	2	8.662	1.254	.686	16.1	668
	60% gasoline	3	8.596	1.254	.681	16.1	668
		Avg			.682	16.1	668

		run	Intake Vacuum in-Hg	Ignition Timing ^{o}BTOC	η_v %	A/F ratio	Air / Gasoline ratio
	3000 RPM	1	11.35	14	41.2	20.8	29.7
	28.9 ft-lbf	2	11.35	14	41.2	21.0	30.3
	40% gasoline	3	11.35	14	41.2	20.4	24.1
		Avg	11.35	14	41.2	20.7	29.7
RPM	3000 RPM	1	9.2	27	58.5	13.8	13.8
Torque	43.4 ft-lbf	2	9.15	27	58.7	14.0	14.0
% fuel	100% gasoline	3	9.15	27	58.7	14.0	14.0
	24.790 hp	Avg	9.15	27	58.6	13.9	13.9
	67.747 PSI BMEP						
	3000 RPM	1	8.3	24	58.5	16.1	17.4
	43.4 ft-lbf	2	8.3	24	58.5	15.8	17.0
	80% gasoline	3	8.3	24	58.5	15.9	17.1
		Avg	8.3	24	58.5	15.9	17.2
	3000 RPM	1	7.4	18	56.2	18.3	22.2
	43.4 ft-lbf	2	7.4	18	56.2	18.1	22.0
	60% gasoline	3	7.45	18	56.2	18.5	22.5
		Avg	7.40	18	56.2	18.3	22.2
	3000 RPM	1	6.75	14	54.7	19.2	26.0
	43.4 ft-lbf	2	6.55	14	55.3	18.9	25.6
	50% gasoline	3	6.55	14	55.3	19.1	25.9
		Avg	6.60	14	55.1	19.1	25.8
	3000 RPM	1	4.55	*1^{o}ATDC	57.3	21.4	34.2
	43.4 ft-lbf	2	4.50	*1^{o}ATOC	57.3	20.5	32.5
	40% gasoline	3	4.50	*1^{o}ATDC	57.3	20.7	33.4
		Avg	4.5	*1^{o}ATOC	57.3	20.9	33.4
RPM	3500 RPM	1	14.75	33	42.8	12.0	12.0
Torque	21.7 ft-lbf	2	14.75	33	42.8	11.9	11.9
% fuel	100% gasoline	3	14.70	33	42.9	11.9	11.9
	14.461 hp	Avg	14.75	33	42.8	11.9	11.9
	33.874 PSI BMEP						
	3500 RPM	1	14.7	27	41.3	15.0	15.5
	21.7 ft-lbf	2	14.7	27	41.3	14.8	15.3
	80% gasoline	3	14.7	27	41.3	15.3	15.8
		Avg	14.7	27	41.3	15.0	15.5
	3500 RPM	1	14.05	23	39.2	16.2	18.6
	21.7 ft-lbf	2	14.05	23	39.2	16.0	18.4
	60% gasoline	3	14.05	23	39.2	16.2	18.5
		Avg	14.05	23	39.2	16.1	18.5

*knock limited spark advance

		run	Gasoline Consumption lbm/hr	Hydrogen Consumption lbm/hr	BSFC $\frac{\text{lbm}}{\text{hp-hr}}$	η_{th} %	Exhaust Temp ^{o}F
	3500 RPM	1	7.228	1.910	.632	15.6	678
	21.7 ft-lbf	2	7.008	1.910	.617	15.9	683
	50% gasoline	3	6.900	1.910	.609	16.0	687
		Avg			.619	15.8	683
	3500 RPM	1	5.365	2.269	.528	16.8	669
	21.7 ft-lbf	2	5.293	2.269	.523	16.9	669
	40% gasoline	3	5.473	2.328	.539	16.4	672
		Avg			.530	16.7	670
RPM	3500 RPM	1	15.609	0	.881	16.5	701
Torque	28.9 ft-lbf	2	15.548	0	.807	16.6	704
% fuel	100% gasoline	3	15.568	0	.808	16.6	703
	19.259 hp	Avg			.809	16.6	703
	45.113 PSI BMEP						
	3500 RPM	1	11.438	.585	.624	19.8	763
	28.9 ft-lbf	2	11.734	.585	.640	19.4	757
	80% gasoline	3	11.524	.585	.629	19.7	758
		Avg			.631	19.6	759
	3500 RPM	1	8.919	1.552	.544	19.6	767
	28.9 ft-lbf	2	9.231	1.552	.560	19.2	769
	60% gasoline	3	8.882	1.552	.542	19.7	768
		Avg			.549	19.5	768
	3500 RPM	1	7.430	2.567	.519	17.9	756
	28.9 ft-lbf	2	7.647	2.567	.530	17.6	757
	50% gasoline	3	7.660	2.567	.531	17.6	757
		Avg			.527	17.7	757
	3500 RPM	1	5.760	3.881	.501	15.8	761
	28.9 ft-lbf	2	5.667	4.179	.511	15.2	763
	40% gasoline	3	6.142	4.179	.536	14.7	764
		Avg			.516	15.2	763
RPM	3500 RPM	1	16.674	0	.577	23.2	878
Torque	43.4 ft-lbf	2	16.848	0	.583	23.0	860
% fuel	100% gasoline	3	16.678	0	.577	23.2	872
	28.922 hp	Avg			.579	23.1	870
	67.747 PSI BMEP						
	3500 RPM	1	13.314	1.672	.518	21.7	847
	43.4 ft-lbf	2	13.136	1.672	.512	21.9	847
	80% gasoline	3	13.133	1.672	.512	21.9	846
		Avg			.514	21.8	847

		run	Intake Vacuum in-Hg	Ignition Timing ^{o}BTOC	η_v %	A/F ratio	Air / Gasoline ratio
	3500 RPM	1	13.35	20	39.6	17.2	21.7
	21.7 ft-lbf	2	13.30	20	39.6	17.6	22.4
	50% gasoline	3	13.25	20	39.6	17.8	22.7
		Avg	13.30	20	39.6	17.5	22.3
	3500 RPM	1	13.25	15	37.5	19.1	28.3
	21.7 ft-lbf	2	13.15	15	37.5	20.1	28.7
	40% gasoline	3	13.10	15	37.5	19.5	27.7
		Avg	13.15	15	37.5	19.6	28.2
RPM	3500 RPM	1	12.8	32	48.8	12.8	12.8
Torque	28.9 ft-lbf	2	12.8	32	48.8	12.8	12.8
% fuel	100% gasoline	3	12.75	32	48.8	12.8	12.8
	19.259 hp	Avg	12.8	32	48.8	12.8	12.8
	45.113 PSI 8MEP						
	3500 RPM	1	12.5	26	47.6	15.8	16.6
	28.9 ft-lbf	2	12.55	26	47.3	15.3	16.1
	80% gasoline	3	12.55	26	47.3	15.6	16.4
		Avg	12.55	26	47.4	15.6	16.4
	3500 RPM	1	11.45	21	46.8	17.9	21.1
	28.9 ft-lbf	2	11.4	21	46.8	17.4	20.4
	60% gasoline	3	11.4	21	46.8	18.0	21.2
		Avg	11.4	21	46.8	17.8	20.9
	3500 RPM	1	10.3	18	46.7	18.4	24.7
	28.9 ft-lbf	2	10.3	18	46.7	18.0	24.0
	50% gasoline	3	10.3	18	46.7	17.9	24.0
		Avg	10.3	18	46.7	18.1	24.2
	33.874 PSI 8MEP						
	3500 RPM	1	10.4	15	45.6	18.8	31.4
	28.9 ft-lbf	2	10.3	14	45.6	18.4	31.9
	40% gasoline	3	10.3	14	46.1	17.7	29.7
		Avg	10.3	14	45.8	18.3	31.0
RPM	3500 RPM	1	8.85	33	61.7	15.3	15.3
Torque	43.4 ft-lbf	2	8.95	33	60.7	14.8	14.8
% fuel	100% gasoline	3	8.85	33	61.1	15.1	15.1
	28.922 hp	Avg	8.90	33	61.2	15.1	15.1
	67.747 PS1 8MEP						
	3500 RPM	1	7.55	23	59.7	15.5	17.4
	43.4 ft-lbf	2	7.55	23	59.9	15.7	17.7
	80% gasoline	3	7.55	23	59.9	15.7	17.7
		Avg	7.55	23	59.8	15.6	17.6

		run	Gasoline Consumption lbm/hr	Hydrogen Consumption lbm/hr	BSFC $\frac{lbm}{hp\text{-}hr}$	η_{th} %	Exhaust Temp °F
	3500 RPM	1	9.719	2.537	.424	23.3	869
	43.4 ft-lbf	2	9.458	2.537	.415	23.7	872
	60% gasoline	3	9.888	2.537	.430	23.1	873
		Avg			.423	23.4	871
	3500 RPM	1	9.190	2.806	.415	23.0	883
	43.4 ft-lbf	2	9.486	2.806	.425	22.6	882
	50% gasoline	3	9.184	2.806	.415	23.0	884
		Avg			.418	22.9	883
	3500 RPM	1	7.055	3.582	.369	23.1	937
	43.4 ft-lbf	2	7.384	3.582	.379	22.6	937
	40% gasoline	3	7.515	3.582	.384	22.5	938
		Avg			.377	22.7	937
RPM	4000 RPM	1	16.178	0	.979	13.7	716
Torque	21.7 ft-lbf	2	16.004	0	.968	13.8	717
% fuel	100% gasoline	3	16.303	0	.986	13.6	719
	16.527 hp	Avg			.978	13.7	717
	33.874 PSI BMEP						
	4000 RPM	1	12.156	.681	.777	15.8	754
	21.7 ft-lbf	2	12.195	.681	.779	15.8	756
	80% gasoline	3	12.276	.681	.784	15.7	756
		Avg			.780	15.8	755
	4000 RPM	1	9.585	1.791	.688	15.3	734
	21.7 ft-lbf	2	9.677	1.791	.694	15.2	737
	60% gasoline	3	9.713	1.791	.696	15.2	737
		Avg			.693	15.2	736
	4000 RPM	1	8.127	2.567	.647	14.7	768
	21.7 ft-lbf	2	8.068	2.567	.643	14.7	769
	50% gasoline	3	8.018	2.507	.637	14.9	772
		Avg			.642	14.8	770
	4000 RPM	1	6.272	2.925	.557	15.6	754
	21.7 ft-lbf	2	6.299	2.925	.558	15.5	753
	40% gasoline	3	6.344	2.925	.561	15.5	753
		Avg			.559	15.5	753
RPM	4000 RPM	1	17.005	0	.773	17.3	802
Torque	28.9 ft-lbf	2	16.756	0	.761	17.6	801
% fuel	100% gasoline	3	16.799	0	.763	17.6	800
	22.010 hp	Avg			.766	17.5	801
	45.113 PSI BMEP						

		run	Intake Vacuum in-Hg	Ignition Timing °BTDC	η_v %	A/F ratio	Air / Gasoline ratio
	3500 RPM	1	7.05	17	57.5	18.6	23.4
	43.4 ft-lbf	2	7.05	17	57.5	19.0	24.1
	60% gasoline	3	7.05	17	57.5	18.3	23.0
		Avg	7.05	17	57.5	18.6	23.5
	3500 RPM	1	6.35	15	58.4	19.2	25.0
	43.4 ft-lbf	2	6.40	14	58.4	18.7	24.2
	50% gasoline	3	6.40	14	58.4	19.2	25.0
		Avg	6.40	14	58.4	19.0	24.7
	3500 RPM	1	5.15	2*	59.3	22.1	33.4
	43.4 ft-lbf	2	5.15	2*	59.3	21.5	31.9
	40% gasoline	3	5.15	2*	59.3	21.2	31.4
		Avg	5.15	2*	59.3	21.6	32.2
RPM	4000 RPM	1	14.15	38	44.5	12.8	12.8
Torque	21.7 ft-lbf	2	14.15	38	44.5	12.9	12.9
% fuel	100% gasoline	3	14.15	38	44.5	12.7	12.7
	16.527 hp	Avg	14.15	38	44.5	12.8	12.8
	33.874 PSI BMEP						
	4000 RPM	1	14.2	28	42.5	15.2	16.1
	21.7 ft-lbf	2	14.2	28	42.5	15.2	16.0
	80% gasoline	3	14.2	28	42.5	15.1	15.9
		Avg	14.2	28	42.5	15.2	16.0
	4000 RPM	1	13.55	24	41.1	16.7	19.8
	21.7 ft-lbf	2	13.55	24	41.1	16.5	19.6
	60% gasoline	3	13.55	24	41.1	16.5	19.5
		Avg	13.55	24	41.1	16.6	19.6
	4000 RPM	1	12.45	19	42.7	18.0	23.6
	21.7 ft-lbf	2	12.45	19	42.4	18.0	23.7
	50% gasoline	3	12.45	18	42.4	18.2	23.8
		Avg	12.45	19	42.5	18.1	23.7
	4000 RPM	1	12.8	14	40.0	20.0	29.3
	21.7 ft-lbf	2	12.8	14	40.0	19.0	29.2
	40% gasoline	3	12.8	14	40.0	19.8	29.0
		Avg	12.8	14	40.0	19.6	29.2
RPM	4000 RPM	1	12.35	35	50.5	13.7	13.7
Torque	28.9 ft-lbf	2	12.35	35	50.5	13.9	13.9
% fuel	100% gasoline	3	12.35	35	50.5	13.9	13.9
	22.010 hp	Avg	12.35	35	50.5	13.8	13.8
	45.113 PSI BMEP						

*knock limited spark advance

		run	Gasoline Consumption lbm/hr	Hydrogen Consumption lbm/hr	BSFC $\frac{lbm}{hp\text{-}hr}$	η_{th} %	Exhaust Temp °F
	4000 RPM	1	13.192	1.015	.645	18.5	819
	28.9 ft-lbf	2	13.26	1.003	.648	18.4	825
	80% gasoline	3	13.394	1.015	.655	18.3	823
		Avg			.649	18.4	822
	4000 RPM	1	10.116	2.388	.568	17.8	818
	28.9 ft-lbf	2	9.908	2.418	.560	17.9	818
	60% gasoline	3	9.956	2.985	.588	16.3	817
		Avg			.572	17.3	818
	4000 RPM	1	8.129	3.164	.513	17.6	846
	28.9 ft-lbf	2	8.478	3.224	.532	17.1	847
	50% gasoline	3	8.593	3.224	.537	17.0	849
		Avg			.527	17.2	847
	4000 RPM	1	4.261	4.299	.389	18.5	845
	28.9 ft-lbf	2	6.499	4.418	.496	15.9	851
	40% gasoline	3	6.554	4.418	.498	15.9	852
		Avg			.497	15.9	852
RPM	4000 RPM	1	19.058	0	.577	23.2	974
Torque	43.4 ft-lbf	2	19.290	0	.584	23.0	974
% fuel	100% gasoline	3	18.765	0	.568	23.6	975
	33.053 hp	Avg			.576	23.3	974
	67.747 PSI BMEP						
	4000 RPM	1	14.682	1.970	.504	22.1	964
	43.4 ft-lbf	2	14.742	1.970	.506	22.0	967
	80% gasoline	3	14.459	1.970	.497	22.3	969
		Avg			.502	22.1	967
	4000 RPM	1	11.074	3.821	.451	20.6	982
	43.4 ft-lbf	2	10.454	3.821	.432	21.2	987
	60% gasoline	3	10.803	3.821	.442	20.9	987
		Avg			.442	20.9	985
	4000 RPM	1	9.146	3.821	.392	22.7	981
	43.4 ft-lbf	2	9.207	3.821	.394	22.6	985
	50% gasoline	3	9.092	3.821	.391	22.7	986
		Avg			.392	22.7	984
	4000 RPM						
	43.4 ft-lbf						
	40% gasoline						

		run	Intake Vacuum in-Hg	Ignition Timing ^{o}BTDC	η_v %	A/F ratio	$\frac{\text{Air}}{\text{Gasoline}}$ ratio
	4000 RPM	1	12.1	28	48.4	15.7	16.9
	28.9 ft-lbf	2	12.05	28	48.4	15.6	16.8
	80% gasoline	3	12.1	28	48.4	15.4	16.6
		Avg	12.1	28	48.4	15.6	16.8
	4000 RPM	1	11.1	20	47.2	17.3	21.4
	28.9 ft-lbf	2	11.1	20	47.2	17.6	21.9
	60% gasoline	3	11.1	20	47.2	16.7	21.8
		Avg	11.1	20	47.2	17.2	21.7
	4000 RPM	1	10.05	16	49.0	19.4	26.9
	28.9 ft-lbf	2	10.1	16	49.0	18.7	25.8
	50% gasoline	3	10.15	16	49.0	18.5	25.5
		Avg	10.1	16	49.0	18.9	26.1
	4000 RPM	1	9.4	4*			
	28.9 ft-lbf	2	9.4	5*	46.7	19.5	32.8
	40% gasoline	3	9.4	5*	46.7	19.4	32.5
		Avg	9.4	5*	46.7	19.5	32.7
RPM	4000 RPM	1	7.45	37	67.1	15.9	15.9
Torque	43.4 ft-lbf	2	7.45	37	67.1	15.7	15.7
% fuel	100% gasoline	3	7.4	37	67.1	16.2	16.2
	33.053 hp	Avg	7.45	37	67.1	15.9	15.9
	67.747 PSI BMEP						
	4000 RPM	1	6.35	25	64.2	17.3	19.6
	43.4 ft-lbf	2	6.35	25	64.2	17.2	19.5
	80% gasoline	3	6.35	25	64.2	17.5	19.9
		Avg	6.35	25	64.2	17.3	19.7
	4000 RPM	1	5.9	15	59.8	18.2	24.4
	43.4 ft-lbf	2	5.9	15	59.8	18.9	25.9
	60% gasoline	3	5.9	15	59.8	18.5	25.0
		Avg	5.9	15	59.8	18.5	25.1
	4000 RPM	1	5.9	6*	59.5	20.9	29.6
	43.4 ft-lbf	2	5.85	7*	59.5	20.8	29.4
	50% gasoline	3	5.85	7*	59.5	21.0	29.8
		Avg	5.85	7*	59.5	20.9	29.6
	4000 RPM						
	43.4 ft-lbf						
	40% gasoline						

*knock limited spark advance

Acknowledgements

Of course it is impossible to thank everyone who assisted in the completion of this thesis, they ranged from former graduate students to factory representatives, but a few specific thanks are in order. First I would like to thank Dr. Herbert Ball, my major advisor for this study, for his advice and encouragement. I would also like to thank those who served on the advisory committee, Dr. J. G. Thompson and Dr. E. C. Lindley. Thanks also to Ms. JoAnn Driggers for typing the manuscript.

Finally I would like to thank my parents, for without their support and encouragement, the long educational process I have just completed would not have been possible.

VITA

Jerry Price Harkey

Candidate for the Degree of

Master of Science

Thesis: PERFORMANCE OF AN INTERNAL COMBUSTION ENGINE USING MIXTURES OF GASOLINE AND HYDROGEN AS THE FUEL

Major Field: Mechanical Engineering

Biographical:

Personal Data: Born at Manhattan, Kansas, June 18, 1954, the son of Malcom W. and Lois P. Harkey.

Education: Received primary and secondary education in the Manhattan, Kansas public school system and graduated from Manhattan High School in 1972; received the Bachelor of Science degree in Mechanical Engineering from Kansas State University, Manhattan, Kansas in December of 1976; completed requirements for the Master of Science degree in Mechanical Engineering at Kansas State University in May, 1978.

Professional experience: Worked one summer for the U.S. Army Corps of Engineers as a fallout shelter survey technician. Worked as a graduate research assistant from January 1977 to July 1978 at the Kansas State University Mechanical Engineering Department.

Professional organizations: Member of the American Society of Mechanical Engineers.

PERFORMANCE OF AN INTERNAL COMBUSTION ENGINE USING MIXTURES OF GASOLINE AND HYDROGEN AS THE FUEL

by

Jerry Price Harkey

B.S., Kansas State University, 1976

AN ABSTRACT OF A MASTER'S THESIS

submitted in partial fulfillment of the

requirements for the degree

MASTER OF SCIENCE

Department of Mechanical Engineering
Kansas State University
Manhattan, Kansas

1978

Abstract

Engine performance tests on a 1968, electronically fuel injected 96.6 cu-in, horizontally opposed, air cooled Volkswagen engine were conducted. Tests were conducted at engine torques of 21.7, 28.9, and 43.4 ft-lbf with fuel that consisted of a mixture of gasoline and hydrogen. The gasoline-hydrogen mixtures that were used were: 100% gasoline, 80% gasoline - 20% hydrogen, 60% gasoline - 40% hydrogen, 50% gasoline - 50% hydrogen, 40% gasoline - 60% hydrogen. These tests were conducted at engine speeds of from 1500 rpm to 4000 rpm in 500 rpm increments. The air-gasoline ratio was controlled by a KIM 1 microprocessor and associated hardware. The spark advance was set manually by the best torque procedure for tests using 100% gasoline. For tests using gasoline-hydrogen mixtures the hydrogen mixture and the spark advance were set manually with the lean best torque procedure. The hydrogen was introduced into the intake stream through a modified propane fuel system and carburetor.

It was found that the methods used to control the air-fuel ratio and spark advance were satisfactory. It was also found that in general intake manifold vacuum and volumetric efficiency decreased as the proportion of hydrogen in the fuel was increased. No dangerously high (equipment threatening) temperatures occured during the tests. Brake specific fuel consumption decreased as the proportion of hydrogen was in-

creased. For the most part the 80% gasoline - 20% hydrogen mixture produced the highest thermal efficiency. As the proportion of hydrogen was increased it was necessary to retard the spark advance to maintain optimum advance, or in the extreme, to maintain engine operation. Finally, it was found that when the engine was run on fuels with a high hydrogen proportion while operating with a high torque output, it was difficult to operate the engine without preignition or backfires. This last occurance led to recommendations that some method be found to control this preignition and backfiring.